Characterizing Viscoelastic Properties of Polyacrylamide Gels

A Major Qualifying Project Report:

Submitted to the Faculty

Of the

WORCESTER POLYTECHNIC INSTITUTE

In partial fulfillment of the requirements for the

Degree of Bachelor of Science

By

Zachary Gautreau[1], Jeremy Griffin[1], Todd Peterson[2], and Ploypan Thongpradit[1]
[1]Department of Biomedical Engineering, Worcester Polytechnic Institute
[2]Department of Physics, Worcester Polytechnic Institute

Date: April 27, 2006

Prof. Kristen Billiar[1], Major Advisor

1. Polyacrylamide
2. Viscoelasticity
3. Cell culture

Prof. Nancy Burnham[2], Co-Advisor

TABLE OF CONTENTS

TABLE OF FIGURES

TABLE OF TABLES

Acknowledgements

Authorship

Zachary Gautreau

 Ball Indentation

Todd Peterson

 Atomic Force Microscopy

Ploypan Thongpradit

 Uniaxial Testing

Jeremy Griffin

 Rheometry

Abstract

Despite its common use in cell culture studies, polyacrylamide gel's mechanical properties remain unclear. To characterize this gel fully, atomic force microscopy, uniaxial testing, rheology, and ball indentation were used. The range of the elastic moduli was 1.9-7.5 kPa and 18.1-39.4 kPa, for 5%/0.025% and 8%/0.08% gel concentrations, respectively, and a Poisson's ratio of 0.45 was found. Future research utilizing polyacrylamide as a cell culture substrate should indicate how the gel was characterized and acknowledge the uncertainty in stiffness values.

1. Introduction

Polyacrylamide has proven to be a popular medium examining the response of cultured cells to the stiffness of their surrounding environment. The interest in polyacrylamide has evolved from its experimentally tested biocompatibility and tunable mechanical properties. Substrates are required to closely mimic the natural conditions of biological tissues for cell culture techniques and it is known that polyacrylamide gels have the ability to be prepared with the identical mechanical properties of soft tissues, normal and pathological. However, polyacrylamide's potential as a cell culture substrate for *in vitro* studies is currently impeded due to a lack of confidence in the established stiffness values generated.

By studying the mechanical properties of polyacrylamide gels, the hope is to generate a range of consistent stiffness values for two gel concentrations. Thus far, there has been limited scientific research aimed at detailing the various mechanical parameters which polyacrylamide shares with natural soft tissues. In an effort to determine relative values of stiffness for varied polyacrylamide concentrations, Dr. Yu-li Wang and colleagues documented a range of stiffness values closely resembling that of native soft tissue which were obtained through mechanical testing (Wang et al., 2002). However, Dr. Wang's published results were recently labeled incorrect "by up to orders of magnitude" by a research group lead by Dr. Dennis Discher at the University of Pennsylvania using an alternative testing technique (Engler et al., 2004). Extensions of these findings, and the results outlined in this report, have practical implications for the study of cellular interactions on a polyacrylamide substrate.

Cell-substrate interactions are known to influence various cell characteristics such as proliferation rates, differentiation pathways, migration, adhesion, and matrix reconstruction. The influence of the substrate on these characteristics can be largely attributed to its mechanical

properties. The mechanical requirements of a substrate are specific in accordance with cell type; therefore the unknown stiffness values of polyacrylamide concentrations greatly restrict the depth of research possibilities.

The primary objective of this project is to find reliable numbers that quantify the mechanical properties of polyacrylamide over a range of concentrations. By using four techniques, it is hoped that a thorough evaluation of technique reliability, benefits, and capabilities can be outlined allowing for a general conclusion. Determination of the elastic properties will be obtained through experimental tests designed for atomic force microscopy (AFM), ball-indentation, dynamic rheology and uniaxial tensile. Following a brief introduction of relevant background subjects, this paper will discuss the experimental procedures and results of each technique. The techniques will be compared and analyzed to provide a range of acceptable stiffness values for two specific concentrations of polyacrylamide gels. The results from this study have the potential to set a standard for the composition of polyacrylamide gel substrates used in cell culturing.

2. Background Information

2.1. Polyacrylamide Gels

Previous studies have shown that cells respond differently when cultured on substrates of varying mechanical stiffness. The mechanical interactions in between the cell and the substrate are known to influence a number of cell behaviors (Beningo et al., 2002). Polyacrylamide gel is quite easily prepared and is thought by many experts to offer a suitable substrate on which to grow cells because it can be made to closely mimic the mechanical properties of natural tissues. Researchers have had much success adhering cells to the polyacrylamide gel substrates; however, it proves to be difficult to accurately evaluate cellular responses provoked by the mechanical properties of the substrate because there is no set standard for determining their mechanical properties. Dr. Yu-li Wang and colleagues have made an attempt to quantify polyacrylamide gel properties using a ball indentation technique. In addition, Dr. Dennis Discher and colleagues have evaluated the comparison between mechanical stiffness values of several natural and polyacrylamide gel substrates using AFM (Engler, 2004). Compelling results were obtained displaying similarities between several substrate types.

In order to mimic the environment and structure of natural soft tissues, researchers produce synthetic polyacrylamide gels with similar properties to both healthy and pathologic human tissue. These gels are formed by dissolving acrylamide and cross-linker monomer N, N'-methylenebisacrylamide (bis). The chemical structure of the acrylamide monomer can be seen in Figure 1.

$$\begin{array}{c}
\mathbf{O}\\[-2pt]
\|\\[-2pt]
\mathbf{H}\;\diagdown\\
\mathbf{C}=\mathbf{C}-\mathbf{C}-\mathbf{N}\\
\mathbf{H}\;\diagup\diagdown\,\mathbf{H}
\end{array}$$
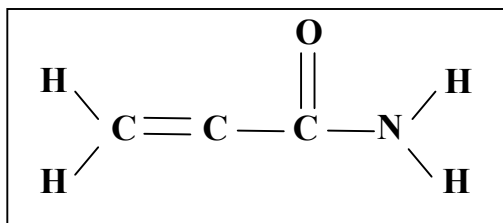
Figure 1: Chemical structure of the acrylamide monomer

The polymerization of a polyacrylamide gel is a free-radical catalyzed reaction and results in long chains that are held together by covalent bonds. Polyacrylamide gels are typically made between two glass plates because oxygen acts a free-radical scavenger and inhibits polymerization (www.amershambiosciences.com [manual], 2005).

There are several advantages beyond its simple fabrication for using polyacrylamide gels as the structure for studying mechanical properties on the microscopic level. The mechanical properties are easily manipulated by simply altering the concentrations of acrylamide and bisacrylamide without making any alteration to the gel's chemical properties. Polyacrylamide gels offer a much more realistic model of physiological tissue than a glass or plastic surface because of its soft flexible nature. The gel material has optical properties that allow for researchers to perform high-resolution imaging to analyze the structure. In addition, some studies involve the implementation of fluorescent beads into the gels to further analyze the mechanical properties with a resolution near 2 μm (Beningo et al., 2002).

A range of stiffness values can be achieved simply by having a constant total concentration of acrylamide while varying the concentration of bisacrylamide cross-linker. Previous research has shown that too low of a concentration of bisacrylamide will cause the surface of the gel to crack and it is possible that the gel will not polymerize. Wang et al. have previously shown that a 5-8 % acrylamide / 0.1 -0.03 % bisacrylamide gel mixture produces an appropriate scaffold for measuring cell traction forces (Engler et al., 2002). Equally as important

to the overall concentrations of the gel's components, is maintaining an appropriate thickness. The thickness of a gel cannot be calculated from the volume of solution used. The actual gel thickness tends to be up to four times greater than the calculated value. This is due to the gel's response to changes in temperature, osmolarity, and hydration. It is therefore extremely important to monitor the experimental atmosphere and constantly maintain suitable experimental conditions when working with polyacrylamide gels. The following sections will outline the principles and techniques for mechanical and viscoelastic characterization of polyacrylamide gels.

2.2. Ball Indentation, Atomic Force Microscopy, and Hertz Contact Mechanics

Ball indentation is considered to be the standard method for determining stiffness values of soft materials due to its simple methodology and basic principles. Following principles of Hertz mechanics, one is able to determine a stiffness value with this simple technique. Doctor Yu-li Wang of UMass Medical School used this method for a polyacrylamide (Pelham and Wang, 1997). The results from this experimentation were eventually published in a 2002 article where the methodology was presented (Engler, 2002). Similar research methods have been utilized in this research with little variation. Observed gaps in the previous research method will be analyzed in order to further evaluate the methods effectiveness.

Hertz mechanics provide the mathematical support and theory behind ball indentation. All Hertz mechanics problems require several assumptions to be made for the mathematical analysis. The assumptions considered in this research are as follows (Emil, 2002):

- at the point of contact the shape of each of the contacting surfaces can be described by a homogeneous quadratic polynomial in two variables;

- both surfaces are ideally smooth;

- contact stresses and deformations satisfy the differential equations for stress and strain of homogeneous, isotropic, and elastic bodies in equilibrium;

- the stress disappears at great distance from the contact zone;

- tangential stress components are zero at both surfaces within and outside the contact zone;

- normal stress components are zero at both surfaces outside the contact zone;

- the stress integrated over the contact zone equals the force pushing the two bodies together;

- the distance between the two bodies is zero within but finite outside the contact zone;

- in the absence of an external force, the contact zone degenerates to a point

Abiding by these assumptions, mathematical derivation leads to the overlying equation used for determination of a substrate stiffness value. Derivation of the overriding equation can be found in Appendix 10.3 (Wang et al., 2002):

$$E = \frac{3(1-\nu^2)P_s}{4d^{3/2}R^{1/2}} \quad (\text{N/m}^2).$$

Equation 1

Where E is Young's modulus, ν is Poisson's ratio, P_s is the applied force for a sphere, d is the measured indentation of the ball and R is the radius of the ball used.

More advanced and more localized research was later conducted on polyacrylamide by use of Atomic Force Microscopy. Similar to ball indentation, an AFM probe is lowered onto a sample and the indentation depth is measured. However, AFM operates on a much smaller scale. A cantilever, including a conical indenter at the tip, is lowered onto the sample which then bends the cantilever. A laser is directed onto the cantilever tip and then deflected onto a photodiode. The position of the laser on the photodiode correlates to how much the cantilever deflects, which allows for precise measurements. Dr. Dennis Discher of University of Pennsylvania is a leading researcher using AFM in his studies of cell substrates (Discher et al., 2004). The creation of

streamlining the process of acquiring data from AFM on a compliant surface is still progressing.
A current technique is described in a report by Margo Frey of Worcester Polytechnic Institute
(Frey et al., 2005).

The AFM conical tips follow both the conical and spherical Hertzian models. The tip
will behave as a sphere and abide by Equation 2 up to a certain indentation depth. Thereafter, it
will follow the Hertzian model of a cone:

$$E = \frac{2P_c(1-v^2)}{d^2\pi\tan\theta},$$ **Equation 2**

with θ equivalent to the tip's half angle that is measured using the a step function grating step
described in the AFM Methodology.
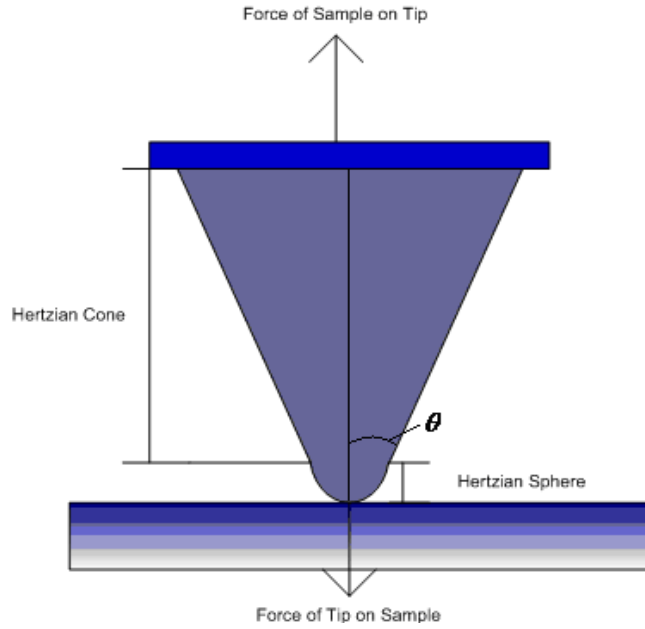
Figure 2: Combination of Hertzian models of a conical AFM tip

For AFM the following equations were used to calculate the Hertzian models. The
Hertzian model of a spherical tip is shown as:

$$P_{s=} bd^{(3/2)}.$$
<div align="right">**Equation 3**</div>

The quantity b is determined by the following equation:

$$b = \frac{4}{3} * \frac{E}{(1-v^2)} * R^{(1/2)} \; (nN/nm^{(3/2)}),$$
<div align="right">**Equation 4**</div>

where R is the radius of the tip, and v is the Poisson ratio.

The two techniques of ball indentation and AFM measure the local properties of a material. The following two sections will outline the principle of two techniques which were utilized in this research to obtain the bulk properties of polyacrylamide gels. The combination of measurements on both scales is hoped to provide a thorough understanding of this complex material.

2.3. Uniaxial Tensile Testing and Viscoelasticity

To compliment the local measurements of ball indentation and AFM, a uniaxial tension test will obtain the bulk properties of the polyacrylamide gel. A uniaxial tension test is a direct mechanical measurement which observes a material's behavior under tension in one direction. The two important parameters for this technique are the amount of force per unit area and the elongation response of the material under a known force. These collected results allow for the creation of a stress-strain curve and a calculated Young's modulus to quantify a material's stiffness.

The applied stress on a material can be found by dividing the force by the initial area of the sample where the force is applied. The stress (σ), found in Equation 5, is defined as the amount of force per unit area:

$$\sigma = \frac{Force}{Area_{Initial}}.$$
<div align="right">**Equation 5**</div>

While the stress is being applied, the sample undergoes axial elongation and the lateral dimension undergoes contraction. A schematic of a sample under a tension load during uniaxial testing is shown in Figure 3.
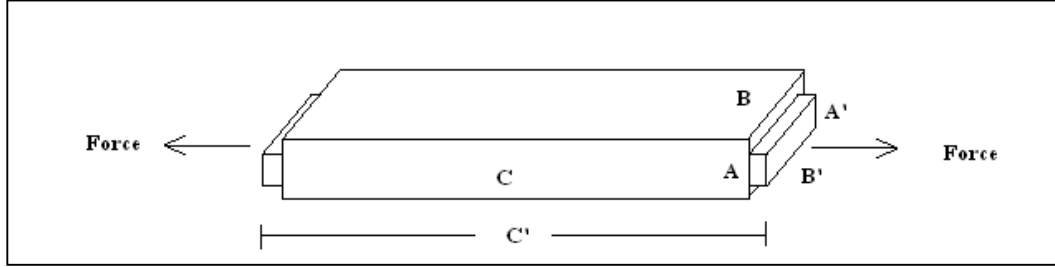
Figure 3: A schematic of a sample undergoing elongation in the axial direction and contraction in the transverse direction during a uniaxial tension test.

The strain value quantifies the deformation of a body when it is subjected to stress. An engineering strain is defined as the change in length divided by its initial length. The fundamental equation is represented by the Greek letter ε (epsilon) shown in Equation 6:

$$\varepsilon = \frac{\Delta Length}{Length_{Initial}}.$$

Equation 6

From Figure 3, the infinitesimal, or engineering axial strain, is represented as:

$$\varepsilon = \frac{C'-C}{C}.$$

Equation 7

There have been several researchers in the past who have studied the properties of polyacrylamide gel using the uniaxial tension technique (Pelham and Wang, 1997). Due to the physical properties of the gel, a common issue in a tension test was gripping. Various grip designs were created as an attempt to inhibit the sample from slipping and tearing during a tension test. One research group used paper clips as a grip attachment technique to the polyacrylamide gel. This technique used the weight of the paperclips to apply tension force from

gravity to the gel sample (Pelham and Wang, 1997). A different group lead by Wong developed a gripping technique that involved gluing pieces of transparency film with glue to both ends of the gel sample and applied known weights using a copper wire (Wong, 2003). While the maximum strain values from past research was not extensively discussed, it is important to keep the strain percentage within the range of cell response. A cell traction study lead by Engler showed that the maximum strain generated from a single cell is about 15-25% (Engler, 2004). Researchers used the equations of stress and strain as mentioned above to find the elastic modulus.

In addition, the Poisson's ratio can be determined using this testing method by calculating the deformation in the transverse and axial strains. Three other techniques in this project involved in this research rely on the accurate Poisson's ratio to calculate the elastic modulus. Researchers have been using a Poisson's ratio in a specified range rather than one specific defined number: Engler's research team found a Poisson's ratio in the range of 0.4-0.45, while Dr. Wang's group assumed a value of 0.3 (Engler, 2004). These values came from a range of 0.3-0.5 by a study on the swelling behavior of polyacrylamide gels in 1980 (Geissler, 1980).

In addition to measuring the Poisson's ratio and Young's modulus, the uniaxial tensile technique can be used to quantify the material's viscoelastic behavior. To examine the viscoelastic behavior of polyacrylamide gel, varying strain rates and a stress relaxation method were used with the tensile tests. The device used for this technique allows the strain rate to vary, while past researchers did not investigate the gel's behavior under different strain rates. A viscoelastic material's stiffness values are expected to increase with a growing strain rate and decrease (relax) over time during a stress relaxation test. Figure 4 further illustrates the behavioral characteristics between elastic and viscoelastic materials.
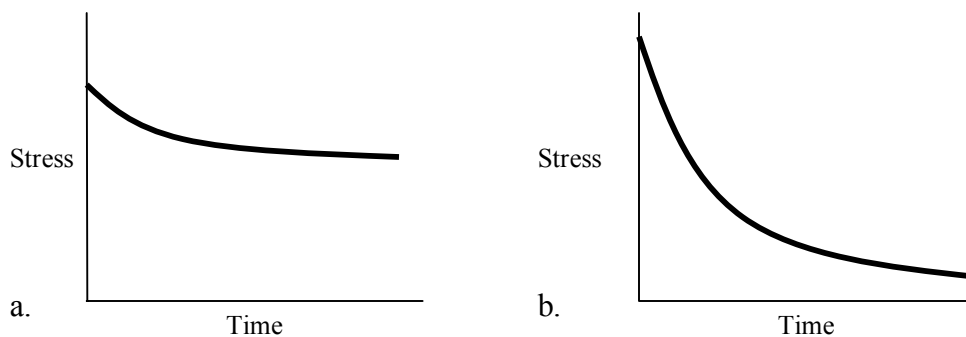
Figure 4: Stress Relaxation Test: a) the material is predominantly elastic because the stress becomes constant b) the material behaves as a viscoelastic fluid with a continuously decreasing stress value.

In order to perform a complete analysis of the viscoelastic property of the polyacrylamide, another theory of viscoelasticity with dynamic testing involving harmonic motion was investigated. The introduced concepts have specific applications to the rheology testing technique used in this research.

2.4. Rheology and Viscoelasticity

Rheology is the flow of fluids and deformation of solids under stress and strain. As previously mentioned, semi-solid, or viscoelastic, materials exhibit liquid and solid like properties depending on temperature and the applied stress and strain over time (Goodwin, 2000). A dynamic rheometer can be used to determine the viscoelastic properties of polyacrylamide by calculating the complex shear modulus under low-frequency oscillating shear deformation. Due to their three dimensional cross-linked network, polyacrylamide gels demonstrate viscoelastic behavior, having the ability to store energy and also flow when put under small deformations. The rheometer applies a harmonic oscillatory torque to the polyacrylamide gel sample and is able to measure the output motions to calculate the viscoelastic

properties. Figure 5 visually demonstrates this concept of an applied shear stress and a resulting deformation, or shear strain.
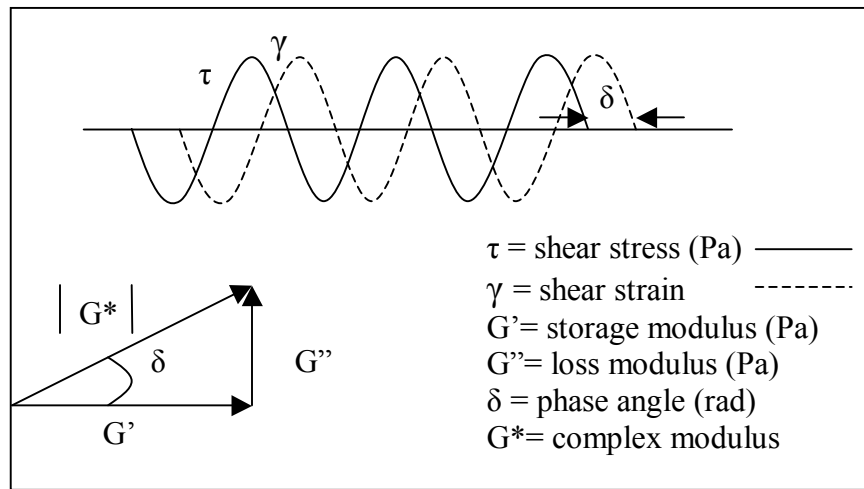
Figure 5: This viscoelastic schematic displays two out of phase sin waves, one representing shear stress and the other being the resulting shear strain. The storage modulus (G') quantifies the amount of elastic energy in the system, while the loss modulus (G") is the mechanical energy lost to viscous forces.

The elastic response of a particular gel is quantified with the storage modulus (G'), a measurement of the gel's ability to "store" elastic energy that can eventually be recovered. A second measurement known as the loss modulus (G'') quantifies the amount of mechanical energy that is "lost" in the form of heat due to the viscous forces acting on the gel. Finally, the ratio of G''/G' represents the tangent of the phase angle between stress and shear during oscillatory shear (Grattoni, 2001). The phase angle quantifies the degree of viscoelasticity of a specific material. Elastic materials have phase angles close to 0° (a shear strain in phase with the applied shear stress) and viscous materials have phase angles around 90° (a shear strain completely out of phase with the applied shear stress). The complex modulus (G*) is known as the viscoelastic, or complex, modulus and is obtained from the ratio of stress to strain. This value quantifies the total resistance to oscillatory shear.

For a linear elastic material, the shear modulus measurements taken with the rheometer may be converted to an elastic modulus value using the following equation:

$$G^* = \frac{E}{2(1+\nu)}$$.

The G* value used in these calculations is the previously mentioned complex modulus. As discussed in the uniaxial tension section, the Poisson's ratio (ν) is the negative of the ratio of the lateral strain to uniaxial strain, in axial loading. The calculation for Poisson's ratio will come from the uniaxial testing of the polyacrylamide gels.

Researchers have used a variety of rheological techniques to quantify the viscoelastic properties of polyacrylamide gels. Butler et al. (1998) utilized small ferromagnetic beads within a gel to quantify its rheological properties. The angular rotation of the beads was measured when the magnetized beads were rotated by an external magnetic field. Butler et al. have reported that it is difficult to interpret the viscosity and elastic modulus of the material from the given parameters. Other research has involved the use of microrheology to characterize the properties of polyacrylamide gels. Dasgupta et al. use embedded probes in the medium to quantify the local viscoelastic properties. This research found that quasielastic light scattering, diffusing wave spectroscopy, and video-based particle tracking techniques successfully measured the properties of polyacrylamide gels (Dasgupta, 2005). It is difficult to compare the results found by the research group lead by Dasgupta, because they used entirely different concentrations of acrylamide monomer and bisacrylamide cross linker to make their polyacrylamide samples. It is interesting to note, that this group did find microrheology and bulk rheology techniques resulted in similar variations of the elastic and viscous moduli. Also on the local level, Schnurr et al. have utilized the laser interferometry technique to measure beads

within the polyacrylamide substrate. This technique's limitation was that it was unable to present clear temporal and spatial resolution on the local level and could not measure a large amount of beads at the same time (Dasgupta, 2005).

Due to the lack of equipment availability, many of the above mentioned microrheology and bead techniques could be utilized within this research. The rheometry methodology chapter will further detail the dynamic oscillatory testing which was performed for this project. It is important to note the differences in the scale of the measured properties of the polyacrylamide gels.

3. Project Approach

This project was unique in the sense that there was no physical object to "design" and validate. The work entailed designing a method for characterizing the viscoelastic properties of polyacrylamide gels. In an attempt to thoroughly understand the properties of polyacrylamide gels, a strategic design process had to be followed. To study the mechanical properties of polyacrylamide gels, it was essential to choose measurement methods which would quantify properties on both the macro and micro scale. The project approach of this research is to use a variety of measuring systems to find reproducibility and consistency in the mechanical properties of polyacrylamide gels.

The team approached the client's original project statement by asking several questions to clearly define client's objectives, constraints, and functions. Previous research involving polyacrylamide gel was thoroughly analyzed and showed that there was not a great deal of work involving the material's viscoelastic properties. The team used project management tools to help conclude that pursuing multiple techniques was necessary to satisfy the client's needs. Further, the team decided to approach the problem from various size scales; allowing for an easy comparison to published values and to thoroughly evaluate the material.

From background research, budget constraints and machine availability, the team decided to use four techniques: ball indentation, Atomic Force Microscopy (AFM), uniaxial tensile testing, and rheology. The three techniques of ball indentation, AFM, and uniaxial tensile testing were performed on the WPI campus; however, the team utilized a rheometer at Malvern Instruments in Southborough, MA. The ball indentation and AFM techniques provide stiffness values on the local scale, while the uniaxial tensile testing and rheometry technique measure the bulk properties. By using these four techniques, the team hoped to clarify some of the

controversial issues with the stiffness values and to provide a better understanding about the

gel's properties in multiple scales.

4. Design

To properly formulate the experimental method for this project, the design process outlined in the textbook, Engineering Design: A Project-Based Introduction by Dym and Little was followed (Dym et al., 2004). The subsequent section will outline the overall process which was used to design the structure of this project. The attempt to develop a novel experimental design separates the design process of this project from a typical design process which consists of developing a physical device.

Several client interview sessions provided the initial analysis of project objectives and constraints. In an attempt to obtain reliable viscoelastic properties of polyacrylamide gels the subsequent objectives were developed from the client interviews: yield reliable viscoelastic properties, stay within the project budget, cannot harm the user, and must be easy to use.

Following the interview process a more specific list of requirements was developed to include in an objective tree and a pairwise comparison chart. The objective tree can be seen in Figure 6, while the pairwise comparison chart can be found in Appendix 10.1. From these tools, it was determined that the main focus of the project was to find reproducible results among the individual measuring techniques.
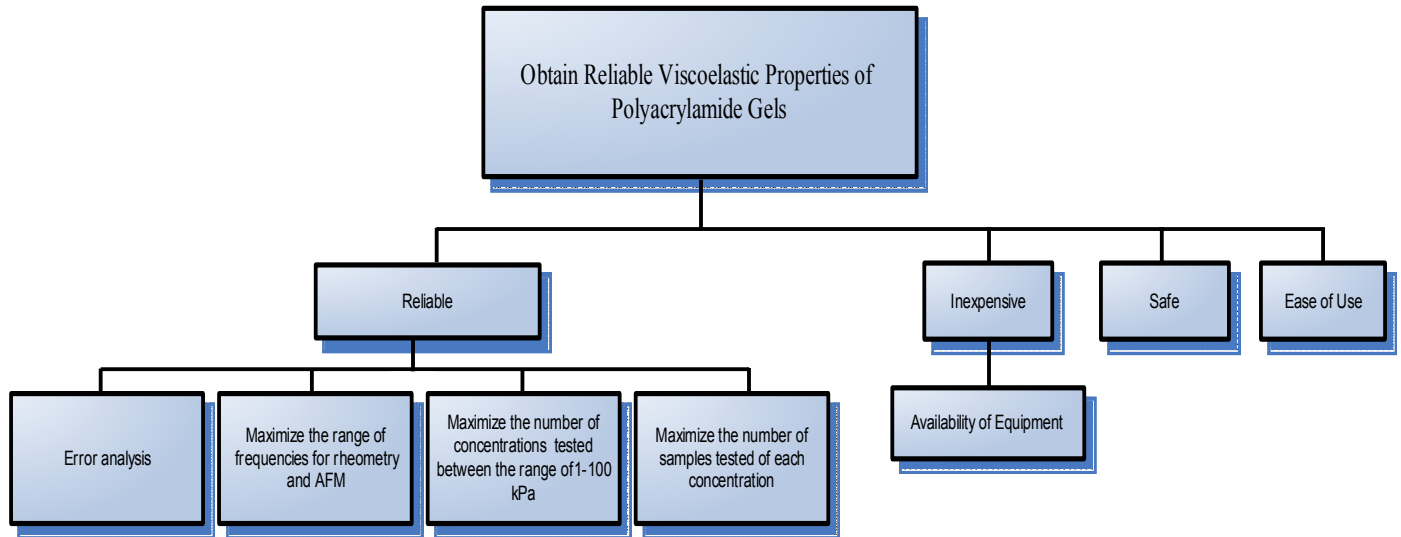
Figure 6: Objective Tree: this design tool aided the team in prioritizing the overall objectives of the project. The ultimate goal of this research was to obtain reliable viscoelastic properties of the polyacrylamide gels.

The pairwise comparison chart (PCC) was sent to all clients including Dr. Billiar, Dr. Burnham, Angie Throm, and Margo Frey. These recipients have been identified as key stakeholders from the corresponding research, therefore outlining their concerns was important. To generate some comparison, we the research team also filled in a PCC. The PCC allowed the client and the team to rank the level of importance of the project's objectives. The PCC chart acts as another medium of communication between the client and the team to evaluate and compare the level of understanding. The numbers 1, 0.5 or 0 are scores that are used to rank the level of objective importance. The magnitude of the score represents the level of importance. The chart works by placing number 1 in the box if he/she feels that the objective in the y-axis is more important than the objective in the x-axis. The number 0 is placed if he/she feels that the objective in the x-axis is more important. In the case where he/she feels that they are both equally important, number 0.5 should be placed in the white box. The responses from clients and our team showed that obtaining reproducible values was placed as the highest priority. The maximum number of concentrations and samples which the team originally thought were more

25

important were proven wrong using this PCC chart. This PCC chart in the design process helped the team greatly in obtaining valuable and satisfying results to our clients. The results from this process are briefly outlined below.

Conclusive results were established by the clients determining that the main research objective was to assure the overall reliability of the testing techniques pursued in this research. Following this in importance was to maximize the testing parameters (e.g. frequency ranges). The third primary objective as determined by the clients was to maximize the number of tests performed in order to generate a large amount of data for analysis.

Upon review of these documents the research team was forced to alter their initial objective of the work. This was determined by a minor difference in perception between the clients and researchers. Initially, the team's goal was to collect as much data as possible over a wide range of polyacrylamide concentrations. As the project progressed, the scope of the project became more concise and it was discovered that data on two specific polyacrylamide gel concentrations were more significant than others (the 8.0% acrylamide / 0.08% bisacrylamide solution and 5.0% acrylamide / 0.025% bisacrylamide). The clients suggested that these concentrations were most important because they are most often used in cell culture research. Dr. Billiar extensively uses these two concentrations in his laboratory; the soft 5%/0.025% represents a healthy normal tissue, while the 8%/0.08% represents a diseased or fibrotic tissue. Using the design process, the team was able to clarify the importance of maximizing the number of samples between these two specific concentrations. In the end, testing less individual samples from multiple concentrations would not have allowed the group to draw conclusive findings.

Each selected technique has its own advantages and disadvantages. The team evaluated the pros and cons of each method as mentioned in Appendix 10.1. In addition to determining the

objectives of the project during the initial stages of the design process, the team had to decide which methods were most appropriate for measuring the viscoelastic properties of polyacrylamide gels. Several tools for measuring viscoelastic properties were mentioned in the literature, but proved to be inappropriate for a variety of reasons including availability of the equipment and the limited budget. While a viscometer was available on the WPI campus, it simply was not suitable for taking the required measurements of the polyacrylamide gels. A viscometer uses a spindle to apply unidirectional shear to sample, limiting its use to viscous or liquid samples. Similar to the viscometer, capillary rheometry proved to be an inappropriate testing method because the sample must have an element of flow in order to yield accurate results.

The many other methods which have been utilized to characterize the viscoelastic properties of gel like substances include: laser trap microrheometry, magnetic twisting cytometry, piezoelectrically actuated linear rheometry, and 1-D ultrasound elasticity.

All of the above mentioned techniques would give intriguing data but could not be used in this project because the equipment was not readily available. The following table outlines the limitations found for each technique.

Experimental Method	Limitations
Laser trap microrheometry	Equipment is unavailable, cost
Magnetic twisting cytometry	Equipment is unavailable, cost
Piezoelectrically actuated linear rheometry	Equipment is unavailable, cost
1-D ultrasound elasticity	Equipment is unavailable, cost
Viscometry	Sample must flow
Capillary Rheometry	Sample must flow

Table 1: Limitations of alternative techniques: this design tool helped narrow down the possible experimental techniques.

Laser trap microrheometry measures local mechanical properties with an infrared laser trap and a galvanometric scanner (Velegol, 2001). Magnetic twisting cytometry uses a magnetic field to rotate small ferromagnetic beads within the gel and measures the angular rotation of the applied torque to allow for specific parameter calculations (Butler, 1998). Piezoelectrically actuated linear rheometry is advantageous because it utilizes a cantilever to apply oscillatory shear stress to the gel sample in a hydrated environment (Parsons, 2002). Finally, the ultrasound elasticity method involves a complex transducer setup which performs uniaxial compressions on the test sample (Chen, 1996). In the end, it was eventually determined that the four methods of atomic force microscopy, ball indentation, uniaxial tension, and rheology were most appropriate. The following methodology chapter of this report will highlight the advantages of each of these four techniques.

To fulfill the project's functions, the team created a morphological chart to show possible ways of obtaining all of the necessary information for what the project must satisfy. A morphological chart is used to help the team evaluate ways to characterize properties of polyacrylamide gels by displaying both the project's functions and means. The functions define what the project must do, while the means clarify possible ways the team can achieve the specific functions.

Function	Possible Means				
Measure elasticity	Rheology	Ball Indentation	AFM	Uniaxial Tension	
Obtain Poisson's Ratio	Uniaxial Tension Technique				
Determine reproducibility of technique	Ball size for Ball Indentation technique	Types of plates for Rheometry	Types of Cantilever tip	Error & statistical analysis	Compare results between technique
Evaluate local & bulk properties of the gel	Comparing AFM and Ball Indentation	Comparing Rheology and Uniaxial tensile testing			
Determine range of reliable stiffness values for specified concentration	Use reliable results determined from AFM, Rheology, Ball Indentation and Uniaxial tensile testing technique to evaluate the stiffness range for a specific concentration				

Table 2: The morphological chart determines possible means for satisfying the functions of the project.

After using this design process we have determined to use the four techniques of ball indentation, AFM, uniaxial tensile testing, and rheology. These techniques are all able to determine the Young's modulus of the polyacrylamide gels and each has their own unique advantages. For example, the uniaxial tensile testing method is able to measure a Poisson's ratio value, while the ball indentation and AFM techniques are able to quantify properties on the local scale. In the end, we have concluded that our clients are more interested in finding a reliable technique rather than maximizing the range of concentrations tested.

5. Methodology

The following chapter aims to detail the experimental procedures of the four testing techniques used in this research to quantify the mechanical properties of polyacrylamide gels. Each technique is explained individually outlining the set-up required, the steps taking to gather data and the calculations used to generate results. Sources of variability were eliminated by controlling environmental conditions (temperature, humidity, and gel hydration) in attempt to maintain consistency for analysis of the results.

5.1. Polyacrylamide Gel Fabrication

The protocol for making polyacrylamide gel from Yu-Li Wang's laboratory, seen in Appendix 10.2, was followed to ensure uniform gel concentration throughout the experimental process. The polyacrylamide gels used in this research were comprised of stock solutions of acrylamide and N, N'-methylenebisacrylamide. The solutions were both obtained from Bio-Rad Inc and were diluted to proper concentrations with distilled water and 1 M Hepes (pH 8.5): 40% weight/volume for the acrylamide and 2% weight/volume for the bisacrylamide. After making a well mixed solution following the protocol outlined in Appendix 10.2, the mixture must be degassed to allow for sufficient polymerization. Finally, 10% ammonium persulfate and TEMED (N,N,N,N'-tetramethylethylenediamine) are added to the solution to induce polymerization. After casting the gels in an appropriate manner, further discussed in the methodology section of this report, the gels are stored at 4°C in a 50 M Hepes (Wang et al., 2002).

The original protocol was intended for making the 70 μm thick gels necessary for AFM; therefore, slight modifications in the polymerization step of the protocol were necessary for each individual technique. The three techniques of ball indentation, uniaxial tension testing, and

rheology required much thicker gels.   The protocol outlined by Wang et al. suggests casting the gels in-between an activated glass slide and a glass cover slip. It is essential to degas the solution and cover the gel during polymerization because oxygen acts as a free radical scavenger and inhibits the polymerization. Insufficient polymerization leads to inconsistent and inaccurate mechanical properties during testing. In an attempt to eliminate experimental sources of error, the polymerization of the gels was completed in between two glass plates with one large solution of acrylamide/ bis solution. The chamber required two parallel glass plates, rubber stops, parafilm, and agarose gel. Two rubber spacers were placed in between the glass plates and the bottom was sealed with 1% agarose gel and parafilm to prevent any solutions from leaking out from the chamber. Binder clips were used to clamp and seal the glass plates against the rubber spacers and agarose gel. Rather than making the traditional 5 mL of solution, the new gelling system required 180 mL of solution. The dimensions of the gap in-between the two glass plates can be found in Figure 7.
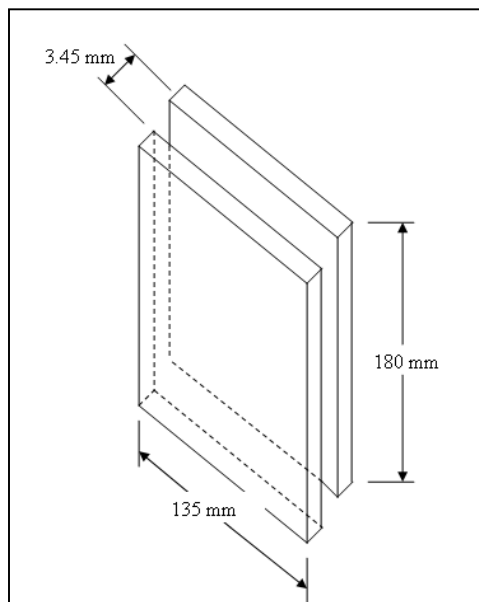
Figure 7: Glass Plate Polymerization Method: rubber spacers on the sides and agarose gel on the bottom inhibited solution leaking.

To ensure a well-mixed solution, the acrylamide solution was placed on a stir plate for five minutes prior to being degassed. In addition, after the degassing the solution was stirred once again while the ammonium persulfate and TEMED was added. The solution was quickly poured in to the gap between the glass plates and allowed to solidify for one hour because of the increase in gel volume. The resulting polyacrylamide gel sheet, seen in Figure 8, was then simply cut into smaller gel samples with scissors.
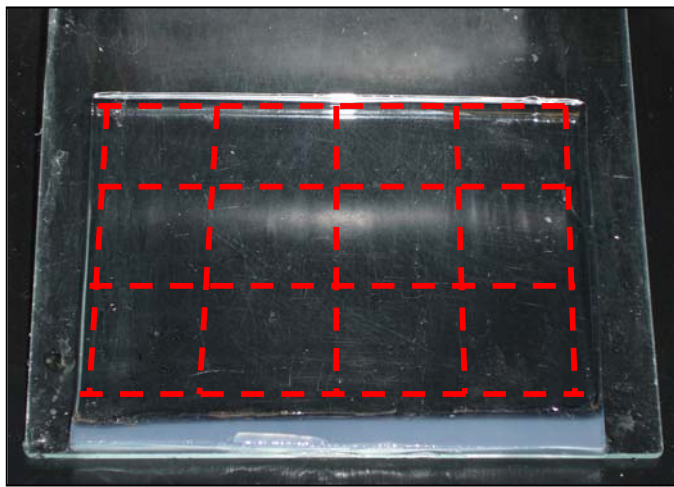
Figure 8: Polyacrylamide Gel Sheet: The large sheet allows for multiple samples made in identical conditions with equal sample thicknesses.

In order to meet specific requirements of the four techniques, slight modifications were made to the above mentioned protocol. The following technique methodologies will cover these specific variations and the reasoning behind them. Any adjustments to the above protocol were made with caution as to not affect the overall properties of the gel being tested.

5.2. Ball Indentation

The objective of the ball indentation testing was to evaluate the effect that ball diameter has on relative stiffness values. This approach is derived from an observed gap in the research conducted by Dr. Wang. This alteration was achieved by perform the test with three steel balls of different diameters (0.64 mm, 1 mm, and 2 mm in diameter). All other components (material,

density and polish) of the balls were equalized in order to eliminate the experimental variables. An inverted microscope with an attached micrometer was used to generate various distances in the z-direction.

Two polyacrylamide gels were made at different concentrations simultaneously in order to eliminate all possible experimental variations (room conditions and time allowed for both degassing and polymerization). Immediately after the polymerization time, each gel was submerged with 50 mM HEPES solution to maintain hydration for consistent swelling of the polyacrylamide. Section 5.1 provides a detailed protocol of the polyacrylamide preparation. One modification involves making the gel with a 1.75 mm thickness, rather than a 3.45 mm thickness, to accommodate for microscope restrictions.

Testing required the removal of the HEPES buffer solution in order to eliminate the need for including buoyancy variables in the calculations of applied force. The surrounding buffer solution was removed only from the gel being tested so that the other two gels remained moist. This step was performed by allowing all of the solution to freely run off the gel surface providing for satisfactory testing conditions when no visible liquid film is present on the surface. Starting with the 0.64 mm ball, ten measurements were taken on a gel of each concentration (5/0.025% and 8/0.08%). Once ten measurements were taken on the first gel, it is placed back in 50 mM HEPES while the next gel was tested. Ultimately, each gel sample was used with each of the three balls. Effects of gel drying are not fully understood which is why consistency was maintained during testing to eliminate this factor.

Due to the large amount of variability with manual measurement of focal points, multiple measurements were taken. The goal was to determine the distance that the bottom of the ball was from the top surface of the gel within a consistent range from over 20 different locations on

the gel. Initially this process was taken as the distance from the top surface of the gel to the point at which the ball was no longer visible when moving the focal point further into the gel. Upon evaluation it was determined that this method did not provide an accurate measurement of the bottom of the ball. Rather, the measurement being made was relative to the diffraction of light through the gel and around the ball on the gel surface. In order to rectify this problem, a new measurement technique was implemented.

Initially, the top of the gel surface was brought into focus and the micrometer was zeroed. This was accomplished by focusing the lens on imperfections of the gel surface. This part of the measurement can be attributed for much of the variation in measured indentation values as particles resting on the gel surface can interfere with the perception of the gel surface location. It was important to make the surface measurement a minimum of one diameter in length away from the outer edge of the ball in order to accommodate for gel adhesion to the ball surface. The centroid of the ball was the second measurement taken for determination of the ball radius' vertical location. The centroid was determined to be the point at which the beam of light was perfectly circular with the highest intensity around the visible edge of the ball. By slightly moving the lens either up or down, there was a clear variation in focused light that made this measurement fairly consistent and required for a range of focus to be assumed. This range constitutes for the standard deviation seen in the results obtained and as a result of variation generated by the human eye. This range was initially 40 μm but through extended testing was reduced to approximately 20 μm.

Calculation of indentation was accomplished with the following equation where M_s is the measured gel surface vertical position, R is the known radius value of the ball, and M_c is the

measured height value of the centroid. A detailed image of these measurement positions is provided in Figure 9.

Indentation (d) = R – (M_c – M_s)   **Equation 9**
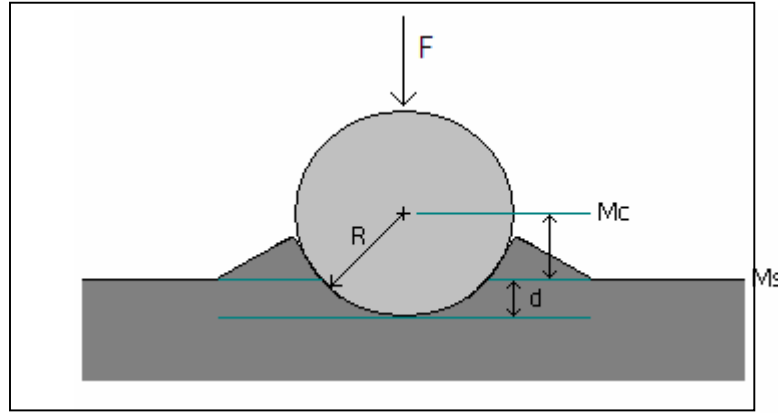
Figure 9: Schematic view illustrating required measurements needed for calculation of the final indentation depth. This indentation value is required for eventual calculation of the Young's modulus.

The values obtained through Equation 9 were used to calculate the Young's modulus using Equation 1 as explained earlier in this paper.

5.3. Atomic Force Microscopy

The difference in preparing the polyacrylamide gel for Atomic Force Microscopy from the protocol given by Dr. Yu-Li Wang (Appendix 10.2) is that a glass cover-slip is required to mount the gel. The glass is activated by applying different coats, described in the protocol. The relative size of the AFM scan head prohibits the use of a Petri dish for containing the polyacrylamide gel during testing. An activated cover-slip is roughly three centimeters in diameter and used as a mounting platform for the samples. Unlike a Petri dish, these activated slips are flat and will not interfere with the wet-cell or the scan head on the AFM. The cover-slips themselves still require activation, which correlates with steps one through six in Dr. Wang's protocol. Once the particular concentration of polyacrylamide is made, roughly 200 mL is placed on the activated cover-slip using a transfer pipette. A smaller circular or square cover-slip is placed over the gel

during polymerization to flatten the gel and give it a uniform thickness. The polyacrylamide gel polymerizes with the activated side of the cover-slip down, easing removal after gel polymerization.

To obtain accurate data with the AFM the cantilever and tip must be well defined. Without knowing the cantilever's stiffness or the tip's radius, the Young's modulus cannot be calculated using the principles of Hertzian mechanics. For each probe, the stiffness and size properties must be measured. It is known that the manufacturer's data on the probe is not always accurate and the results rely heavily on these characteristics.

First, the resonant frequency will be measured by driving the cantilever in non-contact mode. While in non-contact mode the probe will be oscillated above the sample over a range of frequencies. The response of the laser will show displacement peaks as the frequencies vary. The resonance frequency (v_k) will be the maximum measured displacement peak. This value is later used to derive the stiffness of the cantilever.

According to research by Dr. Burnham, one of the most efficient ways to obtain a spring constant of a cantilever is a method known as thermal calibration. A comparison of various calibration techniques that all gave results within 17% of manufacturer's nominal stiffness by researcher's yielded thermal calibration was easier to use and had a wide range of applicability (Burnham et al, 2003).   Thermal calibration stems from the equipartition theorem and utilizes the correlation between temperature and energy to measure the characteristics of the cantilever. According to statistical physics temperature will invoke a slight oscillation in an object, in this case the AFM cantilever, which is described in Equation 10. The Quality Factor (Q) and the mean displacement at resonance $< x^2(v_k) >$ are fit parameters of the following equation:

$$k = \frac{0.97Q}{\pi} * \frac{k_b T}{<x^2(V_k)>} * \frac{\Delta\omega}{v_k},$$ **Equation 10**

where T is the ambient temperature, k the stiffness, k_b the Boltzmann constant, and

$\Delta\omega$ frequency resolution (Thoreson, 2006). The equipartition theorem states that for every

dimension of freedom given, the kinetic energy is represented as (½)k_bT. Therefore, Equation 10

assumes that the only displacement is along the z-direction (vertical).

To obtain the stiffness value this way the cantilever must be placed stationary and not in

contact with any surface so only the temperature is affecting its displacement. Thermal

equilibrium will cause the cantilever will undergo a slight oscillation. This motion is read with

an oscilloscope and the response is used to solve Equation 10 for k.

Once the thermal spring constant of the cantilever is determined, the tip radius can easily

be calculated by using tip imaging. This research could have used both conical and spherical tip

shapes, each with a radius of roughly 30 µm. Conical tips behave like a spherical tip up to a

certain indentation depth, which gives the necessity of knowing the conical's radius as well as

shown in Figure 2. The tip radius is determined by running the tip over a step function grating

and taking a topographic image. In conjunction with a known step height, this topographic

image can be used to find a measurement which is used to calculate the open half angle utilizing

Pythagorean's Theorem. The grating has steps with known depths and when the tip is moved

over them, the resulting image can be evaluated to yield the tip's radius using SPMLab software.

For this particular experiment, conical tips were used on the cantilevers because they were

readily available for the csc12 series from MikroMasch. These cantilevers were chosen because

they have an aluminum coating on the backside which made it easier to align the laser on the tip

especially through a liquid medium. In addition, the csc12 series are manufactured with six

cantilevers per chip, cutting the overall cost of the project. The particular grating which was used in this process was a silicon grating called TGZ03 that has a known step height of 500 +/- 1.5 nanometers.
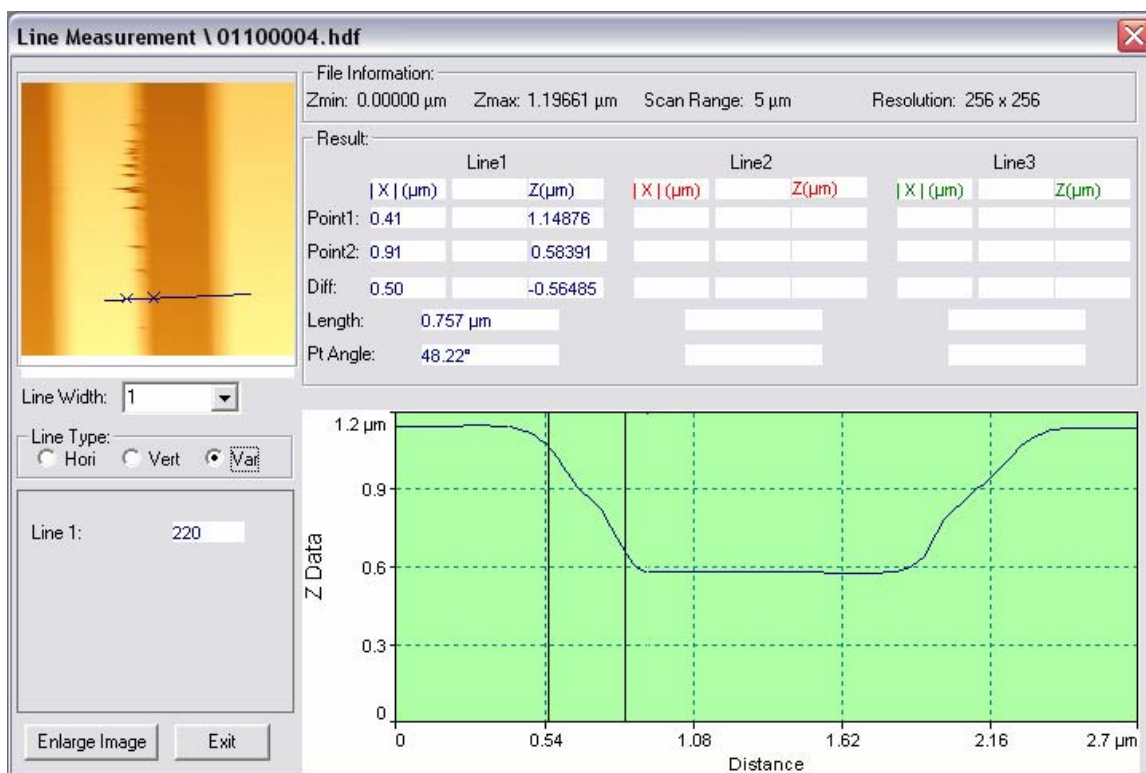
Figure 10: Tip Imaging using SPMlab Program: The trapezoidal shape is broken down and measured by highlighting the displacement of interest.

The tip is shown in Figure 10 to yield an almost trapezoidal response from the TGZ03 step function grating. The diagonal of each trapezoid correlates to the shape of the conical tip as it moves into the grating's "well." From this data the open half angle is calculated as shown in Figure 10.

After the probe characterization, the polyacrylamide gel could be tested. The gels were tested in a liquid medium, using the "wet-cell" attachment, because the material's properties are altered in the dehydration state. The cantilever was placed on the far side of a translucent material in which the laser shined through. Distilled water is slowly added by means of a

syringe, immersing only the cantilever. The other components of the AFM, such as the

photodiode, must stay dry.

As the cantilever is lowered onto the sample its deflection is measured by reflecting a

laser off the tip. The laser's deflection is measured using a photodiode which measures the

change in voltages. These voltages are translated into displacements and forces using a

computer. The forces and displacements are then plotted on what is called a force curve.

The goal of the analyzing the force curve of polyacrylamide gels is to determine the

Young's modulus (E). To calculate the Young's modulus, the raw AFM data F_∂ is compared

with the Hertzian model of the tip (cone F_c or sphere F_s) to minimize the least-square error

between them. The Hertzian model of the tip used is discussed in Section 2.2 of this report. The

least square error equation to be minimized is given with indentation depth ∂ as:

$$\Phi = \sum_{i=1}^{n} (F_\partial - F_{(sorc)})^2.$$

<div align="right">**Equation 11**</div>

The force offset ($P_{intercept}$) is calculated by taking the log of the raw data and "c" for

conical tips, described in the Hertzian mechanics background section, then subtracting conical

Hertizian model from the raw data. This offset is what makes it possible to determine the

Young's modulus. Taking the force offset and substituting into,

$$\log(k) - \log[\frac{E}{(1-v^2)} * \frac{2\tan\theta}{\pi}] = P_{intercept}$$

<div align="right">**Equation 12**</div>

and

$$\frac{k}{10^{Pintercept}} = \frac{E}{(1-v^2)} * \frac{2\tan\theta}{\pi}.$$

<div align="right">**Equation 13**</div>

The previous equation can then be rearranged to determine the Young's modulus:

$$E = \frac{\pi}{2} * \frac{(1-\nu^2)}{\tan\theta} * \frac{k}{10P_{\mathrm{int\,ercept}}} \quad (nN/nm^2 = \mathbf{GPa}),$$ **Equation 14**

The above calculations are performed using a Microsoft Excel spreadsheet (Frey et al, 2005) designed by Professor Nancy Burnham and Margo Frey. A log plot is generated by inputting the raw force curve data into the program and defining the necessary variables. This log plot shows the raw force curve data, along with the Hertzian models of both spherical and conical indenters. Initially, the raw data plot will not be aligned with either of the modeled plots. It is necessary for the program to align the raw data with the Hertzian model plots after minimizing the least square error shown above. The path of the raw data signifies how the tip actually affects the surface as either a conical indenter, spherical indenter or both. For example, when the raw data overlays the line which represents the conical Hertzian model, the tip behaves in a conical manner. Figure 11 shows the log plot of the raw data in initially following the spherical model, but eventually changing to the path of the conical model. This is due to the fact that conical indenters are never infinitesimally sharp, they will always have a rounded tip that follows that of a spherical indenter until a certain indentation depth is achieved. After completing the log plot, the Microsoft Excel program will calculate the Young's modulus automatically using Equation 14.
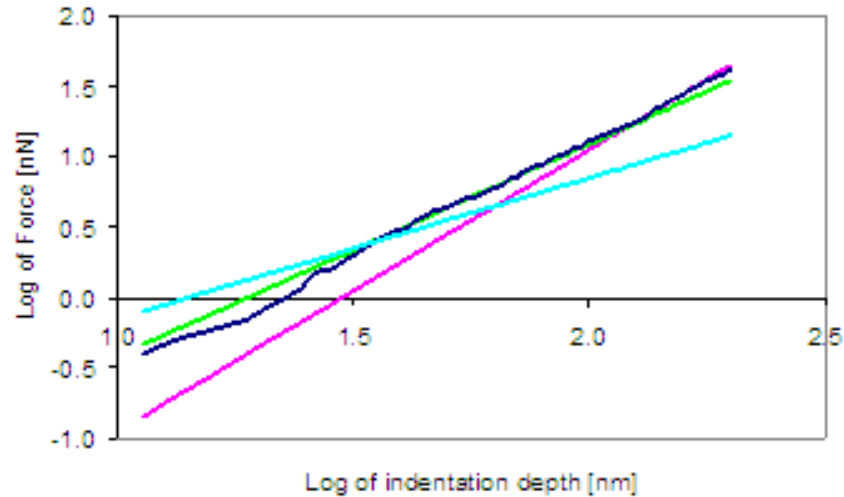
Figure 11: Log/Log Plot: The dark blue line is the raw data from the AFM measurement, light blue is the punch, green is the Hertzian sphere model and the pink is the Hertzian cone model.

5.4. Uniaxial Tensile Testing

A biaxial device was used for the uniaxial tensile test in this research project. The device was modified into a uniaxial tensile testing device by utilizing only one of the two available axes. The device was built by an MQP group in the 2004-2005 academic year for the biomedical engineering department at WPI. It is equipped with a high speed camera, stepper motors, and force transducers and a labVIEW program was used to control, and collect data. For more information on the device assembly and specifications, please refer to the MQP report of the device. This device is located in Dr. Billiar's Biomechanics Lab in Salisbury Laboratory.

Figure 12: A biaxial device is used to perform experiments by utilizing one of the two axes. A LabVIEW program was modified to perform a uniaxial tensile test. The video camera was used to track marker positions on the sample. The lamp was used to increase the contrast between the markers and the background. The stepper motors were used to provide displacements and the force transducers were used for force measurements.
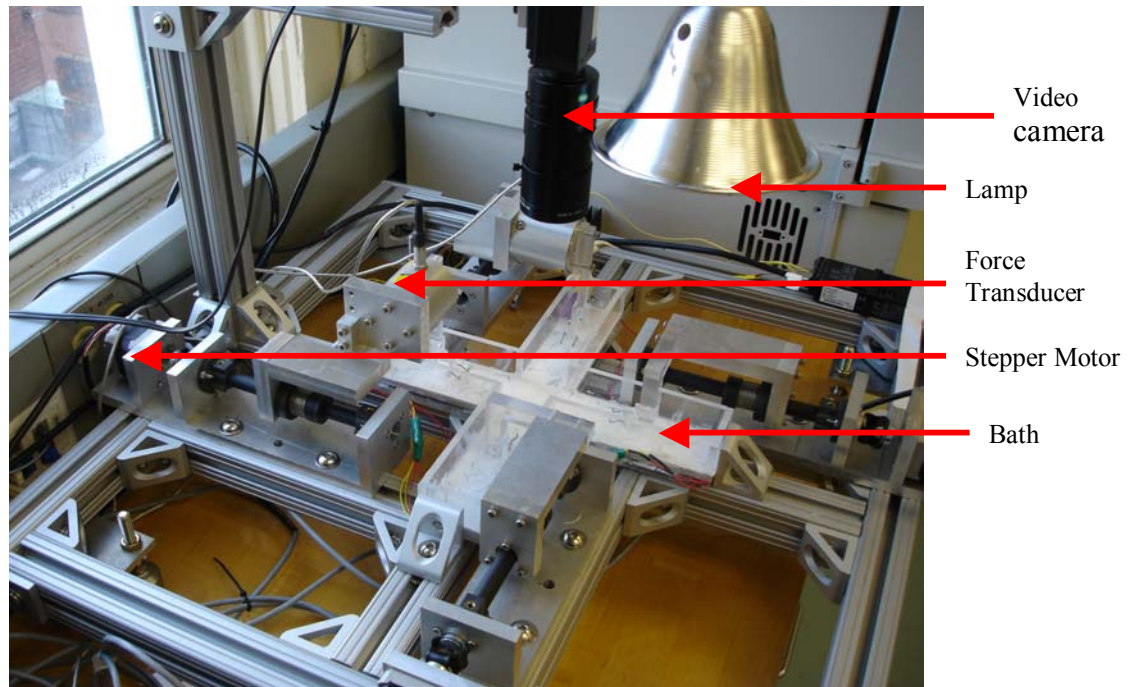
Fish hooks were originally designed on the biaxial device to pull the specimen apart. However, these hooks could not be used as grips to pull the polyacrylamide gel because very high local stresses were created on the gel, causing them to rip. Any direct attachment methods to the gel were unsuccessful. Therefore, the gripping method was modified by embedding Velcro inside the gel. This process was done by polymerizing the Velcro together with the polyacrylamide solution in the glass chamber. After the agarose gel had solidified, Velcro was cut into strips of 10 mm x 70 mm and placed vertically inside the chamber.

A modified version of Dr. Wang's polyacrylamide gel protocol, found in Appendix 10.2, was used to make various concentrations of the gel. After the chamber was disassembled, the sheet of gel was cut into strips of 7 mm in width. Figure 13 represents a schematic of the polyacrylamide sample prior to uniaxial tensile testing.
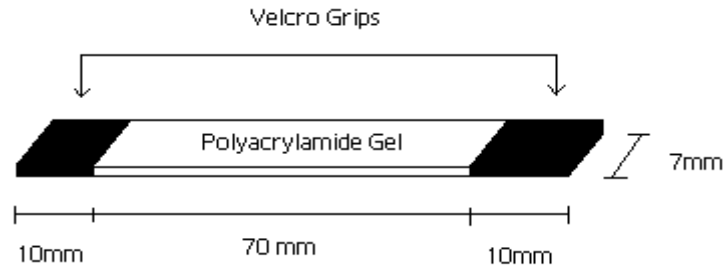
Figure 13: Polyacrylamide sample with Velcro embedded at each end. Velcro allows the gel to be pulled in the experiments without ripping.

To attach the gel sample to the device, another set of Velcro pieces was utilized. This method was used to avoid drilling holes directly to the Velcro grips of the sample. Preliminary experiments found that drilling holes directly to the sample was difficult and could decrease grip strength at the Velcro-gel interface. The improved method allowed the gel to be attached to the device easily which reduces the risks of compromising the grip strength before the test begins. Using an external Velcro attachment avoids jeopardizing the Velcro-gel interface strength before the test. These two extra pieces of Velcro were cut into size 10 mm x 15 mm. Two holes were drilled at one end used to attach to the device, and the other end of the Velcro was used to attach to the sample. Figure 14 is a schematic for the extra Velcro piece used as the means for attachment between the sample and the device.
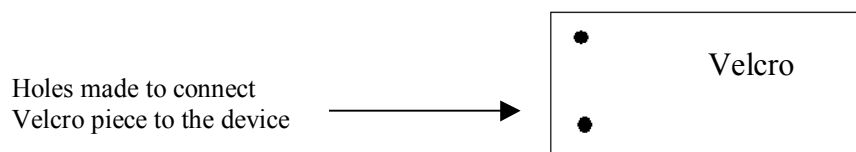
Figure 14: Two extra Velcro pieces with holes were used to ease the attachment of the sample to the device. This method eliminated any drilling to the sample directly, which reduced compromising the gripping capability.

Figure 15 shows a correctly loaded sample ready to be tested. The schematic illustrates how the gel sample should be attached to the device and the location of the sample in relation to the Velcro attaching grips.
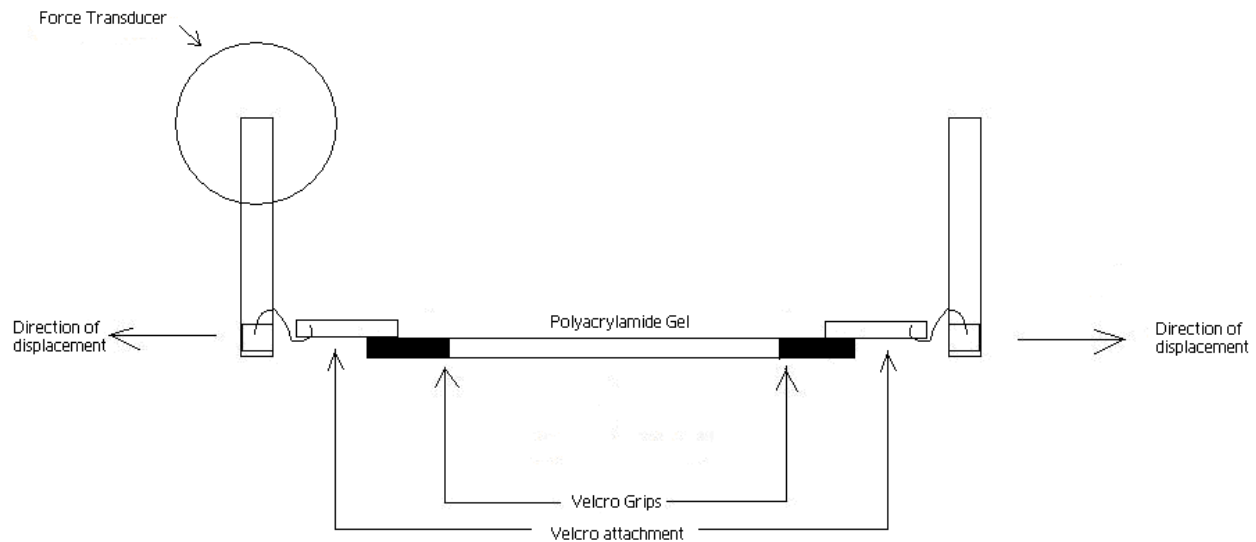
Figure 15: A correct loading position for the sample is shown. The sample is submerged under PBS solution to prevent friction from hindering the results.

Once the sample was placed in its ready position, four black dots were marked on the surface of the gel using a permanent marker. The bath was filled with PBS solution up to the surface of the gel to eliminate the effects of friction forces and to prevent dehydration of the gel. The LabVIEW program known as, 'INITIALIZE COMPLETE', was used to center the sample through a video camera. The camera has the ability to track marker positions using the color contrast between the dark markers and the light background. A lamp was used to enhance the contrasting colors. The viewing screen was set on the program such that only the four markers were displayed in red. The image on the front panel should look similar to Figure 16 below. Detailed instructions for running this program can be found in Appendix 10.5.
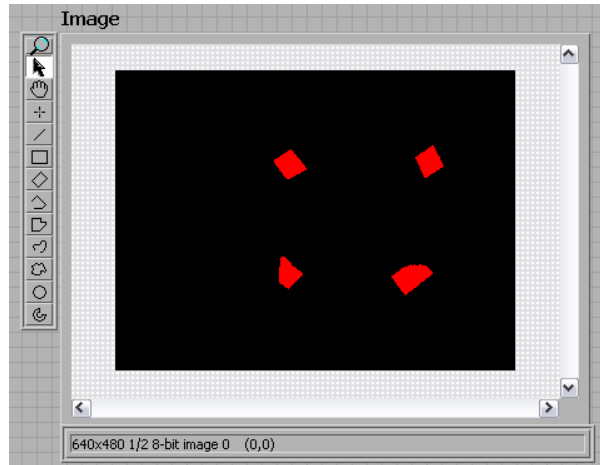
Figure 16: A camera's view in INITIALIZE COMPLETE.vi program is shown in this figure. Four marker positions are centered and showed as red dots

Another labVIEW program known as 'COMPLETE WITH UNIAXIAL.vi' was opened. This program runs the uniaxial tensile test and collects the data. Sample dimensions, strain rate, percent strain, and the number of cycles were inputted in the required fields. Please refer to Appendix 8.5 for detailed instructions for inputting required dimensions before running the test.

The same programs were used for the stress relaxation test. The tab option in the 'COMPLETE WITH UNIAXIAL.vi' allows the user to select the types of test to perform. A more detailed description for running this test can be found in Appendix 10.5.

The results from each test were recorded on a spreadsheet. Every time the camera recorded an image of the marker positions, data points were recorded. The engineering strains and the stress were calculated by the program. The Young's modulus was found by obtaining the slope of the stress-strain curve and the slope was calculated using a linear trend line from the most linear section of the curve. The equation for the Young's modulus, *E*, is given as;

$$E = \frac{\sigma}{\varepsilon}.$$ **Equation 15**

45

It was necessary to perform a limit test to determine the number of cycles and percent axial strain necessary for gathering the average stiffness value. A sample was tested to note its variation under multiple tensile cycles and over a large strain range. The results from each cycle obtained from ten consecutive cycles stretched to 25% were plotted on the stress vs. strain curve. A total of six samples were tested for each concentration at three different strain rates; 0.01, 0.05, 0.1.

The engineering strains calculated by the program were used to find the Poisson's ratio, which represents the physical deformation of the sample under uniaxial tension loading. The equation for Poisson's ratio is,

$$\nu = -\frac{lateral\ strain}{axial\ strain}\ .$$
<div align="right">**Equation 16**</div>

The linear region that was used to calculate the stiffness value for each stress-strain curve was also used to determine the Poisson's ratio. In the end, the Young's modulus obtained from each sample was analyzed using SPSS statistical program to determine whether the variation of the sample and strain rate affected the Young's modulus that was acquired.

5.5. Rheology

As previously mentioned, it was necessary to change the dimensions of the gel from the given protocol for rheometry testing. Typically, the rheological measuring systems which were used in this research required a sample that is at least 1 mm in thickness, while the gels in Dr. Wang's protocol are only 70 μm in thickness. In this research, the rheological measurements that are necessary for quantifying the mechanical properties of polyacrylamide gels were taken with a Bohlin Gemini controlled stress rheometer from Malvern Instruments, seen in Figure 17.
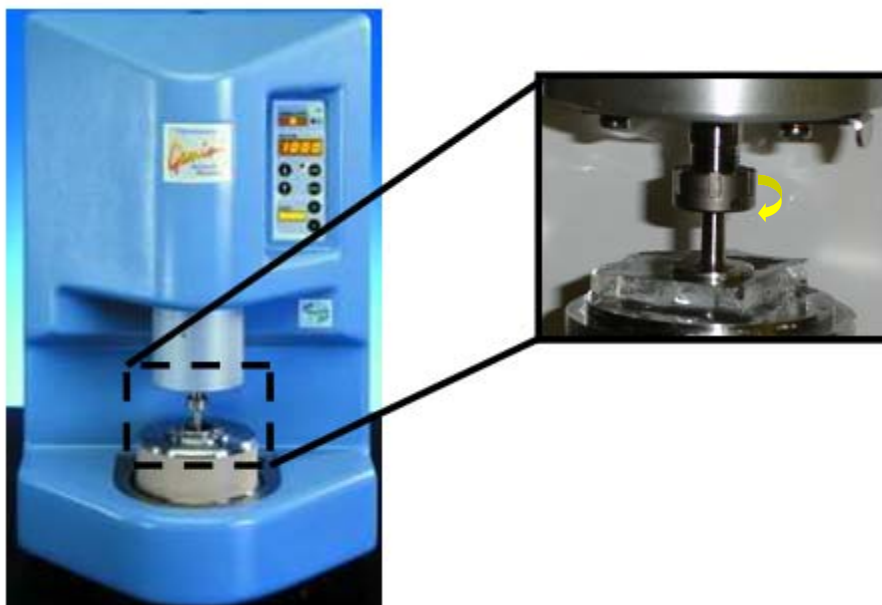
Figure 17: Bohlin Gemini rheometer with the 20mm parallel plate measuring system with a 6310 μm thick polyacrylamide gel sample.

There are a variety of measuring systems which can be used in rheometry testing. The three systems that are best suited for polyacrylamide gel testing are smooth parallel plates, serrated parallel plates, and a titanium vane system. Figure 18 shows a schematic drawing of each system. The smooth parallel plate method has the advantage of provoking very little, if any, damage to the polyacrylamide gel. However, there is the possibility of gel slipping within the two plates, significantly lowering the modulus measurements. To prevent slipping, a serrated parallel plate system with 600 μm teeth was utilized in place of the smooth parallel plate system. However, there is the possibility of structural gel damage when the teeth are forced into the gel. The gel sample must be prefabricated and be at least 1 mm thick for the smooth parallel plate system and 2 mm thick for the serrated parallel plate system. Unlike, the two plated systems, the titanium vane method requires the gel to be solidified within the tube. Typically, a liquid sample size of 5 ml is necessary to completely fill the cup. The interior unit is inserted into the liquid and the gel solidifies around the structure. This is perhaps the best method for testing

polyacrylamide gels because there is a low possibility of slippage and the "gelling process" can be observed by applying a low strain to the central unit.
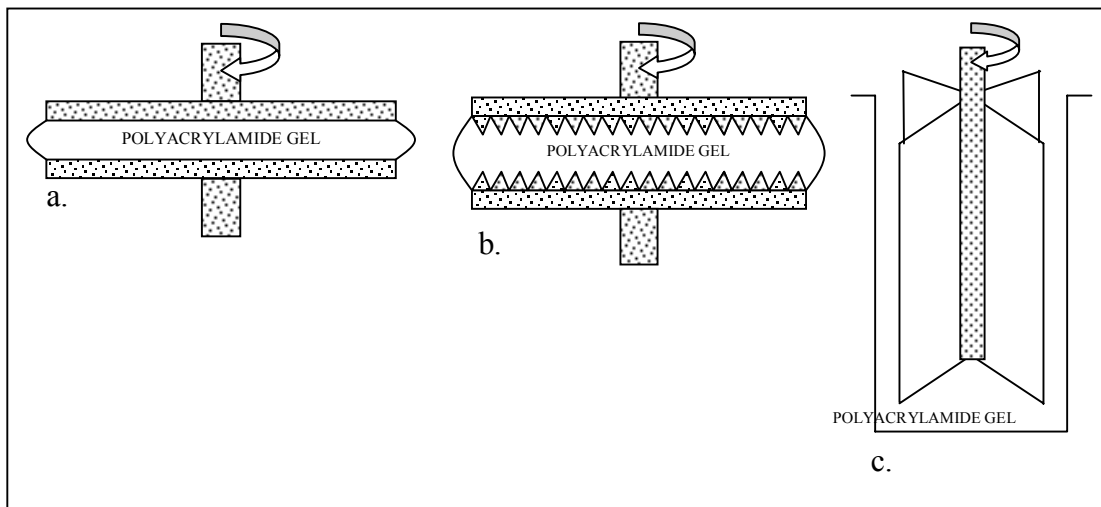
Figure 18: Schematic of, (a) the smooth parallel plate rheological system (b) the serrated parallel plate system (c) the titanium vane system

As mentioned above, the parallel plate measuring system involves a rotating upper plate and a stationary lower plate with the polyacrylamide sample contained between the two. The 20 mm smooth parallel plate system, seen in Figure 17 was chosen as the most effective and accurate for measuring the viscoelastic properties of polyacrylamide gels. The gap varies slightly from sample to sample and is controlled by the rheometer's autotension function. The autotension function of the rheometer controls the upward or downward applied force on the top plate of the smooth parallel plate measuring system. It is necessary to apply a constant compressive force to the polyacrylamide gel to prevent the sample from slipping. One disadvantage with the parallel plate measuring system is that the shear rate is not constant with radial position; it ranges from zero at the center to a maximal value at the outside radius of the upper plate. As can be seen in the calculations section, the rheometer software takes an average value of shear rate. The shear rate proves to be inversely proportional to the gap size.

As recommended by Ferry, to ensure linear viscoelastic properties of the sample, it is necessary to perform testing at more than one torque, angular displacement, or strain to show that creep compliance is independent of stress and strain (Ferry, 1980). The rheometer was used to test polyacrylamide gels in three distinct methods: time sweep, frequency sweep, and strain sweep. A time sweep involved a constant applied frequency over a time range to measure the stability of the polyacrylamide gels. For the samples in this research, a constant frequency of 1 Hz and a constant strain of 5% were applied to the polyacrylamide gel samples. To demonstrate that the polyacrylamide gel's properties did not change significantly with time, the test was run for five minutes.

Following the time sweep was a frequency sweep which involved an applied low strain over a range of frequencies determining the gel's viscoelastic properties as a function of frequency. The schematic in Figure 19 shows the steadily increasing frequency over time. The rheometer measures the phase shift between the stress and the strain and the complex modulus during the sampling period, while the other viscoelastic parameters are calculated. It is important to note that it is only necessary to quantify the properties of polyacrylamide gels in frequencies that cells experience in a physiological environment, between the range of 0.1-10 Hz (Huang et al., 2004). For example, the response of polyacrylamide gels to a frequency of 50 Hz is irrelevant to this study.
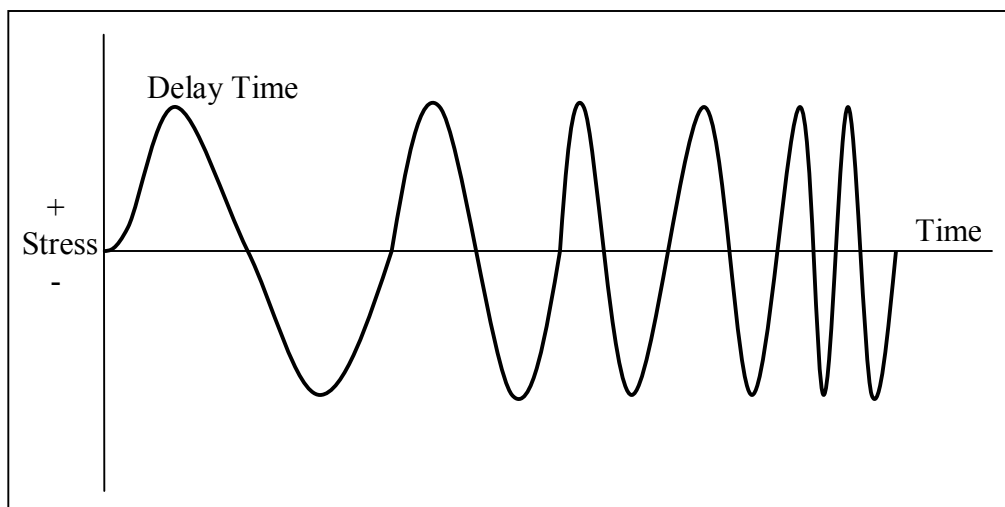
Figure 19: A frequency sweep involves a small delay period with a consistent low frequency of 0.1 Hz followed by an increasing frequency range to an eventual 50 Hz.

The final test which was conducted on the polyacrylamide gel samples was a strain sweep. This method involved a constant frequency over a range of increasing strain and was used to determine the region of linear viscoelastic response of a polyacrylamide sample. The linear viscoelastic region of a sample is a function of strain. This testing method also helped in determining whether or not the gel was slipping or breaking down in structure. These tests were run at a constant frequency of 1 Hz and typically over a range of stress from 0.1-300 Pa. The schematic in Figure 20 shows the increasing stress over time.
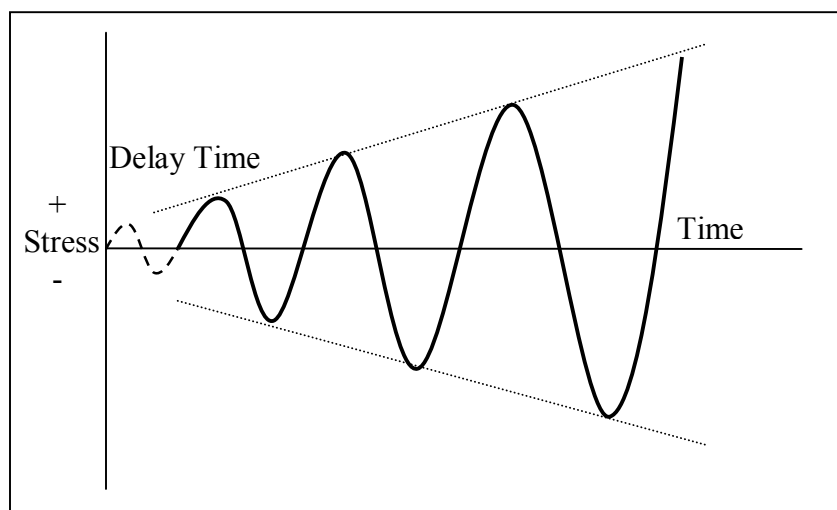
Figure 20: A strain sweep has a delay period where 1 Pa is applied to the sample for a short period of time followed by a sweep up to a final stress of 300 Pa.

In addition to varying the testing mode, it is important to note that rheometers have the capability of controlling sample temperature with a Peltier device. Another interesting component which could have been researched during this project is the effect of temperature on the viscoelastic properties of the polyacrylamide gels. However, because the measured values were eventually compared to the results of the other three tests which are all performed at room temperature (25°C), all rheometry tests were also run at this temperature.

The following equations display how a rheometer converts torque and angular velocity into terms of shear stress and shear rates for the parallel plate measuring system. For demonstration purposes, the shear stress form factor will be C1, and the shear rate factor will be C2:

$$C1 = \frac{3}{2\pi r^3} \, , \qquad\qquad C2 = \frac{3r}{4} \, . \qquad\qquad \textbf{Equation 17}$$

Where the shear stress is equivalent to (C1 x Torque), the shear rate is equivalent to (C2 x angular velocity / gap), the viscosity is equal to (Shear Stress / Shear Rate), and the r value is ¾ the radius of the top plate (Bohlin Instruments Ltd, 2004).

The equations mentioned above assume that the sample under deformation is Newtonian; a fluid which has a viscosity independent of the forces which act upon it. The equations do not consider the effects of surface tension on the mechanical measurements. It is therefore essential to keep samples hydrated during testing in an attempt to eliminate surface tension.

6. Experimental Results

The following section summarizes the individual results obtained in each of the four techniques.

6.1. Ball Indentation

Through the experimental procedures, two separate sets of data were generated using two individually produced samples. These complete data sets are presented in Appendix 10.3 along with the corresponding graph used to show the similarity between the tests and trend caused by the independent variable (ball geometry). From these data sets, an average data set was compiled. Below are the results tabulated from the 5/0.025% polyacrylamide gel tests. Of particular interest are the percent variation values that represent the data variation among all data points for the indicated ball diameter on the 5/0.025% gel. Shown in the following table are the standard deviation values resulting from the test method. It is important to note that these values are corrected for human error in order to produce greater consistency of the results. A value of approximately 40 µm was established as the human error through side experiments. This value had much less of an impact on the softer gel concentration as the indentation distances were much greater.

Summarized Results for 5/0.025% Polyacrylamide			
Ball Diameter (mm)	E (Kpa)	STD	% Variation of Tests
0.64	5.41	0.87	16.11
1	7.40	0.83	11.17
2	9.73	0.08	0.87

Table 3: Ball Indentation Results for the 5/0.025% Gel summarized from two separate tests performed on separately prepared gels. A general trend is displayed showing an increase in stiffness with an increase in ball diameter.

Interpretation of the mean values of elastic modulus for the 5/0.025% gel has been represented as an X-Y scatter plot. The main goal in presenting the results in this fashion is to allow both for visual analysis and to formulate a representative equation for computed elastic modulus (y) with respect to the diameter of ball used for testing (x). The plotted data in Figure 21 shows a clear representation of a logarithmic increase of elastic modulus with increased ball diameter. Representative of this trend line generated is the following equation.

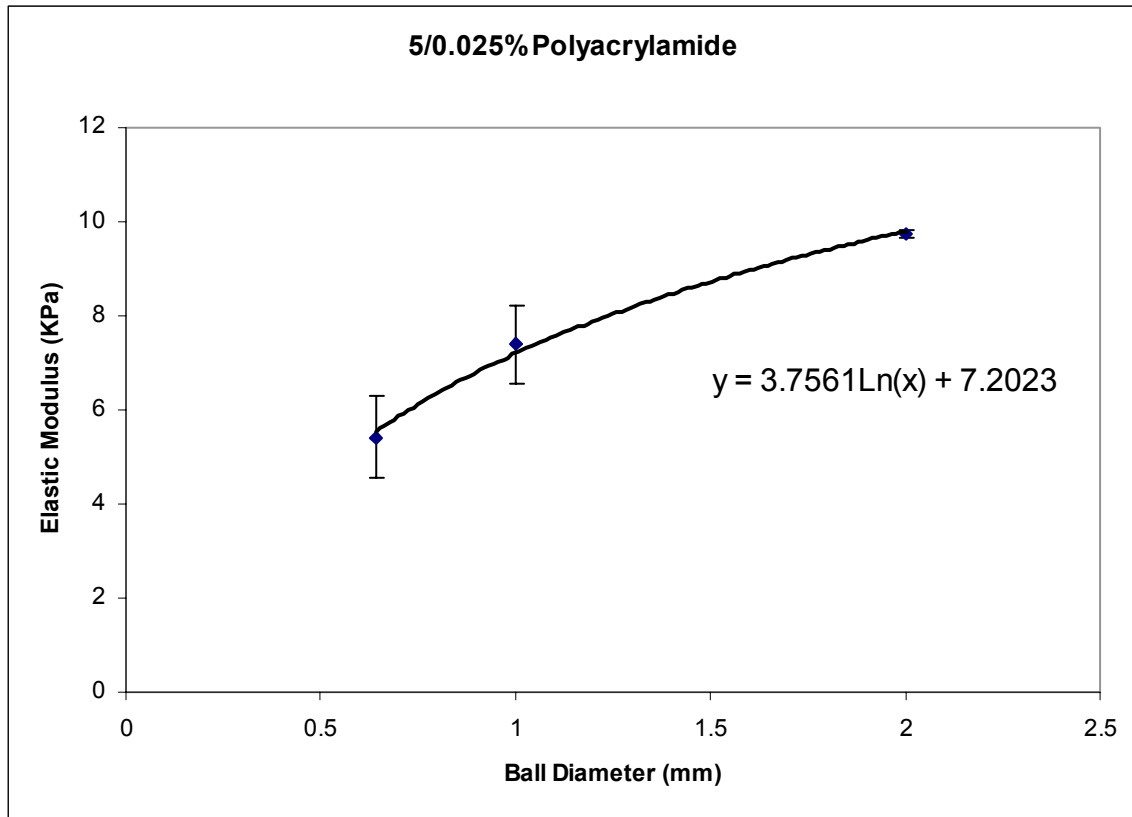$$y = 3.7561 Ln(x) + 7.2023.$$ **Equation 18**

Figure 21: Plotted Results for 5/0.025% Gel display the relationship described in Table 1. The observed trend has been fit with a logarithmic curve solely because this provides the best fit of the data.

In order to verify that the mean values generated are significantly different between the balls sizes used, SPSS software was used to perform a One Way ANOVA from both sets of data collected.

The significance value, of $p < 0.05$, indicates that there is adequate evidence of variation between the generated Young's modulus and the geometry of the ball used for indentation testing. The representative table can be found in Appendix 10.3.

Mimicking the data analysis methods used for the 5/0.025% gel, a representative table was generated for the 8/0.08% gel. The representative data used for the generation of Table 4 is presented in Appendix 10.3. Corresponding to this data set is the graph in Appendix 10.3, which is used to show the similarities between the tests and trend among the independent variable. Most importantly, the table below provides the calculated percent variation among all data points of a given ball on the 8/0.08% gel. Although the computed standard deviation was reduced in accounting for the range of human error, the determined percent variation values would typically be much greater for such a testing technique. The reduced indentation depths from the softer gel lead to a much greater percent variation in the stiff gel results. This is clearly shown by the ability of each gels result to fit a logarithmic trend line. While this is not the expected result, the inability of the stiffer gels results to fit a trend line is indicative of the increased difficulty of measuring indentation on stiffer gels.

Summarized Results for 8/0.08% Polyacrylamide			
Ball Diameter (mm)	E (Kpa)	STD	% Variation of Tests
0.64	12.38	1.33	10.70
1	43.78	8.90	20.33
2	62.15	1.51	2.43

Table 4: Ball indentation results for the 8/0.08% gel averaged from two separate tests. The percent variation of tests is representative of the variation between those two separate tests. Similar to the results from the softer gel, the 2 mm ball showed the most consistency.

Representation of these results is presented in the following X-Y scatter plot. Represented are the mean elastic modulus values with respect to ball diameter used for indentation measures. Error bars have been included to represent the standard deviation values of the data. Indicated by these values is the relative potential for inconsistency among data collected. Compared to the results from the 5/0.025% gel, the 2 mm ball shows consistent precision while the 1 mm ball and 0.64 mm ball shows a low value of inconsistency.

A representative trend line of the data is presented in Figure 22 shows a logarithmic increase of elastic modulus values with increased ball diameter. From this trend the dependant variable (y = elastic modulus) can be determined relative to the independent variable (x = ball diameter).

8/0.08% Polyacrylamide

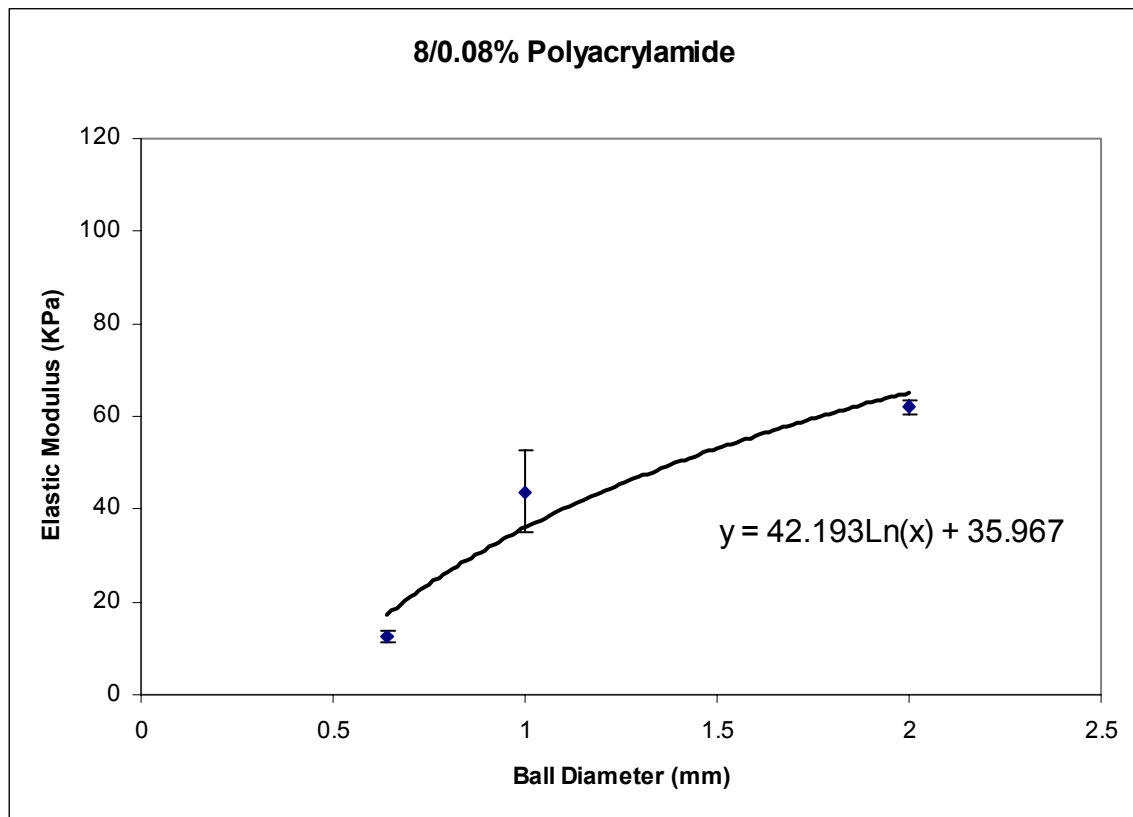$y = 42.193\mathrm{Ln}(x) + 35.967$

Figure 22: Plotted Results for 8/0.08% Gel. There is a clear representation of ball diameter to observed stiffness shown in this data. Similar to the softer gel, this is best represented with a logarithmic trend line y=42.193Ln(x)+35.967.

Further supporting the hypothesis that ball geometry plays a role in the determined elastic modulus value, the significance value of $p < 0.05$ computed from the 8/0.08% polyacrylamide data agrees with the 5/0.025% result. The representative table can be found in Appendix 8.3. This agreement further confirms the hypothesis that computed elasticity by ball indentation technique is relative to the geometry of the ball used for indentation.

Although the generated stiffness values may not be very accurate, the technique does allow for the evaluation of localized verse non-localized properties. Specifically speaking, when the results from the 0.64 mm ball are compared to those of the 2 mm ball, a clear disparity is recognized. AFM will provide further insight into the localized characteristics with a higher reliability due to less potential for human error and greater similarity to actual cells in a physiological environment.

6.2. Atomic Force Microscopy

Following are the results obtained from Atomic Force Microscopy. Initially, the validating steps for determining the conical indenter's dimensions using tip imaging are presented, followed by the thermal calibration method for finding the conical indenter's stiffness. In the end, the force curves yielded consistent results for the stiffer concentration of polyacrylamide when compared to the results of the more compliant samples.

Figure 23 displays an image which was taken using the TGZ03 grating by MikroMasch. The upper left picture is the raw image collected by the AFM probe, while the bottom right image represents a three dimensional model of the image. To give a topographic view, the tip is moved parallel to the sample surface. This topographic view allows for the acquisition of the tip's characteristics.
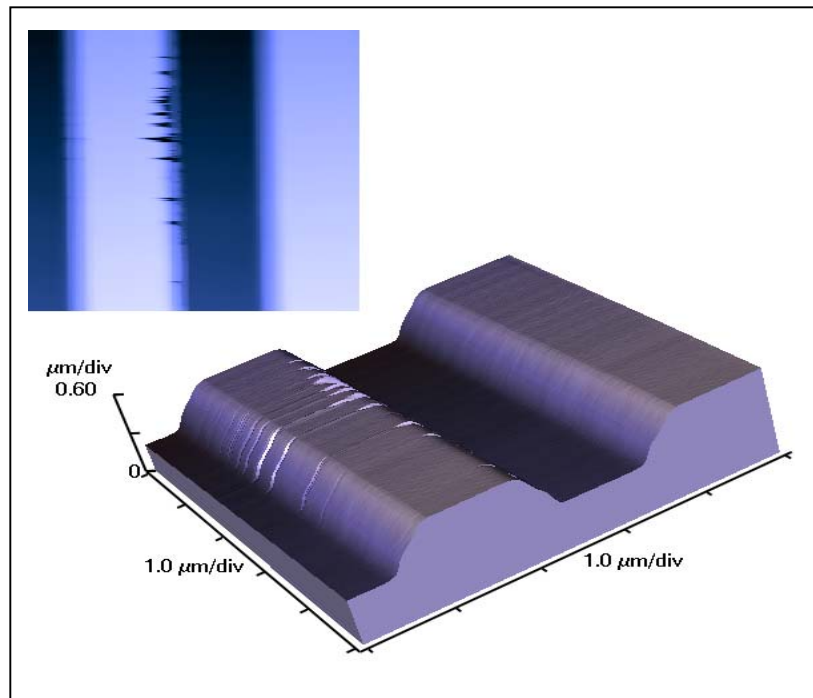
Figure 23: Tip Imaging Result: The trapezoidal shape is due to the dimensions of the conical indenter. Analyzing this yields the tip's open half angle.

Two different cantilevers were tested using this process, the E and B cantilevers shown in Figure 24. The E cantilever proved to be uncooperative because it provided force curves like the one shown in Figure 25. There is no useful data on this curve and cantilevers often broke. The B cantilever, however, was much stiffer and gave force curves which could be analyzed similar to the one in Figure 26.

Fig.1 SEM image of the shorter tipless cantilevers (A, B, C) on chip of the CSC12 series.

Fig.2 Silicon chip of the CSC12 series has 6 rectangular cantilevers. The thickness of the chip is 0.4 mm.

Specification of Cantilevers

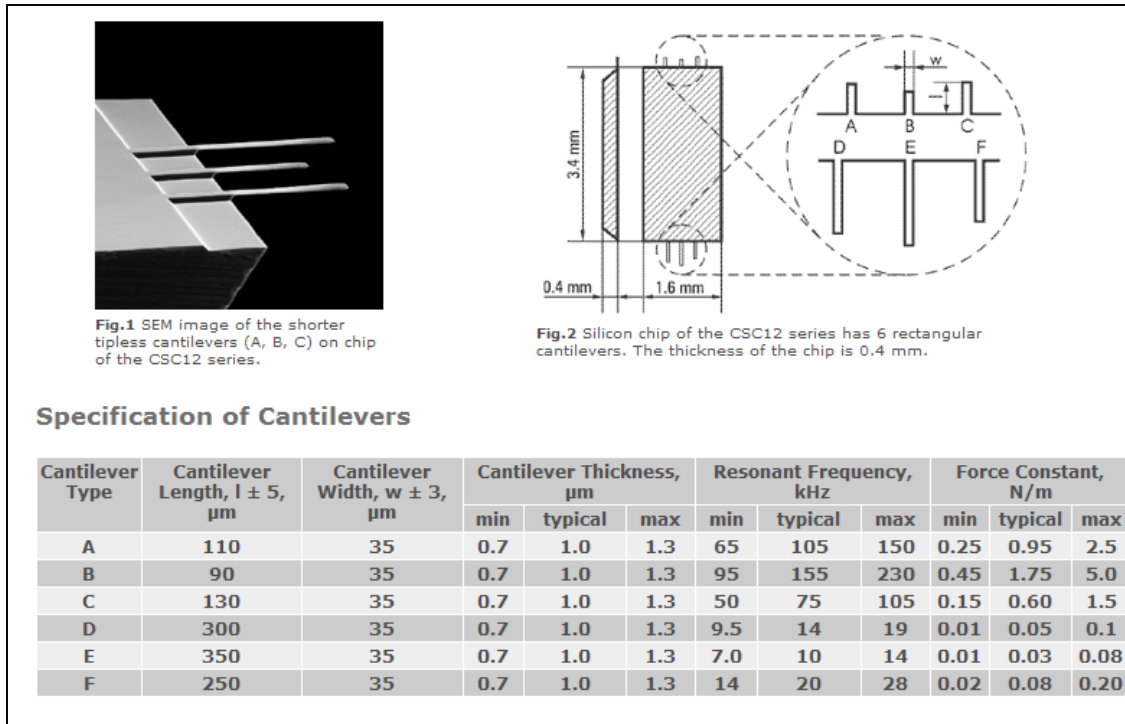| Cantilever Type	Cantilever Length, l ± 5, μm	Cantilever Width, w ± 3, μm	Cantilever Thickness, μm			Resonant Frequency, kHz			Force Constant, N/m		
			min	typical	max	min	typical	max	min	typical	max
A	110	35	0.7	1.0	1.3	65	105	150	0.25	0.95	2.5
B	90	35	0.7	1.0	1.3	95	155	230	0.45	1.75	5.0
C	130	35	0.7	1.0	1.3	50	75	105	0.15	0.60	1.5
D	300	35	0.7	1.0	1.3	9.5	14	19	0.01	0.05	0.1
E	350	35	0.7	1.0	1.3	7.0	10	14	0.01	0.03	0.08
F	250	35	0.7	1.0	1.3	14	20	28	0.02	0.08	0.20

Figure 24: MikroMasch al-bs probes: Specifications of cantilevers used in AFM research (Mikromasch, 2005).

Overall, the tip imaging gave consistent results with few artifacts in the images, shown as crevasses on the leftmost step in Figure 23. The majority of these artifacts are derived from a high gain (feedback loop) when the scan head tries to keep the tip at a constant force. The tip radius and open half angle are determined by importing the raw data into the SPMdata program and interpreting various sections of the image data. For example, in Figure 23 a cross-section of the step is taken, making it possible to measure the distance between the top and bottom horizontal surfaces. This distance translates into one of the "legs" of the tip. Using the knowledge that the TGZ03 step-function gratings have 500 ± 5 nm high steps, the open half angle can be calculated using trigonometry.

For the specific cantilever used in testing the 8%/0.08% and the 5%/0.05% concentrations of polyacrylamide gels the tip was measured to have a 45.2 ± 3.3 micron radius for the sphere at the end of the cone and an open half angle of approximately 38°. The obtained

force curves from the polyacrylamide gel samples can be found in Appendix 10.4. Overall, there

were two generalized forms of the curves acquired when testing these compliant samples.
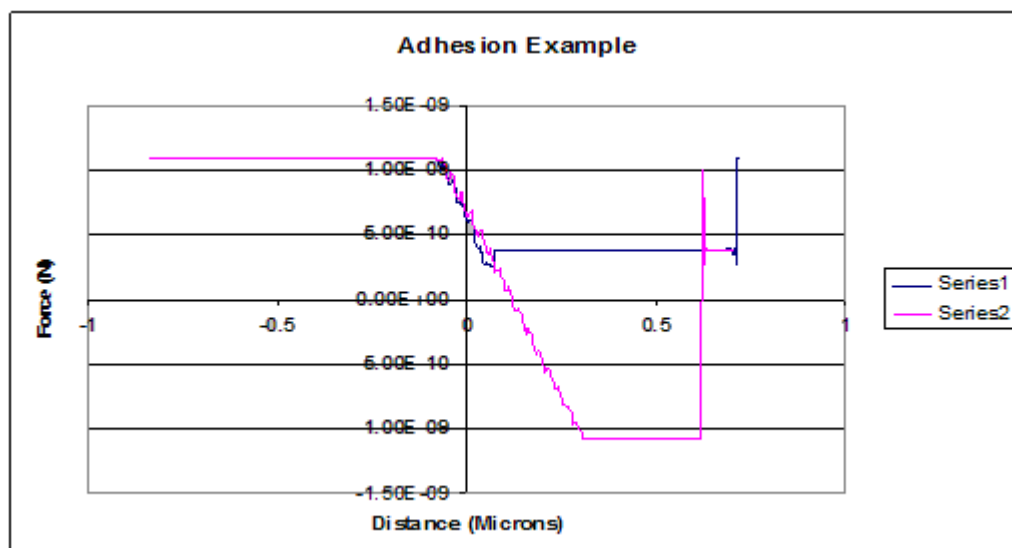
Figure 25: Example of Adhesion: The attractive forces applied to the probe are so great that they will bend the cantilever to a critical force where the cantilever will break or the bond between the tip and sample will, skewing any data obtained.

Figure 26: Workable Force Curve. These curves are usable for when the cantilever is in contact with the sample and does not show adhesion. The area of interest is shown at the bottom right hand corner of the above graph.

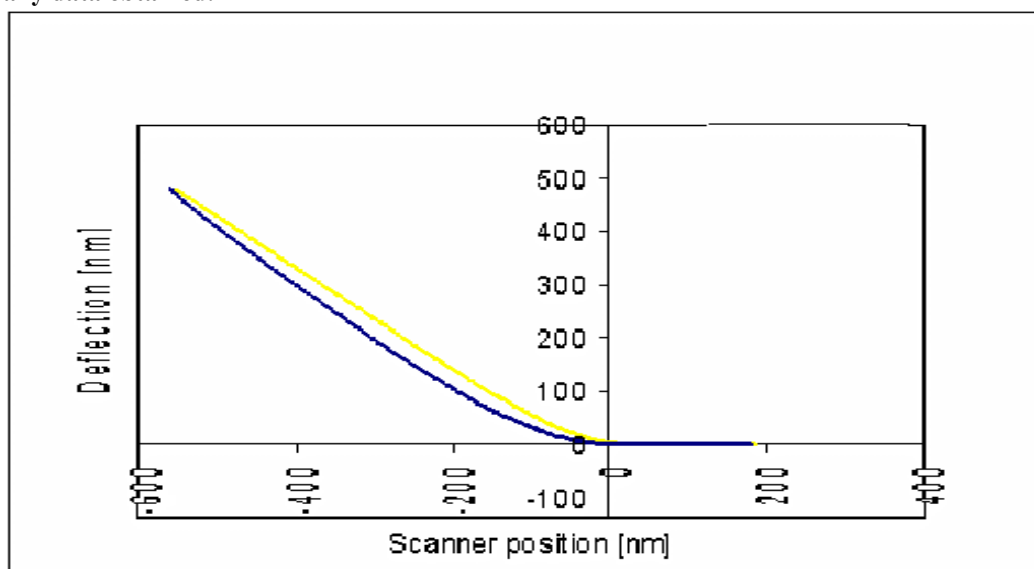To prevent testing a localized defect, both the 8%/0.08% and 5%/0.05% concentrations of polyacrylamide gel were tested twice in each location over four different locations. The data for each test was broken up into a text file with three values; deflection, scanner position and time. This data is the F_d discussed in the AFM Methodology.

The first kind of force curve shown in Figure 25 demonstrates adhesion. This phenomenon occurred during early testing of the 5%/0.025% concentration. The AFM probe was literally "grabbed" by the surface forces present on the sample as it is lowered. As the cantilever attempts to return to its normal position, the gel remains adhered to the tip until enough retraction force is applied to break the bond between the tip and sample or the cantilever.

The Young's modulus is calculated from the force curves similar to the ones found in Figure 26. The analytical results, as shown in Tables 5 and 6, were calculated using the Excel spreadsheet program mention in the AFM Methodology. The previous equations discussed in the AFM background and methodology are implemented into this spreadsheet which allows for relatively quick analysis of the data.

Round 1: 8%/0.08%			
Young's modulus (kPa)	Deviation from Mean (kPa)	Relative Uncertainty	Percent Deviation %
33.53	0.84	0.025	2.51
31.39	2.98	0.095	9.49
33.94	0.43	0.013	1.27
34.9	0.53	0.015	1.52
33.85	0.52	0.015	1.54
35.93	1.56	0.043	4.34
35.58	1.21	0.034	3.40
35.84	1.47	0.041	4.10
Mean 34.37			Standard Deviation 1.53

Round 2: 8%/0.08%			
Young's modulus (kPa)	Deviation from Mean (kPa)	Relative Uncertainty	Percent Deviation %
29.53	1.765	0.060	6.0
29.00	2.295	0.079	7.9
30.26	1.035	0.034	3.4
30.23	1.065	0.035	3.5
32.65	1.355	0.042	4.2
31.91	0.615	0.019	1.9
33.30	2.005	0.060	6.0
33.48	2.185	0.065	6.5
Mean 31.3			Standard Deviation 1.76

Table 5: Results from 8%/0.08% Bis/Acrylamide Concentration for AFM

Round 1: 5%/0.025%			
Young's Modulus	Deviation from Mean	Standard Deviation	Percent Deviation
(kPa)	(kPa)	(kPa)	%
4.63	0.17	0.04	3.67
4.62	0.18	0.04	3.9
4.75	0.05	0.01	1.05
4.99	0.19	0.04	3.81
4.85	0.04	0.01	0.82
5.13	0.32	0.06	6.24
Mean (kPa) 4.81			Standard Deviation (kPa) 0.2

Round 2: 5%/0.05%			
Young's modulus	Deviation from Mean	Standard Deviation	Percent Deviation
(kPa)	(kPa)	(kPa)	%
5.30	0.30	0.06	5.66
5.12	0.48	0.09	9.38
5.26	0.34	0.06	6.46
5.78	0.16	0.03	2.77
5.85	0.23	0.04	3.93
5.82	0.20	0.03	3.44
Mean (kPa) 5.62			Standard Deviation (kPa) 0.33

Table 6: Results from 5%/0.025% Bis/Acrylamide Concentration for AFM

When reviewing the data presented in Tables 5 and 6 the most noticeable trend is the fact that the gels appear to become stiffer as the test progresses. The test time for this technique is close to one hour; therefore, this "stiffening" effect is most likely due to the sample becoming dehydrated. Although the sample is in a liquid medium, the wet cell does not cover the entire sample during testing. The sample is exposed to open air where the gel is outside of the wet-cell. Another explanation of the values becoming stiffer over time includes the fact that the probe eventually breaks down. The constant cyclic motion in the z-direction fatigues the cantilever, changing its effective stiffness. For this reason, only eight tests total were performed on each sample. The results become dramatically skewed when more than eight tests are attempted.

Although AFM is a precise technique to implement when measuring localized areas of a sample, it could not determine the Poisson's ratio or the gel's bulk properties. To validate these results the group required pursued the two techniques of uniaxial tension testing and rheometry.

6.3. Uniaxial Tensile Testing

Multiple tension tests were performed to determine the elastic modulus, Poisson's ratio and stress relaxation behavior of polyacrylamide gel. Before the tension test began, the limit test was done to test the integrity of the Velcro grip at the maximum axial strain of 25%. The linear region of the resulting stress-strain curve was used to determine the slope. This region consistently occurred between 2-25% axial strain in each cycle, which led to the determination that the rest of the experiments would be performed up to 10% axial strain and six cycles without damaging the sample. The limit test showed that the elastic modulus values from ten consecutive cycles were within the allowable error of 20% and that there was not an observable trend relating the elastic moduli and the number of cycles, found in Table 7 below.

Cycle #	Stiffness	Average	STDEV	Percent Error from 10 cycles
1	2998			
2	2115			
3	2240			
4	2114			
5	2062	2196	287	13.1%
6	2094			
7	2111			
8	2045			
9	2068			
10	2111			

Table 7: The limit test result confirmed that the gripping technique did not fail when 25% axial strain was applied and showed that the overall elastic modulus did not vary more than the allowable error of 20%.

Six samples were tested from each concentration. The resulting stress and strain values were plotted to obtain the elastic modulus as shown in Figures 27 and 28. The resolution on the

video camera was not able to detect such small displacements below roughly 2%, which resulted in noise at the start of each curve. The noise region was not included in the slope calculation.

The Stress-Strain Curve of 5/0.025% Polyacrylamide Gel (Sample X)
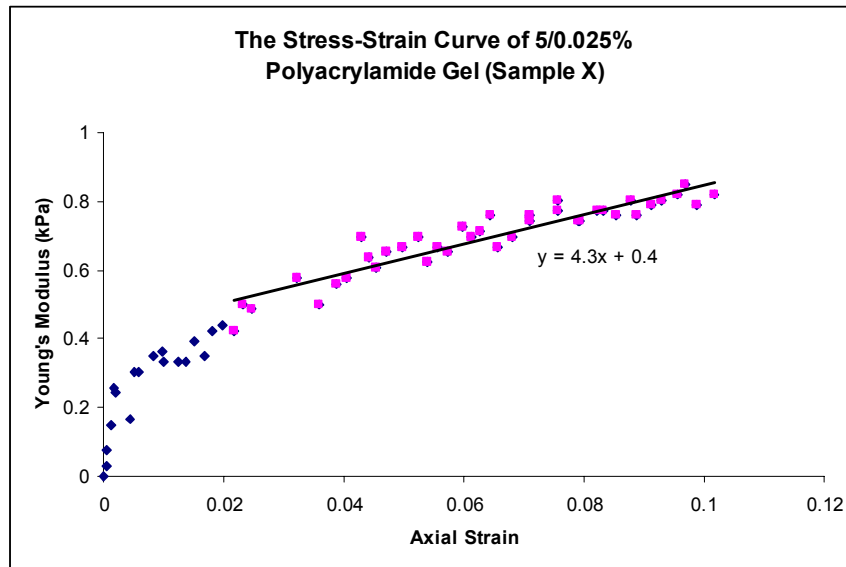
y = 4.3x + 0.4

Figure 27: The stress-strain curve was plotted to obtain the Young's Modulus value for 5/0.025% polyacrylamide gel. The linear trend was fitted in the linear region of the graph to accurately estimate the slope of the curve. The Young's Modulus for this example graph is 4.3kPa. The error in the small strain range occurred due an insufficient resolution in the video camera.

The Stress-Strain Curve of 8/0.08% Polyacrylamide Gel (Sample Q)
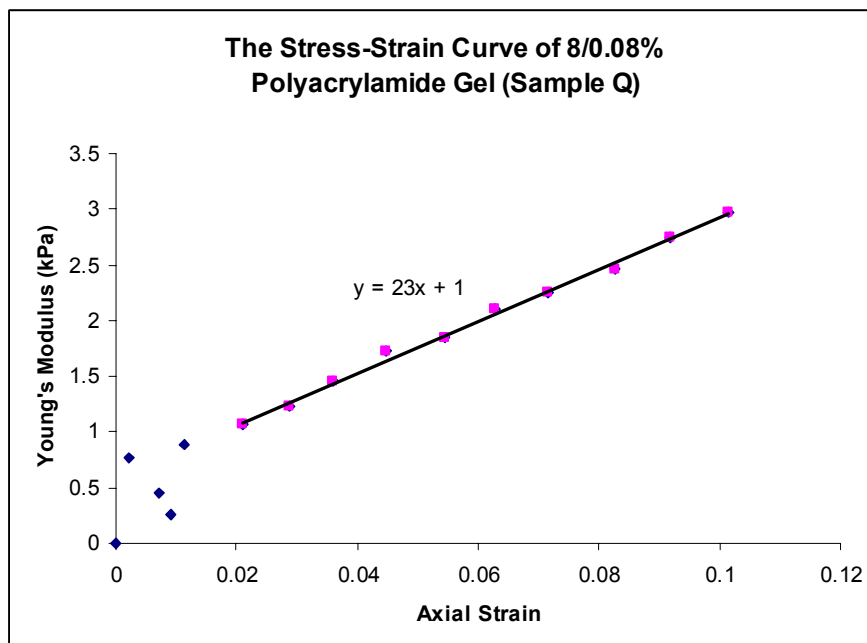
y = 23x + 1

Figure 28: The stress-strain curve was plotted to obtain the Young's Modulus value for 8/0.08% polyacrylamide gel. The linear trend was fitted in the linear region of the graph to accurately estimate the slope of the curve. The Young's Modulus for this example graph is 23kPa. The error in the small strain range occurred due an insufficient resolution in the video camera.

The average stiffness values and their standard deviations obtained from the linear region on the stress-strain curves are shown in Table 8 and 9. These average values were used to perform statistical analysis and to compare with other techniques.

Sample	Strain Rate					
	0.01	stdv	0.05	stdv	0.1	stdv
5/0.025%	(kPa)		(kPa)		(kPa)	
T	2.5	0.3	2.3	0.4	3.4	0.5
U	3.2	0.1	3.1	0.3	2.8	0.4
V	2.1	0.2	1.9	0.3	2.7	0.4
W	2.4	0.4	3.1	0.3	3.6	0.5
X	3.2	0.3	3.2	0.3	5.3	0.5
Y	1.9	0.2	3.4	0.6	5.3	0.8
Avg.	2.6	0.3	2.8	0.4	3.9	0.5

Table 8: Summary of the Young's modulus from 6 samples of 8/0.08% bis/acrylamide concentration are averaged from 6 cycles and shown below.

Sample	Strain Rate					
	0.01	stdv	0.05	stdv	0.1	stdv
8/0.08%	(kPa)		(kPa)		(kPa)	
P	28.4	1.8	22.6	2.3	29.2	1.3
Q	24	0.8	24	0.9	22.8	1.2
R	24.6	0.6	23.7	1.1	23.3	1.8
G	24.3	1.7	20.9	1.1	25.7	1.2
O	26.2	2.3	22.2	3.9	27.8	2.9
J	20.4	0.9	17.9	1	19.9	0.7
Avg.	24.7	1.4	21.9	1.7	24.8	1.5

Table 9: Summary of the Young's modulus from 6 samples of 5/0.025% bis/acrylamide concentration are averaged from 6 cycles and shown below.

The results obtained did not show a consistent relationship or trend between strain rate and stiffness. The elastic modulus of the 5%/0.025% concentration increases with an increased strain rate, but when factoring in the standard deviations to the results from 0.01 and 0.05 strain rates, the elastic modulus values were shown to be in the same range. These results suggest that the difference in strain rates may need to be greater than an order of magnitude to clearly observe the behavior more clearly. Graphical representation of the strain rate and the elastic modulus are shown in Figures 29 and 30.
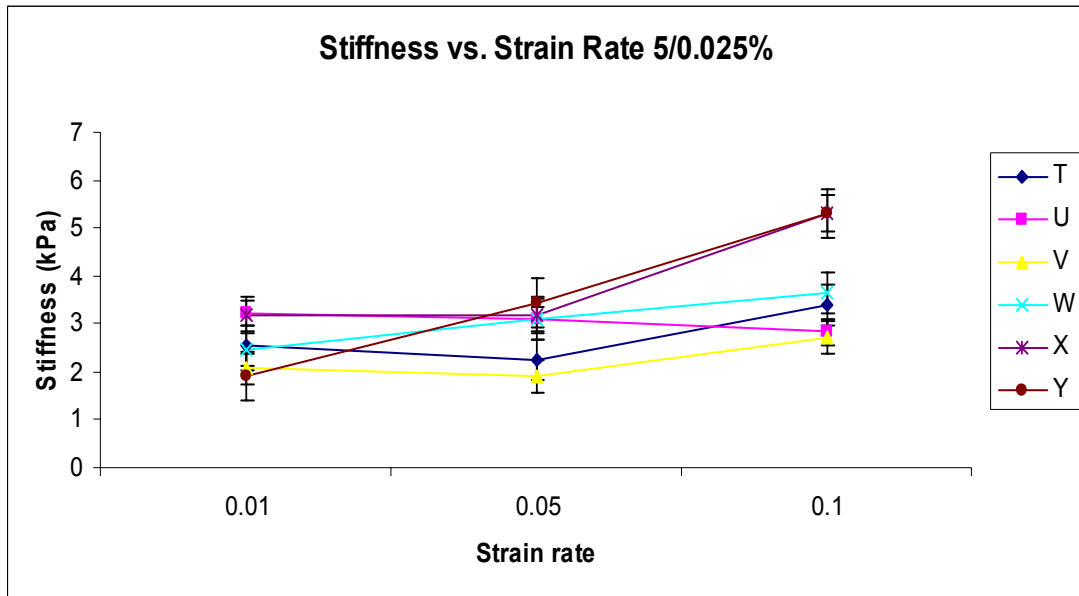
Figure 29: The elastic modulus of polyacrylamide gels with 5/0.025% concentration did not increase with an increase in axial strain.
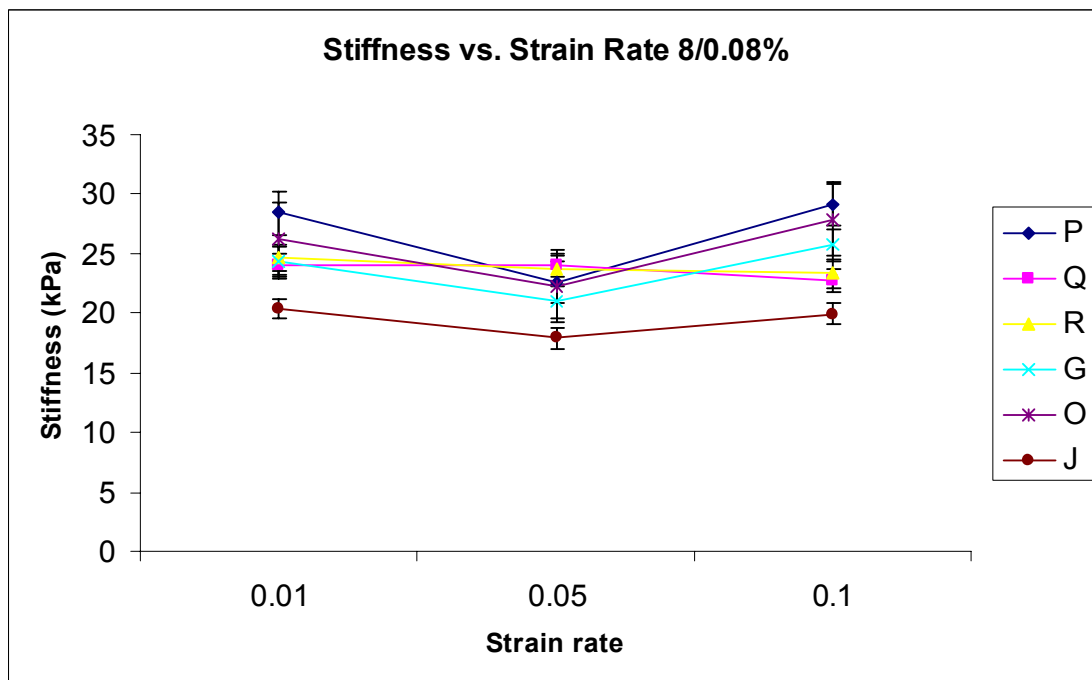

Figure 30: The elastic modulus of polyacrylamide gels with 8/0.08% concentration did not increase with an increase in axial strain.

Further, the results and their standard deviations were analyzed statistically using a two-way ANOVA to observe any effects from sample and strain rate variations. It was chosen to

observe whether the variation between samples and strain rates affect the stiffness values obtained. The results displayed that the stiffness values from both concentrations were affected by the variation between samples and variation between strain rates, found in Appendix 10.5. These findings were taken into considerations in the discussion of the final range for polyacrylamide gel from uniaxial tension test.

Table 10 below shows a summary of the Poisson's ratio values from each tension test and the final average value with its standard deviation. The Poisson's ratio values were in the expected range and correlated with previous studies in the literature as mentioned in the uniaxial and viscoelasticity section. The average value was 0.45 ± 0.5, which is very close to that of an incompressible fluid of 0.5. This value is reasonable because the polyacrylamide gels are mostly comprised of water that is incompressible.

Sample	Poisson's Ratio
G	0.47
J	0.36
O	0.35
P	0.44
Q	0.47
R	0.47
T	0.49
U	0.49
V	0.50
Y	0.47
W	0.44
X	0.41
AVE	**0.45 ± 0.05**

Table 10: The Poisson's ratio found from each sample were averaged and used as the final value.

The stress relaxation test reveals that polyacrylamide gel with the 8/0.08% concentration behaves like an elastic solid, while the 5/0.025% concentration behaves like a viscous fluid. After the initial strain, the stress remained above 50% of its initial value and did not decrease

over a ten minute period as shown in the nearly horizontal line in Figures 31 and 32. The time is plotted on a log scale, which allows the small initial relaxation to be seen more clearly. This test allows an observation to be made qualitatively.
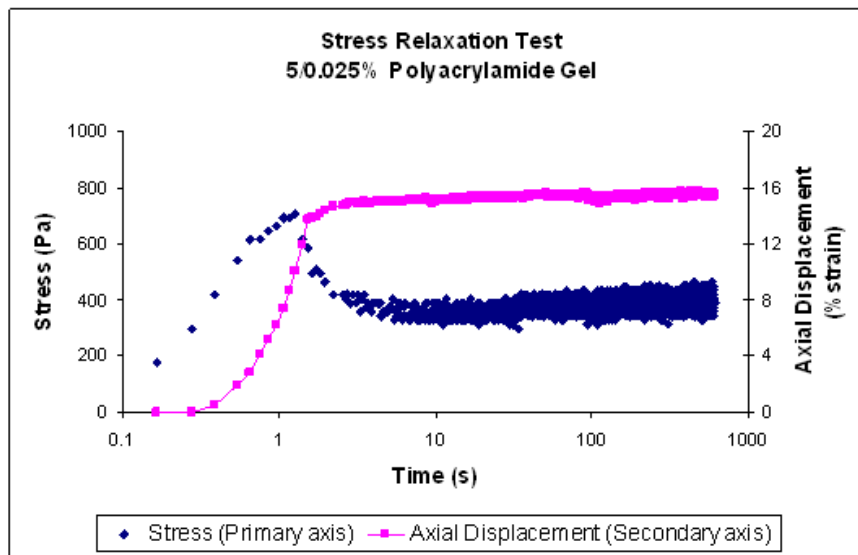

Figure 31: The stress relaxation graph of the 5/0.025% polyacrylamide gel shows that the stress remained constant after the initial relaxation. The initial relaxation shows that at a lower stiffness value, the gel's behavior is more viscous that a higher stiffness.
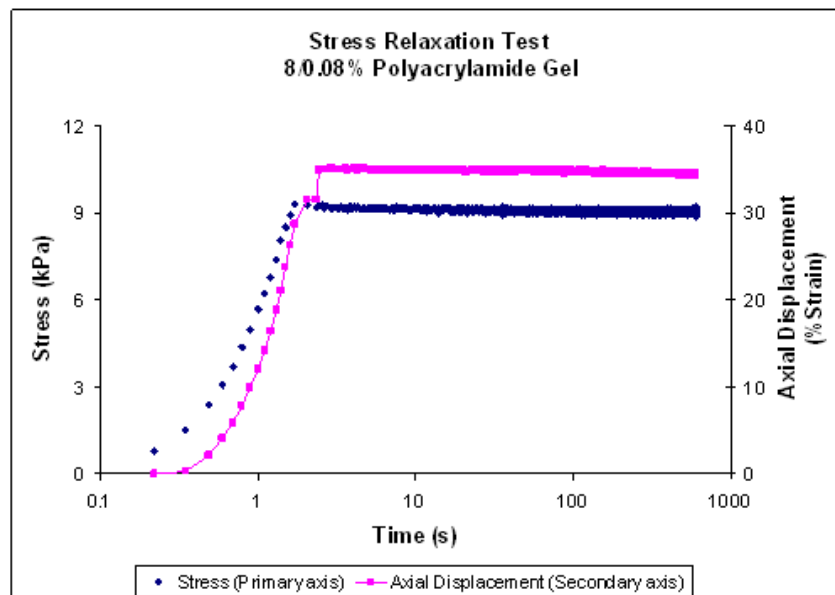

Figure 32: The stress relaxation graph of the 8/0.08% polyacrylamide gel shows that the stress remained constant after a very small initial relaxation. At a higher concentration, the gel's behavior is similar to an elastic solid.

6.4. Rheology

In an effort to further characterize both the viscoelastic properties and the bulk scale properties of polyacrylamide gel, several types of rheometry methods were employed. The inconsistent data (found in Appendix 10.6) obtained in the initial rheometry testing may have been due to the fact that the gels were cast in an open environment in the 35 mm cell culture wells. As previously mentioned, polymerization of acrylamide is a free-radical catalyzed reaction and oxygen is a free-radical scavenger which significantly inhibits gel polymerization. The gels, which were cast in the cell culture wells, were exposed to atmospheric oxygen, and therefore it was difficult to find any consistency in the rheometry results. This initial test data can be found in Appendix 10.6. The glass plate method was utilized to ensure adequate polymerization, leading to reproducible and accurate results. The following section outlines the results from testing of the 8% acrylamide / 0.08% bisacrylamide and 5% acrylamide / 0.025% bisacrylamide concentrations of polyacrylamide gels.

As mentioned in the methodology chapter, to ensure linear viscoelastic properties of the sample, it is necessary to perform testing at more than one torque, angular displacement, and strain to show that creep compliance is independent of stress and strain. The three rheometry testing methods that were used to demonstrate the viscoelastic properties of polyacrylamide gels were a frequency sweep, a time sweep, and a strain sweep.

A frequency sweep was initially performed on a gel sample in order to observe the materials overall response to different frequencies. The test involved an applied low strain of 5% over a wide range of frequencies (0.1-50 Hz). Figure 33 shows that the complex modulus is linear at lower frequencies (<15 Hz) for the 8%/0.08% polyacrylamide gels. A frequency sweep for the 5%/0.025% gel can be found in Appendix 10.6 and appeared to be almost identical to

Figure 33. At frequencies above 15 Hz, the material appears to behave erratically with a large increase in the complex modulus because the machine is unable to distinguish the wave forms to create an accurate signal. This instrument artifact is caused by the inertia of the parallel plate system and instead of detecting the output motion of the gel material; the machine is simply measuring the motion of the parallel plate system. For this reason all tests must be run at a lower frequency than 15 Hz to ensure accurate linear behavior. It was determined that the time sweeps and strain sweeps must be run at a frequency of 1 Hz for all gels because it is in the middle of the linear range.
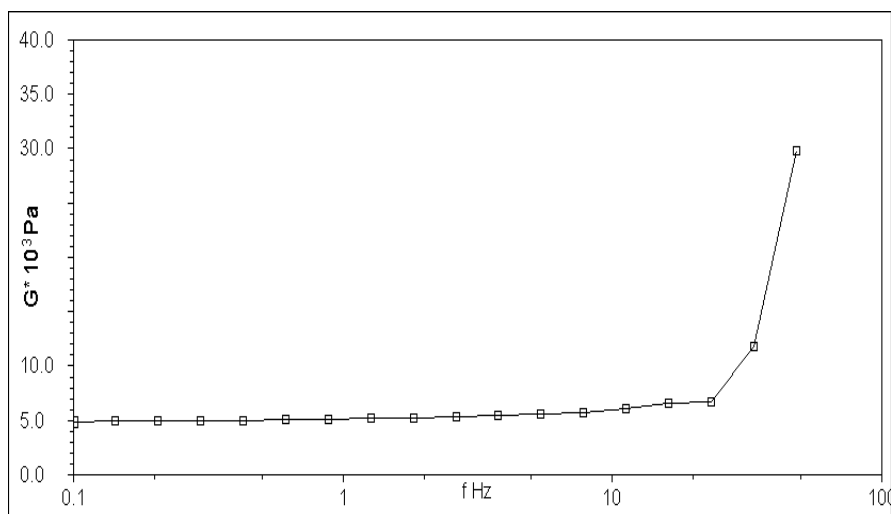

Figure 33: Frequency Sweep 8%/0.08% of 0.1-50 Hz: complex modulus is linear at low frequencies and instrument artifact causes inaccurate results at frequencies greater than 15 Hz. The large increase in G* is instrument artifact caused by the high inertia of the parallel plate system.

The time sweep was used to measure the gel's stability and involved a constant applied frequency of 1 Hz and a constant low strain of 5% over a five minute time period. Hydration is believed to play a large role in the mechanical properties of the polyacrylamide gels; therefore, it was essential to show that in short time periods there is not a drastic change in the complex modulus of the sample. Figure 34 demonstrates that the modulus is linear over a five minute time period for the 8%/0.08% gel. This indicates that during all test periods under five minutes,

the gel samples will behave in a consistent manner. If the gel's complex modulus increased

during the test, it would be indicative of the sample drying out; however, a linear display

signifies that the sample is not altered within five minutes of being removed from the buffer

solution. Throughout all testing, a gel sample was tested immediately after being removed from

the buffer solution and was never left out of the buffer for longer than five minutes. The time

sweep for the 5%/0.025% gel is included in Appendix 8.8 and is also linear, signifying all

concentrations of the gels are able to be tested for a five minute time period without any
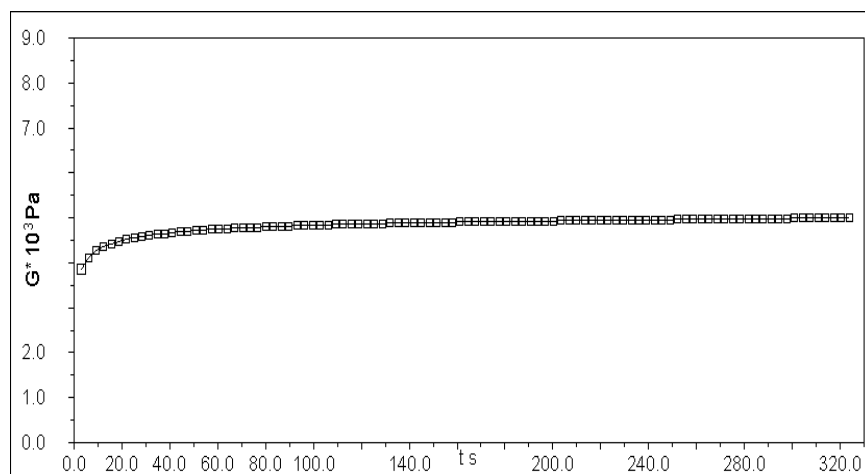
dehydration affects.

Figure 34: Time Sweep of 8%/0.08% gel: the complex modulus remains linear throughout the five minute testing period, signifying that drying does not affect the gels properties and that slippage or gel breaking is not an issue.

The final test which was conducted on the polyacrylamide gel samples was a strain

sweep. This method again involved a constant frequency of 1 Hz over a range of increasing

stress, resulting in increasing strain. This test method was used to determine the region of linear

viscoelastic response, where the stress is a function of strain, of a polyacrylamide sample. Figure

35 displays that when a low stress of 0.1-10 Pa is applied to the sample, the complex modulus is

not linear. The initial sloped appearance is most likely due to the fact that the programs testing

method is not optimized to measure such small strain values. The preliminary small stresses of the sweep result in minute strains that are incorrectly portrayed by the software as non-linear behavior. As a solution, a higher stress range of 50-300 Pa was applied to the sample and the resulting display was linear for numerous samples.

In addition, this testing method also determined whether or not the gel was slipping or breaking down in structure. A characteristic of slip on a complex modulus vs. strain graph is a dip, or simply a nonlinear region in the middle of a linear portion of the graph. If there was consistent slip, the complex modulus would go to zero and the strain sweep would take on the sine wave shape. However, it is apparent that the linear region in Figure 35 is reproducible among several samples signifying that the rheometer is accurately characterizing the properties of the polyacrylamide gel.
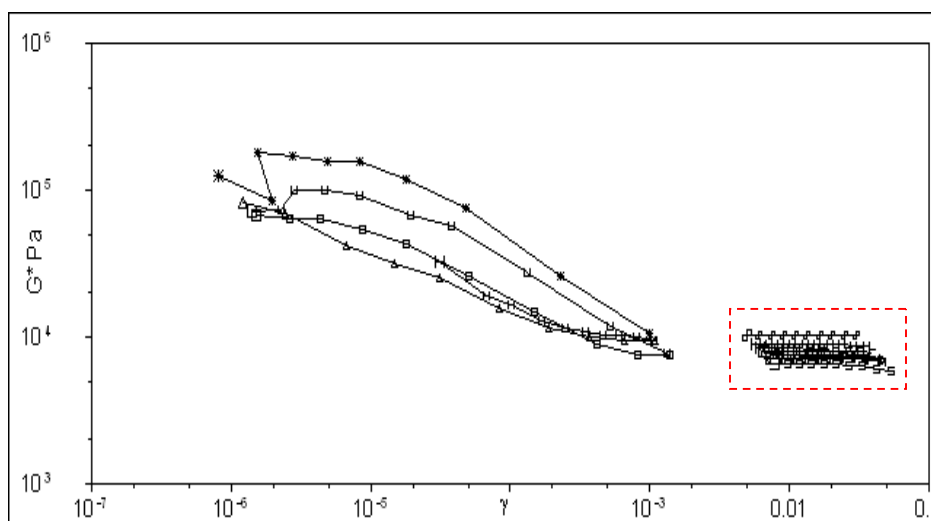

Figure 35: Strain Sweep of 8% acrylamide / 0.08% bis gel: highlighted linear viscoelastic region of the material signifies reproducible and accurate results for the complex modulus values of the gel.

After completing the three previously mentioned test methods, the linear viscoelastic region was able to be consistently found amongst all samples. Figure 36 shows the linear region of a frequency sweep (0.1 – 10 Hz) with the representative elastic modulus (G'), viscous

modulus (G"), and the phase angle (δ). It is quite apparent that the elastic modulus is the

dominant variable in this material. In addition, the phase angle is less than 10°. The extent of a

material's viscoelasticity is quantified by this phase angle value; a viscous material will have a

phase angle close to 90°, while a completely elastic material will have a phase angle of 0°.
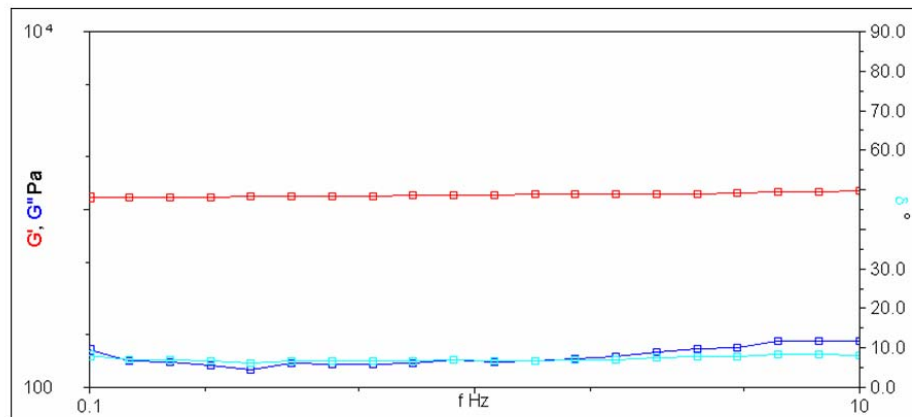

Figure 36: Linear region of a frequency sweep of 8% acrylamide / 0.08%: The elastic modulus (G') is shown to be much greater than the viscous modulus (G"). The phase angle (δ) is less than 10°, also signifying dominant elastic material properties.

As can be seen in Figure 37, the 5%/0.025% concentration has a slightly larger phase

angle under identical conditions, representing behavior which is more viscous. Another

indication of a more viscous like material is the fact that the viscous modulus appears to be more

prevalent in the 5%/0.025% plot than in Figure 36. In both Figure 36 and Figure 37, if the

complex modulus was to be plotted, it would closely resemble the elastic modulus values. This

signifies that although the 5%/0.025% concentration has proven to be more viscous than the

8%/0.08% concentration, it is still predominately elastic in behavior. It is important to note that

in combination with the uniaxial tensile testing, the overall confirmation of consistent linear

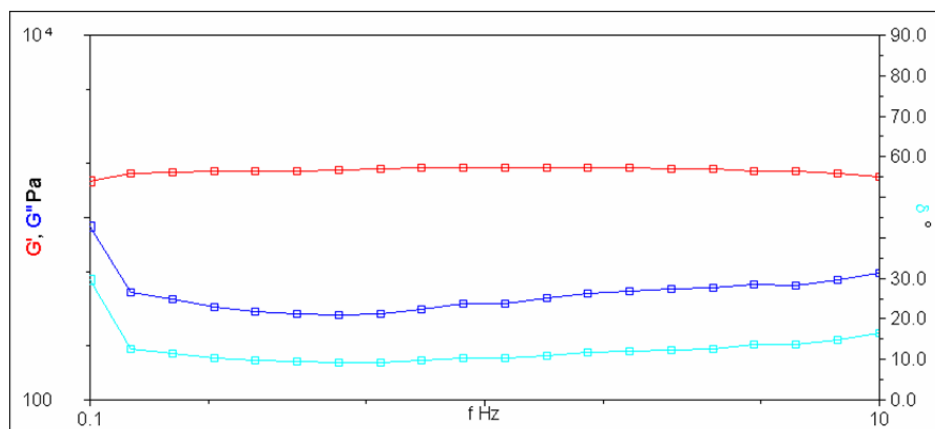viscoelastic results verify the assumptions made in Hertzian mechanics.

Figure 37: Linear region of a frequency sweep of 5% acrylamide / 0.025%: The viscous modulus (G") is shown to be quite larger than that in Figure 36, indicating less of an elastic behavior. The phase angle (δ) is greater than 10°, also signifying more viscous like material properties than the 8%/0.08% concentration.

As previously mentioned, the time sweep proved that the gel samples did not have a change in the mechanical properties over a five minute time period of consistent frequency and applied stress. In an attempt to further quantify the behavior of the polyacrylamide gel in the absence of hydration over time, a single gel was tested at thirty minute increments over a three hour time period. As can be seen in Figure 38, there is no trend in the complex modulus values as time increases.
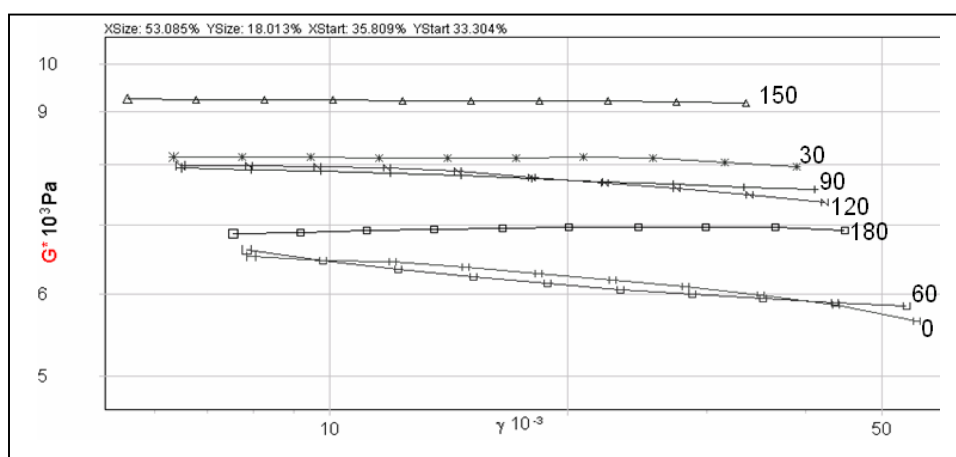

Figure 38: Strain Sweep 8%/0.08% Linear Region Dehydration: inconsistent alteration of the complex modulus values over drying time. The numbers represent the time in minutes that the sample was left out to dry.

The only conclusion that can be drawn from this data set is that dehydration does affect the stiffness properties of the gel. Over the three hour time period, the complex modulus range

was from 6127 Pa to 9214 Pa. There are no observed trends in the change of the complex

modulus and the inconsistency is greater than the normal error seen amongst samples of the same

concentration. Along with the fact that there will be ample hydration when these gels are used as

a cell substrate, this finding signifies the importance of hydrating the samples during testing.

Figure 39 shows the visible change in gel appearance with significant curling on the edges.
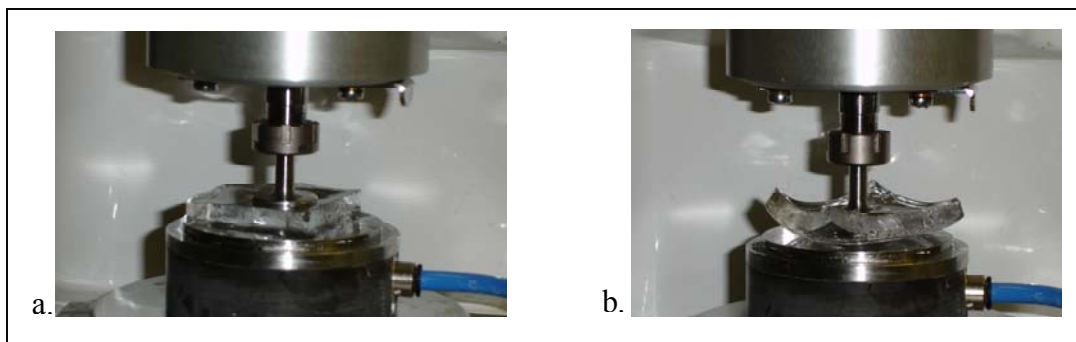

Figure 39: a) Initial hydrated polyacrylamide gel sample during testing b) Identical gel sample after three hours of dehydration with curling at the edges

In addition to quantifying the effects of dehydration on the gels, it was important to study

the change in complex modulus when the thrust force is altered on the sample. As previously

mentioned, the protocol for making the polyacrylamide gels was changed in an attempt to find

more consistent results with the two glass plates being used to seal the polymerization

environment from oxygen. An additional modification from the original testing procedure also

included a higher compressive thrust force of 70 grams on the sample. An increased

compressive force was applied to avoid the possibility of slipping. Figure 40 shows that thrusts

smaller than 70 grams result in inconsistent data collection; most likely caused by the slipping

phenomenon. All thrusts of 70 grams or larger resulted in linear complex modulus values that

were essentially identical, signifying an adequate thrust force on the sample with no slip.
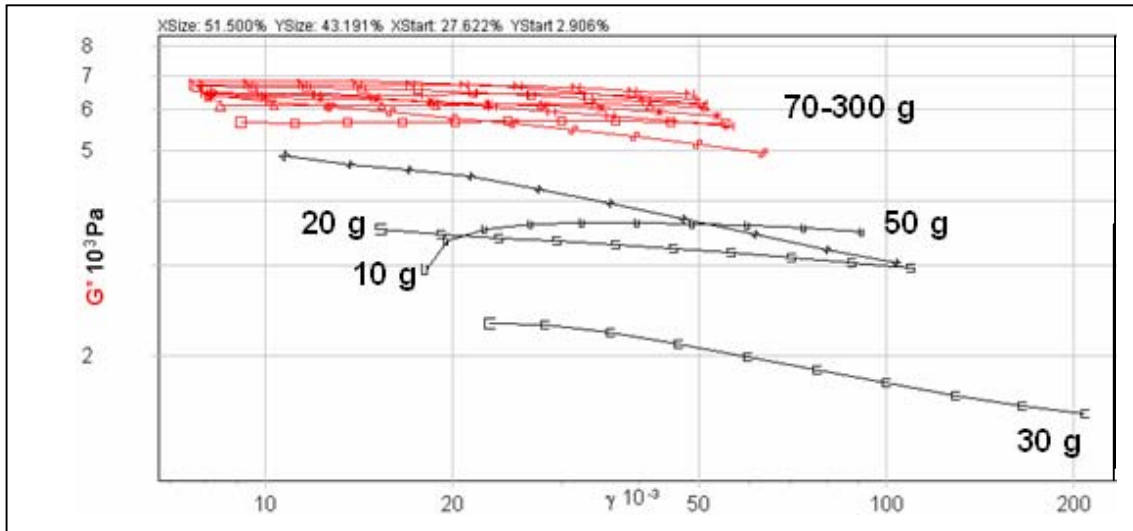
Figure 40: Strain Sweep 8%/0.08% Linear region thrust range: low thrusts (< 70 g) result in inconsistent data, while high thrusts do not appear to significantly alter the properties of the gel.

Due to the drastic difference in gel mechanical properties, a significantly smaller thrust was applied to the 5%/0.025% gels. The results shown in Figures 41 and Figure 42 are strain sweeps for the 8%/0.08% gels and 5%/0.025% gels respectively. The autotension was set to 5% for the 8%/0.08% samples (70.0 grams of thrust) and 3% for the 5%/0.025% samples (30 grams of thrust). The softer, 5%/0.025%, samples were significantly more compressed even with less applied tension. As previously mentioned, both thrusts were determined to be sufficient enough to avoid slip. Ideally, identical thrusts would be applied to both samples, however, it was determined that 30 grams of force was the maximum force the 5%/0.025% samples could undergo without severe deformation.

The two groups plotted in Figure 41 represent two different sheets, or batches, of polyacrylamide with the 8%/0.08% concentration. The elastic modulus is calculated using Equation 9 and a Poisson's ratio of 0.45. The average elastic modulus of Set 1 (black) is 19.1 kPa, while the elastic modulus of Set 2 (green) is 17.1 kPa. Tables with the complete results can be found in Appendix 10.6. One explanation for this variation is the degree of which the gel is hydrated. Under identical thrusts, there are many different gap sizes, or sample thicknesses,

ranging from 5297-6247 μm. Although, the small difference may seem negligible, it signifies

that there is an uneven hydration of the material. All samples do start off at identical thicknesses

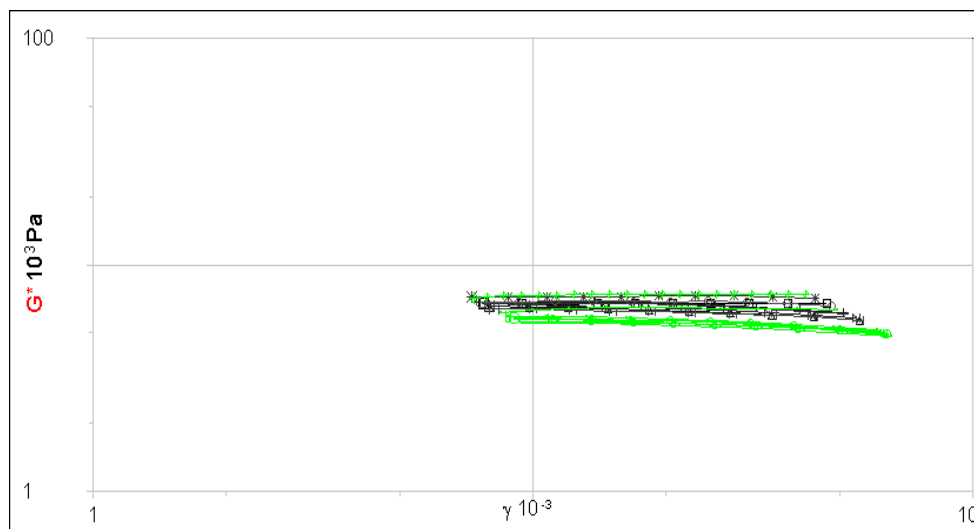before they are placed in the buffer solution after complete polymerization.

Figure 41: Strain Sweep 8%/0.08% [Set 1 – black] and [Set 2 – green]: both sets underwent a gradual increase in stress from 50-300 Pa with consistent changes in strain. The average complex modulus between the two sets is 18.1 ± 1.5 kPa.

The plot in Figure 42 represents two sets of polyacrylamide gels with a concentration of

5% acrylamide / 0.025% bisacrylamide. The top red group underwent a stress range of 1-300 Pa

while the bottom black group was subject to 50-300 Pa, both well within the linear range of the

material. There is a great deal of reproducibility in the complex moduli amongst the samples of

both groups. As can be seen in the tables in Appendix 10.6, the average elastic modulus of Set 1

is 2.0 kPa and 1.9 kPa for Set 2. These values are thought to accurately represent the properties

of the gel because there is such small variation between the two sets of gels.
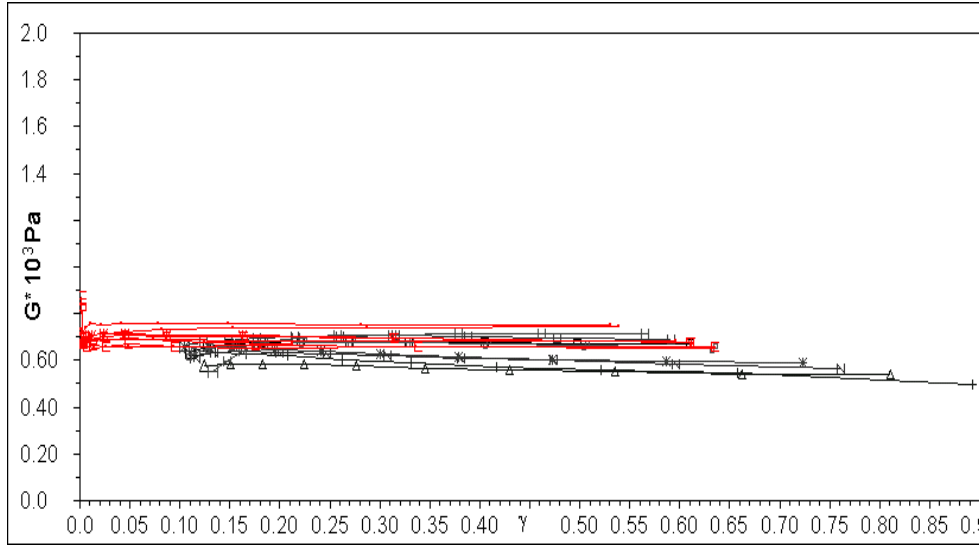
Figure 42: Strain Sweep 5%/0.025% [Set 1 – red] and [Set 2 – black]: both sets underwent a gradual increase in stress, from 1-300 Pa for Set 1 and from 50-300 Pa for Set 2. The complex modulus values are reproducible with an average complex modulus between the two sets is 1.9 ± 0.1 kPa.

Table 11 summarizes the elastic moduli found in the above strain sweeps for both the "stiff" and "soft" concentrations of polyacrylamide gel. These values were found by calculating the elastic modulus from the measured complex modulus values using Equation 9. It is important to note that in all gel samples the elastic modulus was much more dominate than the viscous modulus. Typically, the complex modulus had a value which was almost identical to the elastic modulus, while the viscous modulus was four times less. For the 8%/0.08% gels, the phase angles were consistently smaller than 10°, signifying a large degree of elasticity. Signifying a more viscous component, the 5%/0.025% gels had slightly greater phase angles, but still less than 20°.

	Average Elastic Modulus (kPa)
(8%/0.08%)	18.1 ± 1.5
(5%/0.025%)	1.9 ± 0.1

Table 11: Summary of elastic modulus values from 8%/0.08% and 5%/0.025% gel compositions. The average values were obtained from two sets of 9 samples for each concentration.

These stiffness values generated through rheometry studies provide the final bulk scale analysis of polyacrylamide gels. The following analysis section will detail the speculations of the findings from each technique.

7. Discussion

This research has progressed from the ball indentation technique, which was once considered the "standard test" for obtaining the mechanical properties of polyacrylamide gels to the rheometry testing technique, which had the capability to quantify the gel's complex viscoelasticity properties. The ball indentation technique was originally performed by Dr. Wang at UMASS and was replicated in this research. As can be seen in Figure 43, Dr. Wang's results are quite similar to the results obtained in our research for the 5%/0.025% ("soft") concentration of polyacrylamide gel. Also on this graph, one can see that Dr. Discher's AFM results are considerably lower than all of the values found with the other techniques involved in this research. There are many possible means for the discrepancy between Discher's results and the values obtained in this project. It has been proven that cantilever calibration is a large source of variability for any AFM procedure involving a compliant material. In combination with the different equipment used, any small variation in cantilever calibration has ability to skew results. The large error bar with the more compliant 5%/0.025% concentration of polyacrylamide that is primarily associated with the AFM technique is due to the adhesion of the material to the tip.
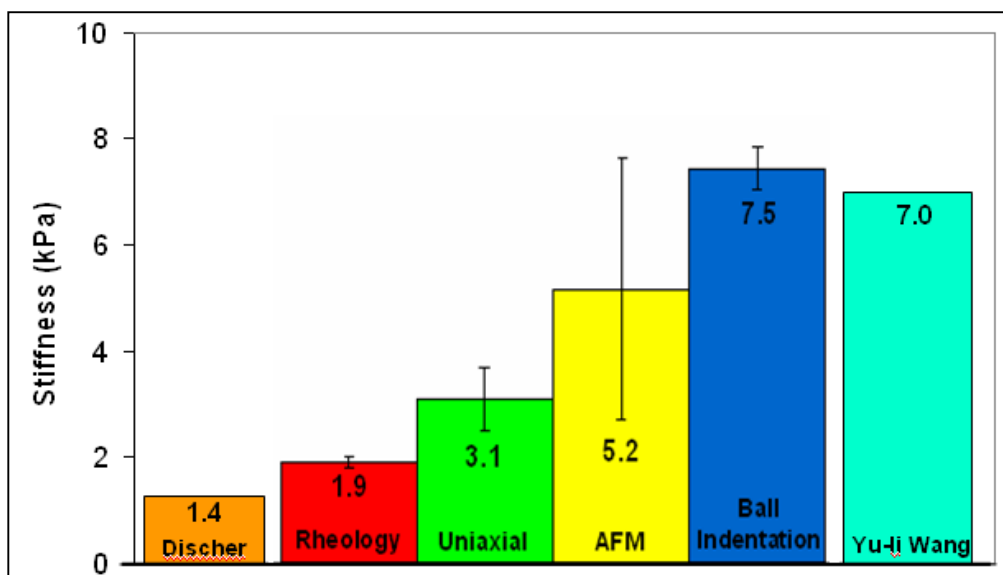
Figure 43: 5%/0.025% Young's modulus values with representative standard deviation bars. There is a clear difference between the two groups of techniques: rheometry and uniaxial testing (bulk properties) and ball indentation and AFM (local properties). Dr. Wang published a stiffness value of 7 kPa for the same gel concentration while Dr. Discher's AFM value is considerably lower at 1.4 kPa (Engler, 2005).

Figure 44 represents the values found in testing the 8%/0.08% ("stiff") polyacrylamide gel. Dr. Wang's value is drastically greater than any value measured by any of the four methods in our research. A large range of error is expected with the ball indentation technique because the conditions are extremely variable. The ratio of human error to indentation is much greater with a "stiff" gel because the ball does not indent the gel as much, making the distance that one must measure with the eye extremely small. One can notice that the error bar associated with the AFM technique is much smaller because adhesion was much less of a factor with the more elastic behaving 8%/0.08% concentration of polyacrylamide gel.
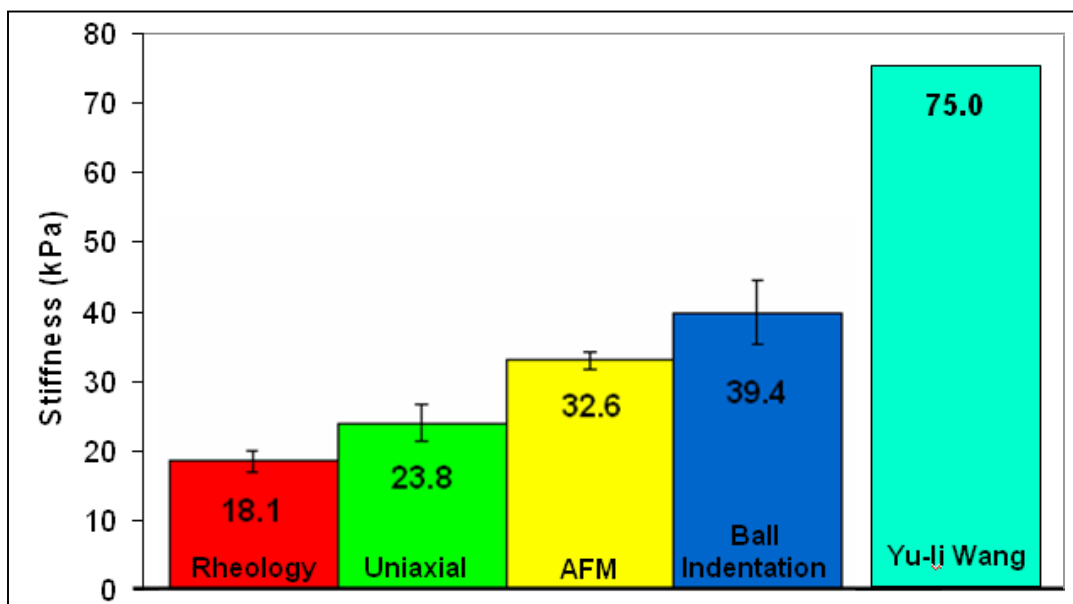
Figure 44: 8%/0.08% Young's modulus values with representative standard deviation bars. The same trend can be found as in Figure 43. Wang published a stiffness value of 75 kPa with an identical gel concentration and Dr. Discher did not perform testing at this particular concentration.

Due to such a high amount of variability in the ball indentation technique, the team utilized the precisely calibrated AFM tool with laser measurements as a comparison. It is interesting to note that the results are slightly less than the ball indentation technique but consistently greater than the two techniques of uniaxial tension and rheology. The distinct difference between the two groups of techniques is that ball indentation and AFM measure the gel properties on the local scale, while uniaxial testing and rheometry testing quantify the bulk properties of the material.

The hydrated three-dimensional complex network of polyacrylamide is responsible for the varying properties on different scales; however, the difference between AFM and ball indentation can be attributed to the level of precision each technique is capable of. Ball indentation relies heavily on human interpretation and more specifically the consistency of the human eye. The variability of the human eye is very large when measuring increments on the micron level; therefore, a large error is ascertained with the obtained results. In this research, this

error was found to be approximately 40 µm for measurements ranging from 120 to 200 µm. In addition, the measurement scale at which AFM is capable of is another cause of variation. The AFM device takes measurements at approximately 20 µm in diameter for the spherical tips, and the smallest ball used for indentation measurements was 640 µm.

Figures 43 and 44 clearly show that the two techniques of ball indentation and AFM yield consistently greater results than uniaxial tensile testing and rheometry. In addition to this large difference in results being due to the fact that the two groups are testing on different scales, there are other factors which alter the obtained values. In the case of ball indentation and AFM, the buffer medium surrounding the matrix plays a much more influential role in the generated results. The localized measurements are also affected by possible surface characteristics which potentially possess great variation from the internal structures. Uniaxial and rheometry methods better characterize the three dimensional matrix which is of primary interest when considering cell culture research. However, it is thought that cells sense the surface properties, rather than the bulk properties. *In vivo*, cells interact with an extra cellular matrix for mechanisms such as migration and adhesion.

Despite individual technique's limitations and assumptions, each technique provided a valuable support to compensate for some if not all of the others. The gel's properties were examined on multiple scales. The overall results from the individual techniques were able to show that each technique's limitations and assumptions played an important role in defining the gel's elastic modulus. However, by showing the differences in each technique's findings, future research will now be able to use this project as a guide to determine the allowable limitations and assumptions to their research.

Technique reliability was a main focus of this research as the objective was to provide the most accurate stiffness values for the various gel concentrations. Tables 3 and 4 in the ball indentation results section clearly show that the results obtained were typically within the 20% variation that was requested. What these tables do not show is the standard error observed in the testing method. A side experiment was used to evaluate this claim and provide quantifiable numbers for the technique reliability. This was conducted by repeatedly focusing on a single point defect made on a Petri dish. While the distance never changed, the resulting measurement of a focal point varied by approximately 40 μm. Upon evaluation it was determined that the reported technique variation would need to be more than doubled to accommodate for standard inaccuracies of the human eye generating an overall technique variation between 40% and 50% for the more localized measurements.

Technique variation of the less localized properties obtained with the 2 mm ball is slightly smaller at approximately 25% to 35%. A prediction was made that polyacrylamide demonstrates higher variation locally due to non-homogeneity surrounding the cross-linked matrix whereas the matrix itself has more consistent characteristics. Atomic Force Microscopy was able to further investigate this assumption by use of highly localized indentation.

The use of AFM to measure compliant materials requires time and patience. On average it takes five to six hours to go through the process of characterizing and calibrating the cantilever on a stiff surface to get to the point where force curves can be acquired. The sensitivity of the AFM probes allows for considerably precise results which are excellent for nano-scale work; however, ideal working conditions are required. The AFM must be enclosed in an insulated hood and placed on an air table to reduce vibrations that could affect the data. Overall, the

Atomic Force Microscope is adaptable enough to accommodate the study of compliant samples as long as adequate resources are allocated to the process.

In comparison to the other techniques used in this project, the AFM required a great deal of more time per test, but obtained rather precise data for the stiffer 8%/0.08% concentration. The time constraint did not allow time to expand on the project scope to determine the viscoelastic properties. In addition, the use of an atomic force microscope requires a larger budget then the other techniques. This is due partly to the fact the equipment requires a vibration free environment and each cantilever costs approximately $20.00 each.

While the results from AFM yielded consistent values for the stiffer gel, the variability of the softer gel still remains quite large when compared to ball indentation technique, which also quantified the properties on the local scale. This large variability could occur due to the surface properties of the gel such as a skinning effect. To observe the similarities or differences in the stiffness values and the range of errors, a uniaxial tension technique was used to examine the gel on the bulk scale and also to observe its viscoelastic behavior.

A uniaxial tensile test yielded repeatable results for both concentrations. The elastic modulus for the 8/0.08% and 5/0.025% concentrations were between 19-25 kPa and 2-4 kPa respectively. For both concentrations, these values were lower than those found by Dr. Wang, but greater than those found by Dr. Discher. Although these results were not expected, they were well within the range found using other techniques in this research. The uniaxial technique provides a direct mechanical measurement of the bulk properties of the gel. It assumes homogeneity in the sample and that the maximum average strain region occurred at the center. The results from this technique correlate well with results from the rheology technique, which also examine the material's bulk properties.

The error associated in uniaxial tension test as seen at the beginning of each stress-strain curve could be resulted from the equipment used to gather data. The error could be reduced if the resolution of the video camera was higher. An attempt to reduce this error was made by placing marker positions further apart from each other. The results yielded small improvements, but a significant change to the overall results was not observed. The strain rates chosen for this project did not seem to affect the stiffness in an observable range. The gel's properties did not allow for a much faster rate to be performed; the majority of the gels were damaged after a few cycles at a rate faster than the maximum strain rate in this experiment. In the future, it is recommended that the chosen strain rates be greater than an order of magnitude in order to emphasize the behavioral differences.

Overall, the Poisson's ratio correlated well with previous research mentioned in the background section. However, the lateral displacement of the black dots was quite small, resulting in a large error when calculating the strain for the Poisson's ratio. Again, the standard deviation associated with the Poisson's ratio could be reduced if the resolution on the high speed camera was increased. The stress relaxation test is simple and consistent, but has several limitations as well. The viscoelastic behavior could not be seen clearly using this technique, especially in the stiffer 8%/0.08% concentration. It is possible that the gel may have relaxed a very small amount in the ten minute test period, but remained undetected by the video camera. In the future, one could allow for a longer relaxation time and observe the difference in the stress response.

The uniaxial stress relaxation method is just one way of analyzing the viscoelastic behavior of the polyacrylamide gel. The device used for this method did not allow for frequency

to vary. To completely examine viscoelasticity, dynamic oscillatory research was performed with a rheometer.

The initial inconsistent results found in Appendix 10.6 were originally thought to be caused by slipping or drying out of the sample. However, both of these theories were proven wrong with the strain and time sweeps. Although, the three hour dehydration test proved that there is inconsistent data after long periods of drying (> 30 minutes), the five minute time sweep test confirmed that the gel was not quickly drying out because the complex modulus was linear throughout the entire test. In addition, the strain sweeps on multiple gel samples proved that there was a consistent linear and non-linear region. If the gel was slipping at all, there would not be such consistency in the non-linear region at low stress values.

Serrated parallel plates were explored on several occasions throughout the course of this research. It is interesting to note that the results collected from the serrated plate test method were consistently larger than that of the parallel plate method. The results from the testing involving the serrated plates can be found in Appendix 10.6. Serrated plates may damage the gel sample, resulting in inaccurate results. In the end, smooth parallel plates proved to give reproducible results with no signs of slipping under low strain values and a high thrust, eliminating serrated plates as a method.

As previously mentioned, the variation in the 8%/0.08% samples may have been caused by the degree of gel hydration. In an effort to eliminate any inconsistencies in the gel structure, the solution was thoroughly stirred prior to polymerization. In addition, all samples were removed from in-between the glass plates with the same thickness. After being cut into small samples, the polyacrylamide gels were stored in a buffer solution at 4°C. However, there may have been some discrepancy in the amount of buffer solution within the Petri dishes in which the

gels were stored, resulting in varying degrees of hydration. In the future, it is recommended that all samples be kept under identical conditions prior to testing. The buffer solution should completely submerge the gels to ensure complete and consistent sample hydration.

Stiffness values generated through rheometry studies provided the final bulk scale analysis of polyacrylamide gels. Overall, the various testing methods of rheology consistently proved that the material predominately behaves in a linear elastic manner. In combination with the uniaxial tensile testing results, proof of polacrylamide's linear properties fully validate the Hertzian mechanic assumptions made in both the AFM and ball indentation techniques.

The exact accuracy of both the uniaxial tensile device and the rheometer is unknown. It is thought that the rheometer should have the lowest relative uncertainty out of all the techniques, because the test method is simple, with very little room for human or mechanical error. The uniaxial tensile method was not as refined as that of rheometry; rheometry simply involved placing samples on the device, while uniaxial tensile testing involved a great deal of physical handling of the polyacrylamide material. An increase in gel handling has the potential to greatly alter the overall structure. The overall measuring capabilities of the uniaxial tensile device was much less than the rheometer, however the Poisson's ratio value obtained from the uniaxial tensile test was used in the elastic modulus calculations for the rheometry technique. In the end, there is no exact accuracy value that can be assigned to either of the two techniques; however, it is believed that the rheometry results would be more accurate simply because of the device's capabilities.

On the local scale, the AFM technique clearly represents a more accurate technique than ball indentation. The calibrated cantilever and laser measurements leave a significantly less amount of room for error than the ball indentation depths that are judged by the human eye. It

has clearly been displayed that the AFM technique will yield more accurate results with the 8%/0.08% concentration than the 5%/0.025% concentration because of the adhesion properties. In the end, it is thought that the AFM technique would most accurately describe the stiffness that a cell would experience on a substrate because the tip size is very close to that of a cell.

8. Future Recommendations

In the end, our results have proven that it is quite difficult to characterize the properties of the polyacrylamide gel. It is often assumed that the polyacrylamide material is a homogeneous material; however, we have consistently shown that there is a range of appropriate values when utilizing these two specific concentrations of acrylamide monomer and bisacrylamide cross-linker. To fully understand this discrepancy in results a complete polymer analysis must be performed. There may be slight structural differences on the surfaces of the material that act slightly "tougher" yielding higher results when the ball is dropped or the cantilever tip is lowered onto the material.

To ensure experimental uniformity and to avoid potential sources of error, the individual gels used for each of the four testing techniques would ideally be made from the same acrylamide / bisacrylamide solution. Although, a strict protocol was followed for making the polyacrylamide gels in this research, there are constant sources of variability which could lead to inconsistent results. For example, lack of consistency in the simple task of stirring the solution has the potential to cause insufficient polymerization and results that are not reproducible. It was discovered that it is essential to stir the solution thoroughly before degassing and during the time when the ammonium-persulfate and TEMED was added.

When utilizing this material in future research, it is crucial to understand that the behavior of the gel is quite complex with an obvious variation in properties when measured on the two different scales of local and bulk. An immediate affect which our results will have on the research world involves Dr. Billiar's on going investigation of cell differentiation pathways relative to substrate stiffness values. Incorrect substrate properties have the ability to dramatically skew the measurements and observations involved in cell culture studies; therefore,

it is crucial to note the method of substrate mechanical characterization and mention that there is

a possible range of values dependant of the scale of interest.

9. References

Beningo, Karen A., C.M. Lo, and Wang, Yu-Li (2002). "Flexible Polyacrylamide Substrata for the Analysis of Mechanical Interactions at Cell-Substatum Adhesions." <u>Methods in Cell Biology</u> **69**: 325-340.

Bohlin Instruments Ltd (2004). "Basic Introduction to Rheology [manual]: 143-184.

Burnham, N., (2003) "Comparison of Calibration Methods for Atomic Force Microscopy" <u>Cantilevers. Institute of Physics Publishing PII</u>: S0957

Butler, J.P., Kelly, S.M., (1998). "A Model for Cytoplasmic Rheology Consistent with Magnetic Twisting Cytometry." <u>Biorheology</u> **35**: 193-209.

Carter, D. G., Beaupre G.S., Giori N.J., Helms, J.A., (1998) "Mechanobiology of Skeletal Regeneration." <u>Clin Orthop Rel Res</u> **355S**: S41-S55.

Chen, Eric J., Novakofski, Jan, Jenkins, Kenneth W., O'Brien, William D., (1996). "Young's Modulus Measurements of Soft Tissues with Application to Elasticity Imaging." <u>IEEE Transactions on Ultrasonics, Ferroelectrics, and Frequency Control</u> **43**: 145-154.

Collinsworth (2002). "Apparent Elastic Modulus and Hysteresis of Skeletal Muscle Cells Throughout Differentiation." <u>Duke University</u>.

Dym, C.L., Little, P. Engineering Design: A Project Based Introduction. 2nd Ed. John Wiley and Sons, Inc., 2004.

Emil W. Deeg, (2004) "New Algorithms for Calculating Hertzian Stresses, Deformations, and Contact Zone Parameters," Tyco Electronics Corporation.

Engler, Adam L. B., Cynthia Newman, Alina Hategan, Maureen Griffin, and Dennis Disher (2004). "Substrate Compliance versus Ligand Density in Cell on Gel Responses." <u>Biophysical Journal</u> **86**: 617-628.

Engler, Adam J. M. A. G., Shamik Sen, Carsten G. Bonnemann, H. Lee Sweeney, and Dennis E. Discher (2004). "Myotubes differentiate optimally on substrates with tissue-like stiffness: pathological implocations for soft or stiff microenvironments." <u>The Journal of Cell Biology</u>.

Engler, A. J., Richert, L., Wong, J. Y., Picart, C., Discher, D. E., (2004). "Surface probe measurements of the elasticity sectioned tissue, thin gels and polyelectrolyte multilayer correlations between substrate stiffness and cell," <u>Surface Science</u>, In press.

Ferry, John D., (1980). "<u>Viscoelastic Properties of Polymers</u>." Wiley Publishers. New York: 96-147.

Frey et al. (2005) Excel workbook for determination of Young's Modulus from AFM force-indentation profiles. Department of Biomedical Engineering and Physics, Worcester Polytechnic Institute. 100 Institute Road, Worcester MA.

Geissler E., Hecht, A. M., (1980). "The Poisson's Ratio in Polymer Gels," Macromolecules **13**: 1276-1280.

Goodwin, James W. (2000) "Rheology for Chemists: an Introduction." Cambridge : Royal Society of Chemistry.

Grattoni, Carlos A. H. H. A.-S., Canghu Yang, Ann H. Muggeridge, and Robert W. Zimmerman (2001). "Rheology and Permeability of Crosslinked Polyacrylamide Gel." Journal of Colloid and Interface Science **240**: 601-607.

Huang H, Kamm RD, Lee RT. (2004) "Cell mechanics and mechanotransduction: pathways, probes and physiology." Am J Physiol Cell Physiol: 287 (1) : C1-11

Li, Yong, Zhibing Hu, and Chunfang Li. (1993) "New Method for Measuring Poisson's Ratio in Polymer Gels." Journal of Applied Polymer Science 50: 1107-1111.

Lo, C.-M., Wanh, H.-B., Dembo, M., and Wang, Y.-L. (2000). "Cell movement is guided by the rigidity of the substrate." Biophysical Journal **79**: 144-152.

Mathur "Endothelial, Cardiac Muscle and Skeletal Muscle Exhibit Different Viscous and Elastic Properties as Determined by Atomic Force Microscopy." Duke University. Durham, NC. 2001

MikroMasch: http://www.spmtips.com/products/cantilevers/datasheets/tipless/

Parsons, Jeffrey W., Coger, Robin N., (2002). "A New Device for Measuring the Viscoelastic Properties of Hydrated Matrix Gels." Journal of Biomechanical Engineering **124**: 145-154.

Polyacrylamide Gels [manual] www.amershambiosciences.com (2005)

Pelham, Robert J. J., and Yu-Li Wang (1997). "Cell locomotion and focal adhesions are regulated by substrate flexibility." Proc. Natl. Acad. Sci. **94**: 13661-13665.

Thoreson, E. (2006). "From nanoscale to macroscale, using the atomic force microscope to quantify the role of few-asperity contacts in adhesion." Worcester Polytechnic Institute, Department of Physics.

Timoshenko, Thomas. (1970). "Theory of Elasticity." McGraw-Hill Companies; 3rd edition: 124-138.

Walker (2004). "Using the Adhesive Interaction between Atomic Force Microscopy Tips and Polymer Surfaces to Measure the Elastic Modulus of Compliant Samples." Duke University.

Wong, Joyce Y., Velaso, A., Rajagopalan, P., Pham, Q. (2002). "Directed Movement of Vascular Smooth Muscle Cells on Gradient-Compliant Hydrogels." Langmuir. **19**: 1908-1913.

10. Appendix

10.1.   Pairwise Comparison Chart

	Determine testing reliability using error analysis	Maximize the number of samples tested of each concentration	Maximize range of frequencies for rheometry and AFM	Maximize the number of concentrations tested between the range of 1-100 kPa	Determine concentrations of acrylamide and bis to produce a stiffness of 1 kPa and 100 kPa	Maximize the number of individual testing modes**	Score
Determine testing reliability using error analysis							
Maximize the number of samples tested of each concentration							
Maximize range of frequencies for rheometry and AFM							
Maximize the number of concentrations tested between the range of 1-100 kPa							
Determine concentrations of acrylamide and bis to produce a stiffness range of 1-100 kPa							
Maximize the number of individual testing modes **							

** Rheometry: smooth parallel plates, rough parallel plates, serrated plates, and   concentric circles

AFM: cantilever stiffness, tip half-angle,

Ball Indentation: ball radius, ball density, and sample geometry

Uniaxial: strain rate, sample dimensions, and percent strain

10.2. Polyacrylamide Protocol

PREPARATION OF POLYACRYLAMIDE SUBSTRATES
(Revised version of Yu-Li Wang's Lab Protocol)

"Stiffness" MQP

Materials

1. No.1 coverslip, 45x50 mm rectangular and 22 mm circular.

2. NaOH, 0.1 N, 100 ml.

3. 3-aminopropyltrimethoxy silane.

4. PBS, 500 ml.

5. Glutaraldehyde, 0.5%. Mix 357 ul of 70% glutaraldehyde with 50 ml of PBS. Keep the 70 % stock tightly sealed in zip bags in a closed container at 4°C.

6. HEPES, 1 M, pH 8.5, 1 ml and 50 mM, pH 8.5, 500 ml. Use at room temperature.

7. Acrylamide (40%, Bio-Rad) and Bis (2%, Bio-Rad).

8. Ammonium persulfate (Bio-Rad) solution, 10 mg in 100ul distilled water. Prepare immediately before use in step 10.

9. TEMED (Bio-Rad).

Procedure

1. Mark one side of a #1 cover slip with a diamond tip pen. Pass the marked side over the inner flame of a Bunsen burner.

2. Place the cover slip, flamed side up, on a test tube rack. Smear the surface with 0.1 N NaOH in the hood and allow the surface to air dry.

3. Smear the dried surface with 3-aminopropyltrimethoxy silane, wear gloves and do this in the hood. Incubate at room temperature for 5 minutes.

4. Collect the cover slips in a pan. Wash with distilled water on a shaker until the cover slip surfaces are clear.

5. Put the cover slips back on test tube rack. Pipette 0.5 % gluteraldehyde to cover the treated surface of the cover slips. Incubate for 30 minutes at room temperature in the hood. Wear gloves.

6. Collect the used glutaraldehyde in liquid waste. Wash as in step 4 and let air-dry. Activated cover slip may be stored in a dessicator for two weeks. Cover slips may be mounted onto chamber dishes before proceeding with the following steps.

7. Mix 5 ml of acrylamide solution in a small beaker according to the dilution scheme below.

Final Acryl/Bis	40%Acrylamide	2%Bis	1M HEPES	H$_2$0+Beads	Young's Modulus
8%/0.1%	1000 ul	250 ul	50 ul	3700 ul	?? kN/m2
8/0.08	1000	200	50	3750	75
8/0.06	1000	150	50	3800	30
8/0.05	1000	125	50	3825	23
8/0.04	1000	100	50	3850	17
8/0.03	1000	75	50	3875	14
8/0.02	1000	50	50	3900	10
5/0.12	625	300	50	4025	33
5/0.10	625	250	50	4075	28
5/0.08	625	200	50	4125	24
5/0.06	625	150	50	4175	15
5/0.05	625	125	50	4200	??
5/0.025	625	63	50	4262	7
3/0.10	375	250	50	4325	??

8. Degas the solution for 20 minutes to remove oxygen, which inhibits acrylamide polymerization.

9. Add 30 ul ammonium persulfate and 20 ul TEMED. Seal the beaker with parafilm and mix gently by swirling.

10. Pipette the acrylamide mixture onto the activated cover slip. Use 15 ul for a 75 um-thick gel. Quickly place a 22 mm circular cover slip onto the acrylamide droplet and invert the chamber dish.

11. Let acrylamide polymerize for 30 minutes.

12. Flood the surface with ~2 ml of 50 mM HEPES. Remove the circular cover slip with two pairs of fine tipped tweezers.

13. Rinse the substrate well with 50 mM HEPES. The substrate may be stored at 4°C for 2 weeks.

10.3.   Ball Indentation

7 Kpa			
Indentation Depth	Ball Diameter	Elasticity	Force
0.351	*1*	9162.296	0.00004414
0.348	*1*	9281.029	0.00004414
0.344	*1*	9443.377	0.00004414
0.358	*1*	8894.887	0.00004414
0.345	*1*	9402.348	0.00004414
0.37	*1*	8465.691	0.00004414
0.255	*0.64*	5085.828	0.00000971
0.245	*0.64*	5400.361	0.00000971
0.24	*0.64*	5569.998	0.00000971
0.242	*0.64*	5501.091	0.00000971
0.239	*0.64*	5604.993	0.00000971
0.238	*0.64*	5640.355	0.00000971
0.718	*2*	11138.99	0.000314
0.729	*2*	10887.82	0.000314
0.714	*2*	11232.72	0.000314
0.733	*2*	10798.82	0.000314
0.715	*2*	11209.16	0.000314
0.727	*2*	10932.78	0.000314
5/.025% Polyacrylamide			
Ball Diameter (mm)	Average E (Kpa)	STD	% Variation
0.64	5.47	0.21	3.75
1.00	9.11	0.37	4.08
2.00	11.03	0.18	1.66

75 Kpa			
Indentation Depth	Ball Diameter	Elasticity	Force
0.124	*1*	43634.75	0.00004414
0.14	*1*	36372.48	0.00004414
0.119	*1*	46413.52	0.00004414
0.119	*1*	46413.52	0.00004414
0.136	*1*	37988.89	0.00004414
0.12	*1*	45834.56	0.00004414
0.136	*0.64*	13057.61	0.00000971
0.144	*0.64*	11984.73	0.00000971
0.13	*0.64*	13971.95	0.00000971
0.135	*0.64*	13202.96	0.00000971
0.132	*0.64*	13655.61	0.00000971
0.14	*0.64*	12502.01	0.00000971
0.239	*2*	58001	0.000314
0.194	*2*	79310.32	0.000314
0.24	*2*	57638.87	0.000314
0.2	*2*	75768.26	0.000314
0.22	*2*	65674.73	0.000314
0.19	*2*	81827.99	0.000314
8/.08% Polyacrylamide			
Ball Diameter (mm)	Average E (Kpa)	STD	% Variation
0.64	13.06	0.73	5.60
1.00	42.78	4.48	10.48
2.00	69.70	10.72	15.38

	5/.025% Polyacrylamide			
	Ball Diameter (mm)	Average E (Kpa)	STD	% Variation
Test A	0.64	5.5	0.21	3.75
	1.00	9.1	0.37	4.08
	2.00	11.0	0.18	1.66
	5/.025% Polyacrylamide			
	Ball Diameter (mm)	Average E (Kpa)	STD	% Variation
Test B	0.64	6.9	1.15	16.74
	1.00	7.8	0.39	5.06
	2.00	11.2	0.56	4.98

	8/.08% Polyacrylamide		
Test A	Ball Diameter (mm)	Average E (Kpa)	STD	% Variation
	0.64	13.1	0.73	5.60
	1.00	42.8	4.48	10.48
	2.00	69.7	10.72	15.38
	8/.08% Polyacrylamide		
Test B	Ball Diameter (mm)	Average E (Kpa)	STD	% Variation
	0.64	15.2	1.31	8.63
	1.00	57.1	8.84	15.47
	2.00	72.1	5.24	7.27

Force Displacement Curve
5/.025%Polyacrylamide

y = 0.1404Ln(x) + 1.8263

Effect of Ball Geometry on Applied Force

$y = 0.0001x^2 - 0.0001x + 3E{-}05$
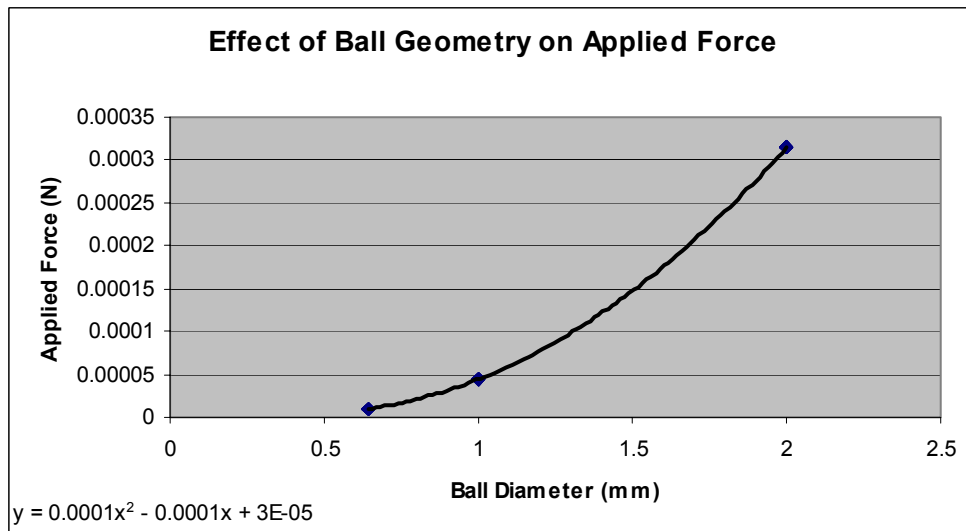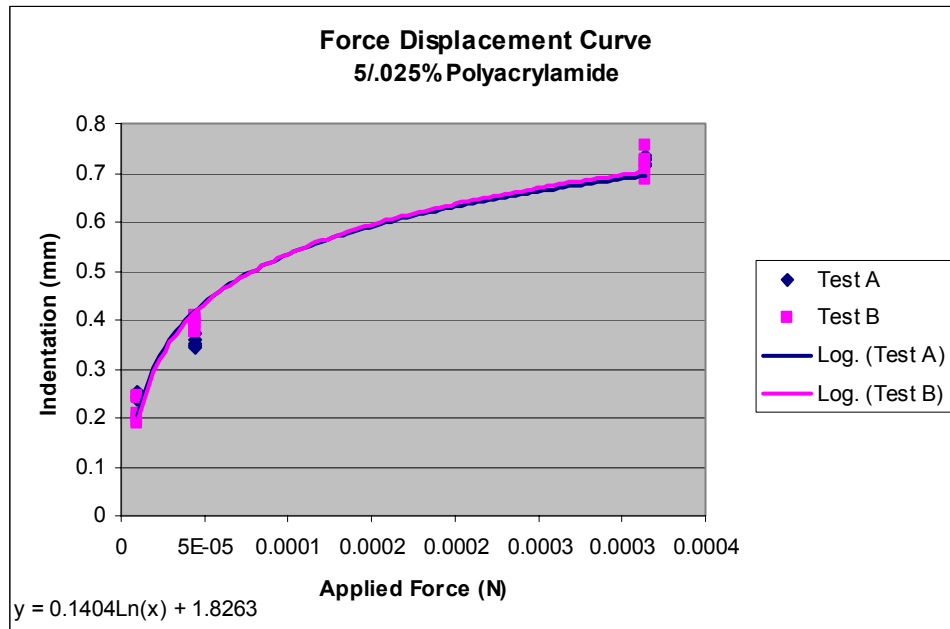
10.4. Atomic Force Microscopy

5%/0.025% Concentration

Raw Data

Raw Data

Raw Data

103

8%/0.08% Concentration:

Raw Data

Raw Data

Raw Data

Raw Data

Raw Data

Raw Data
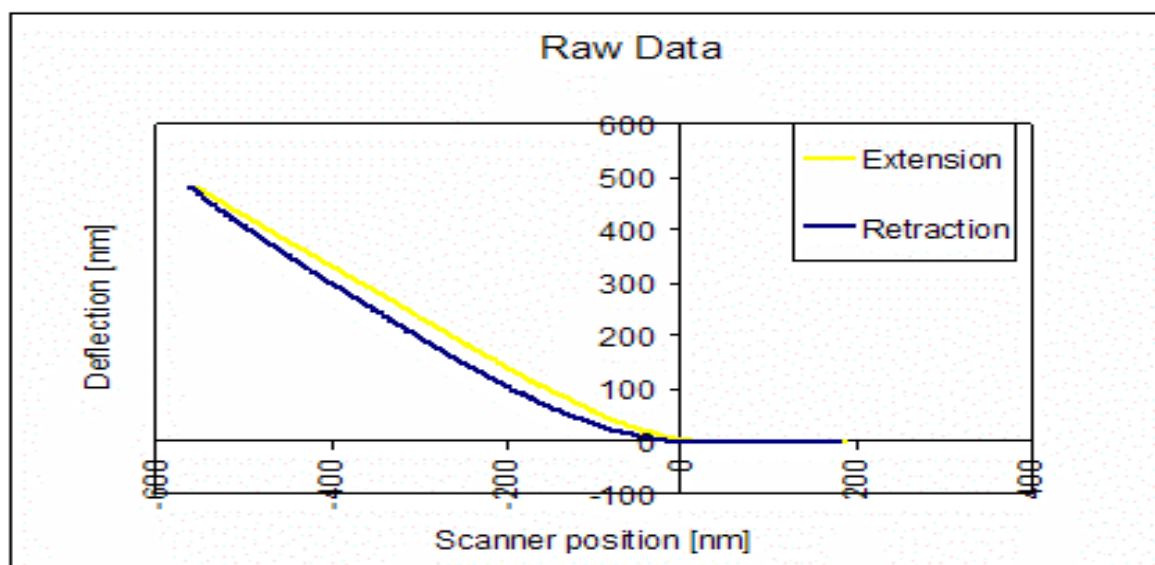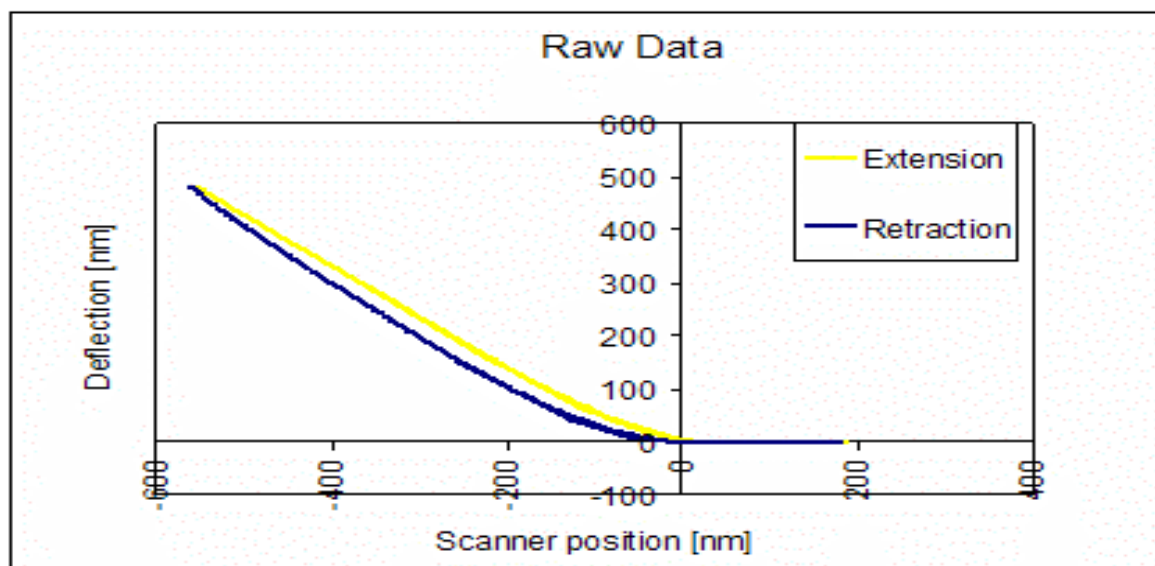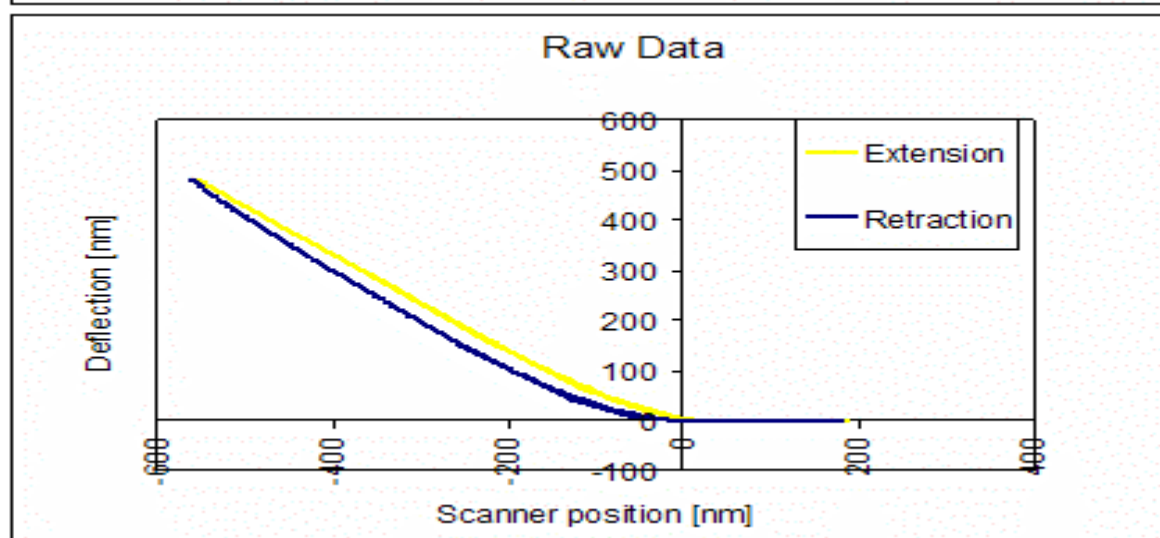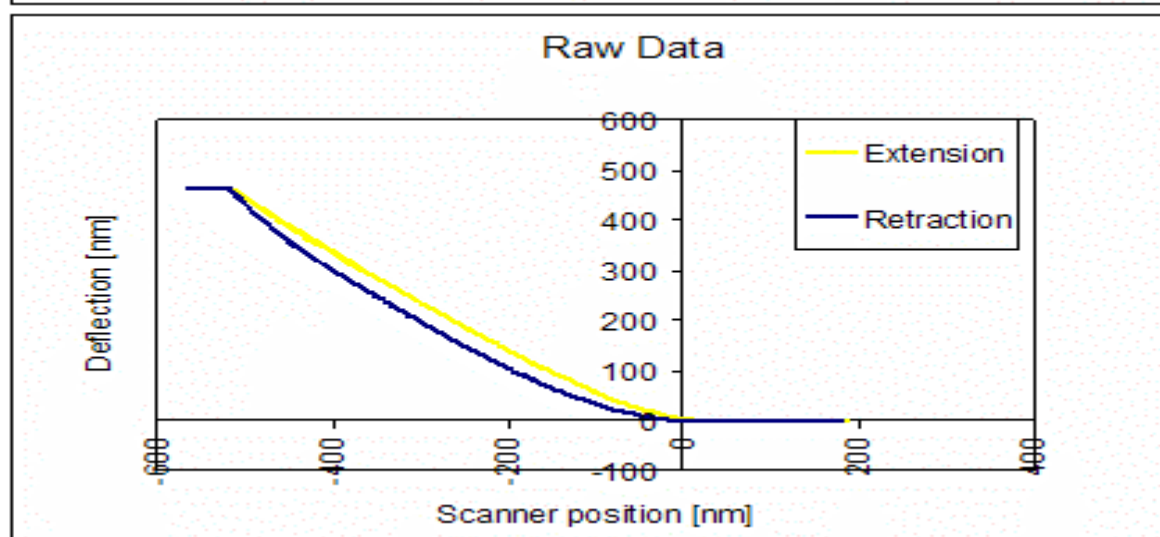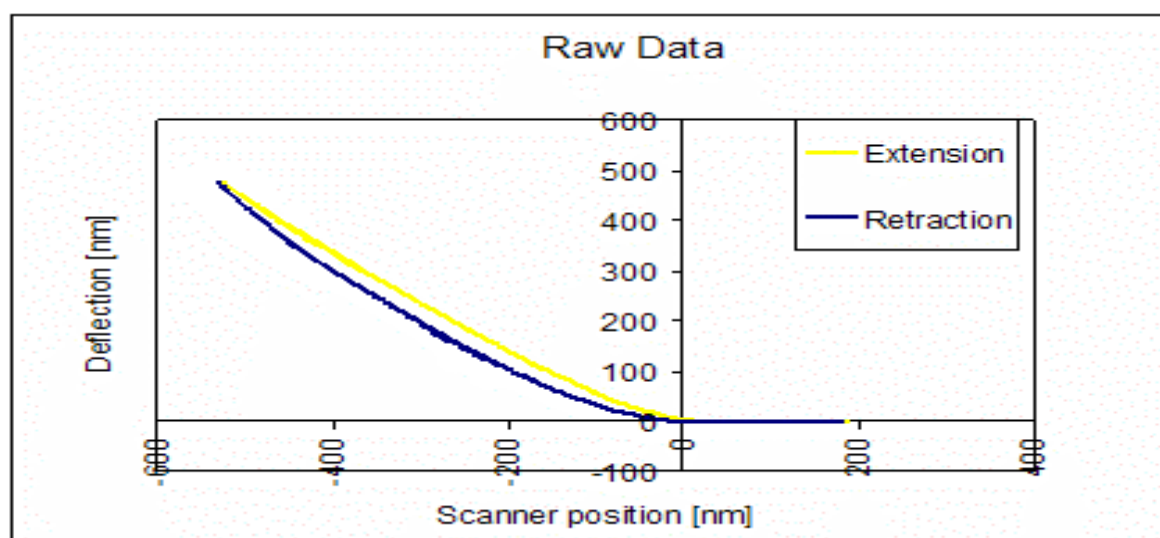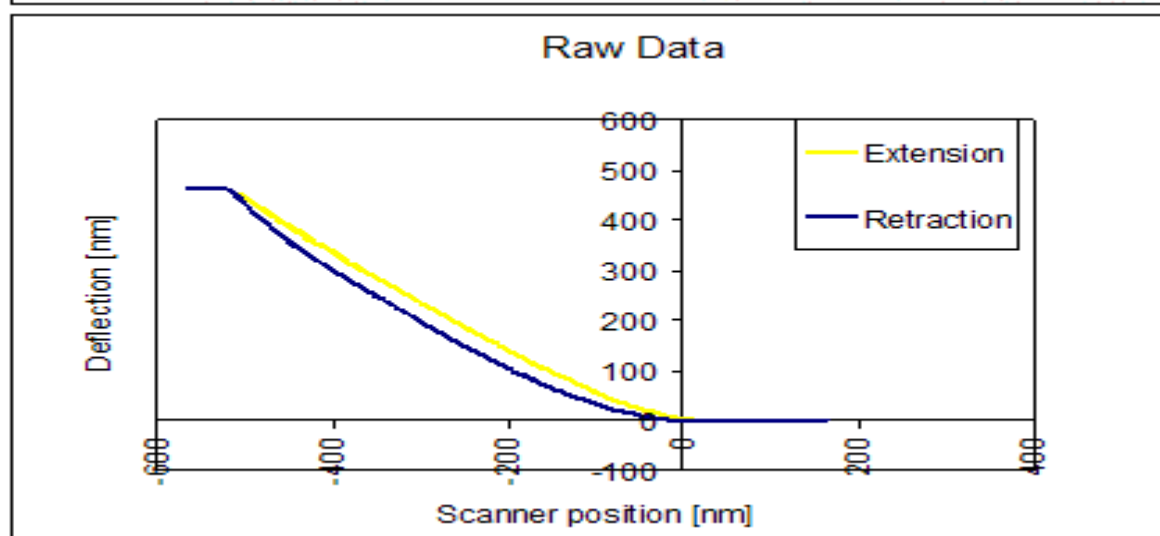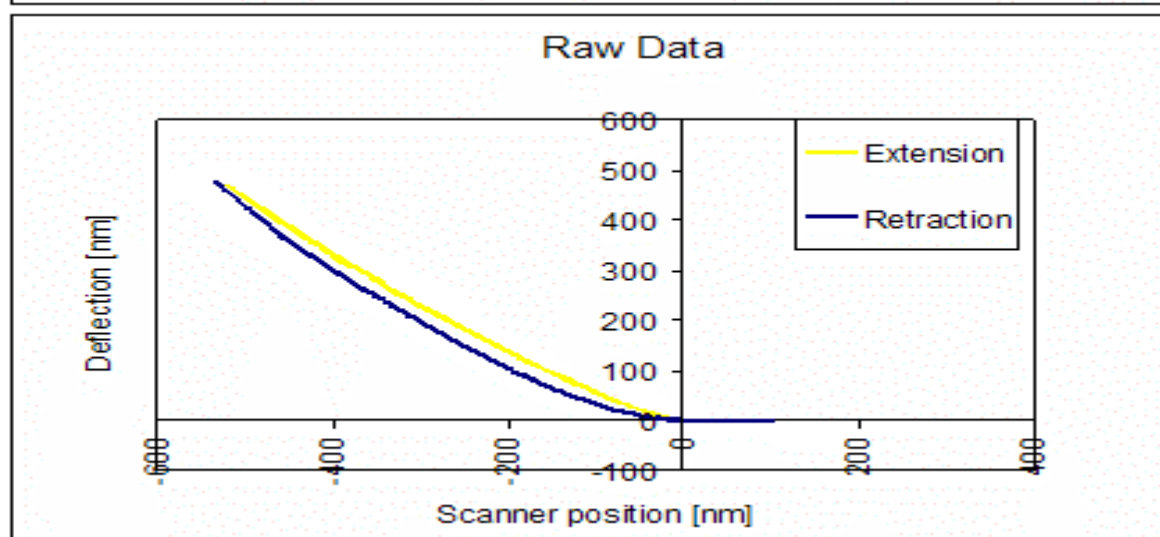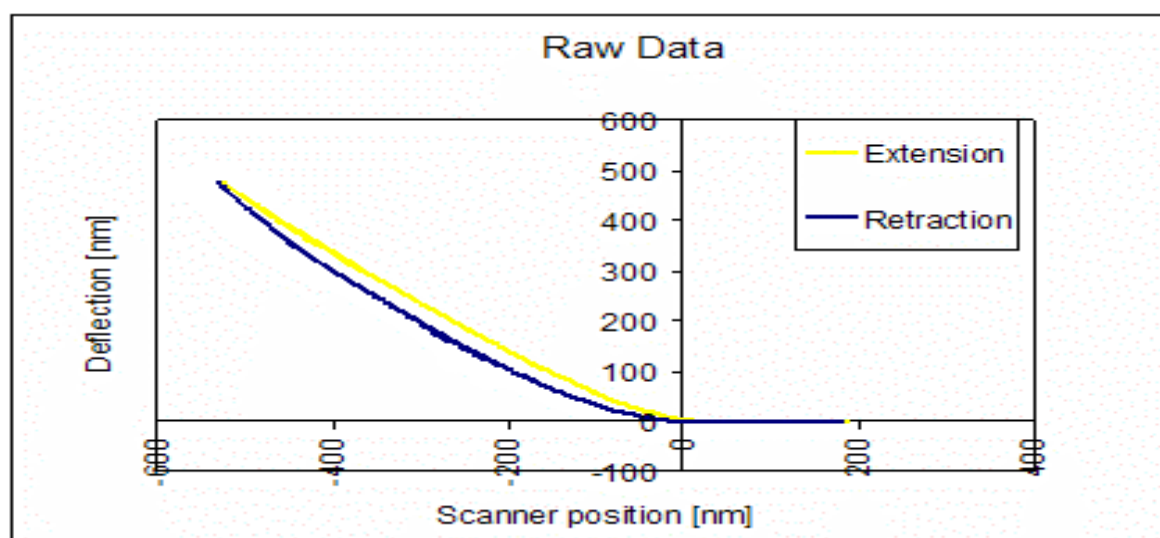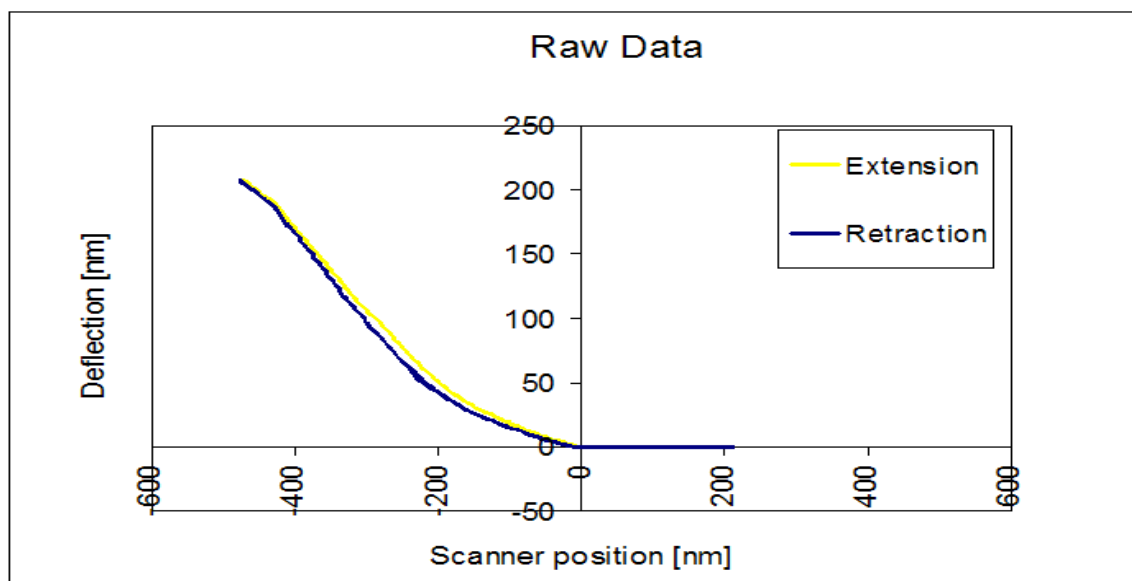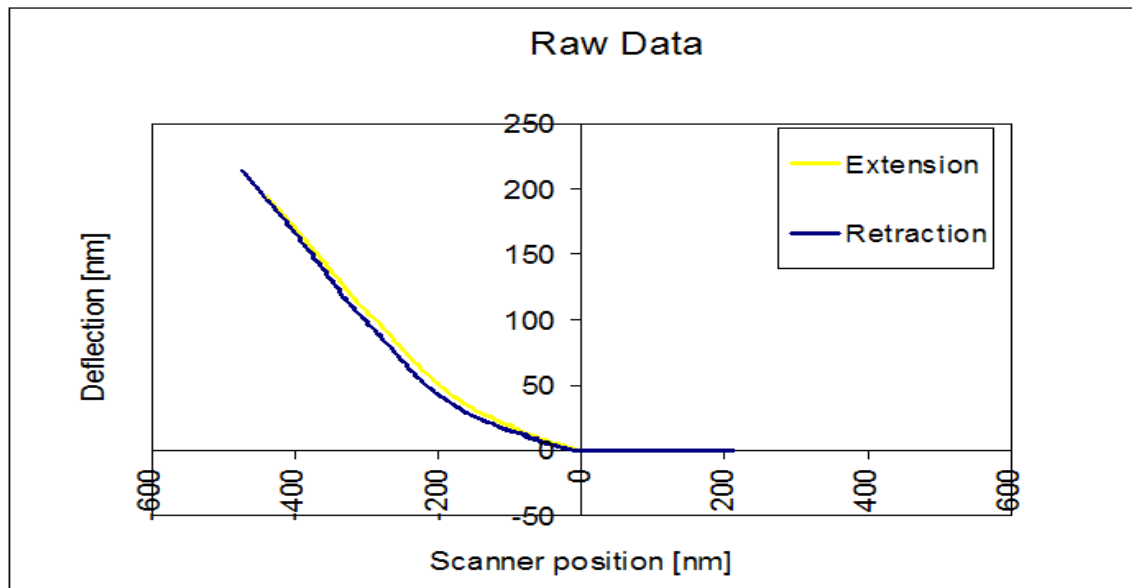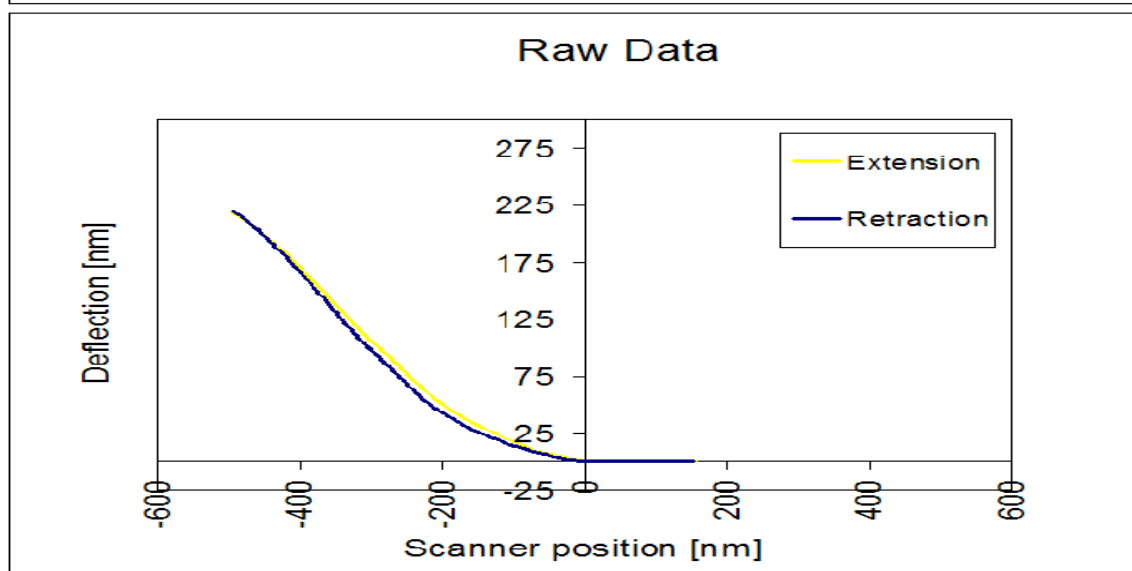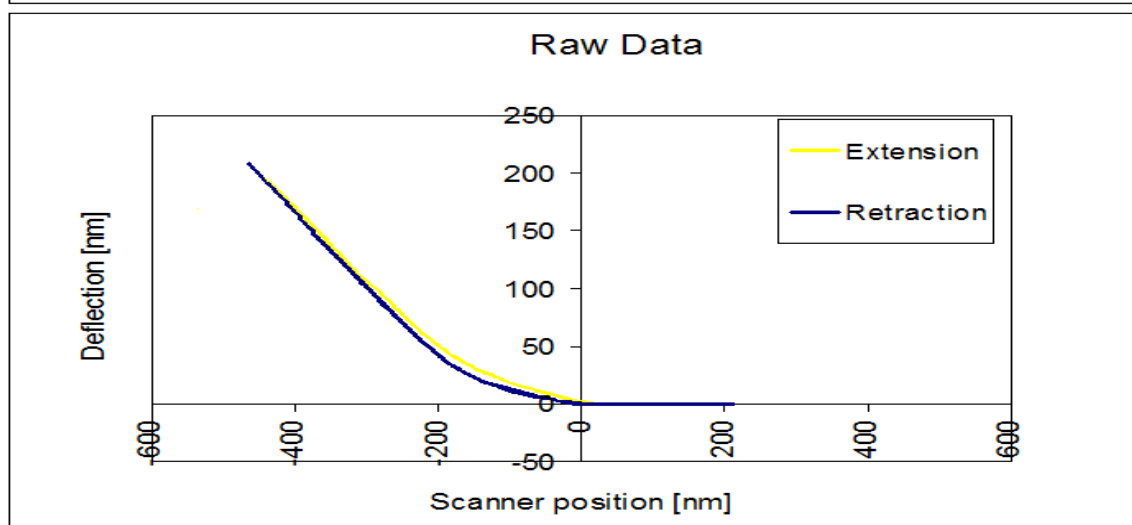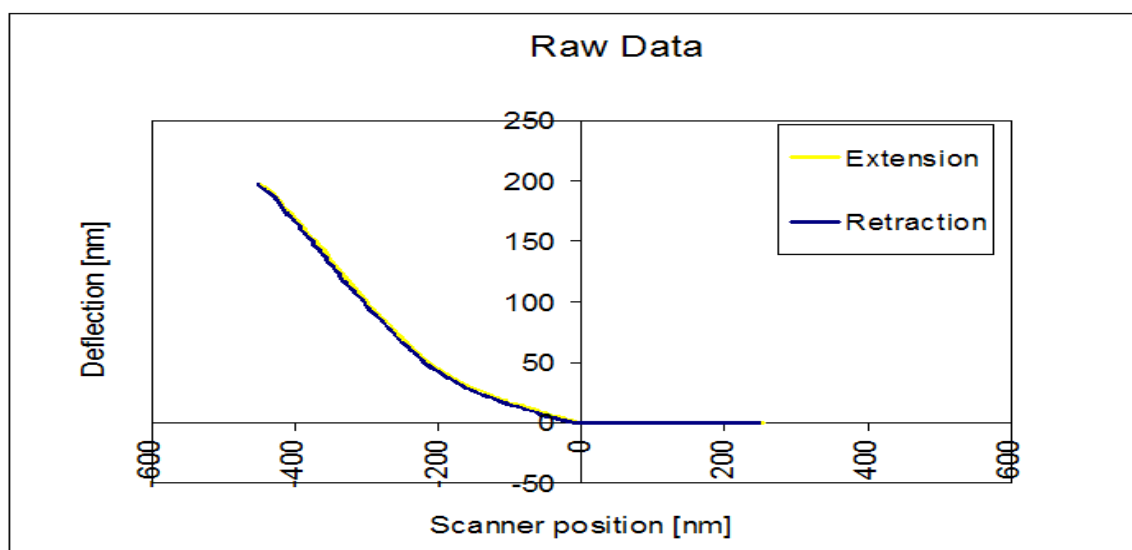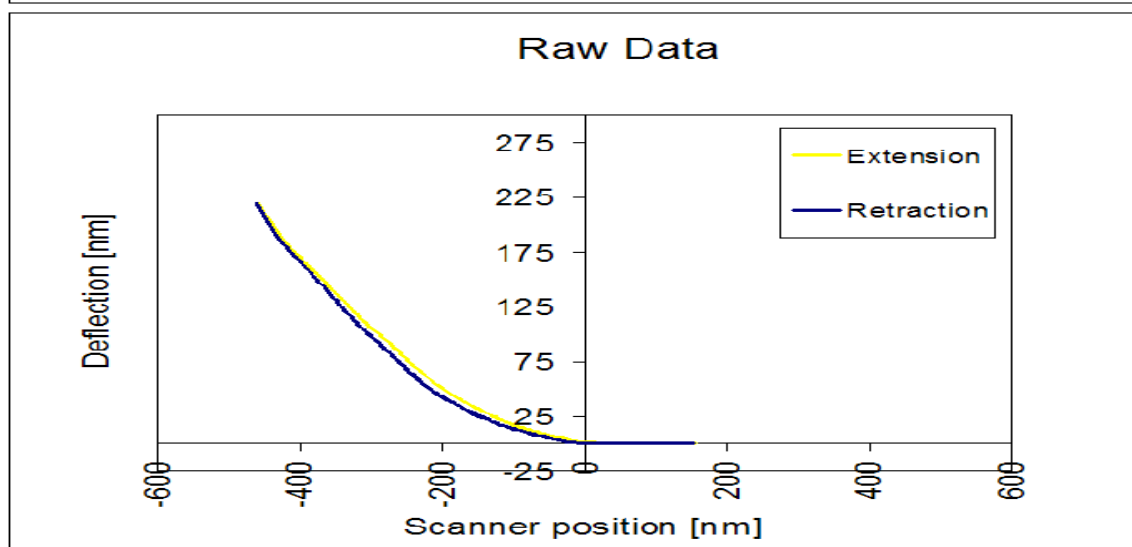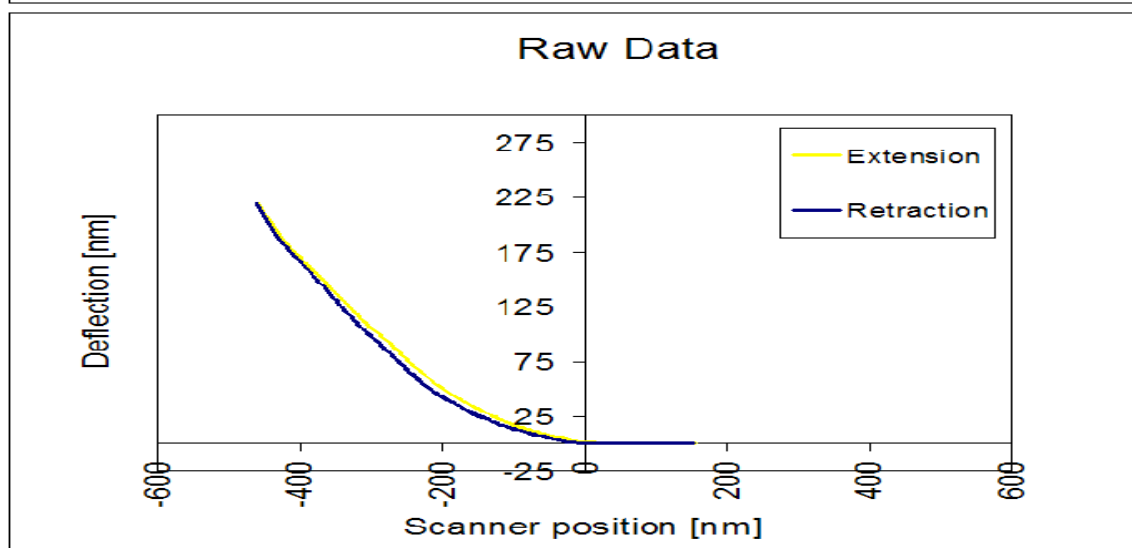
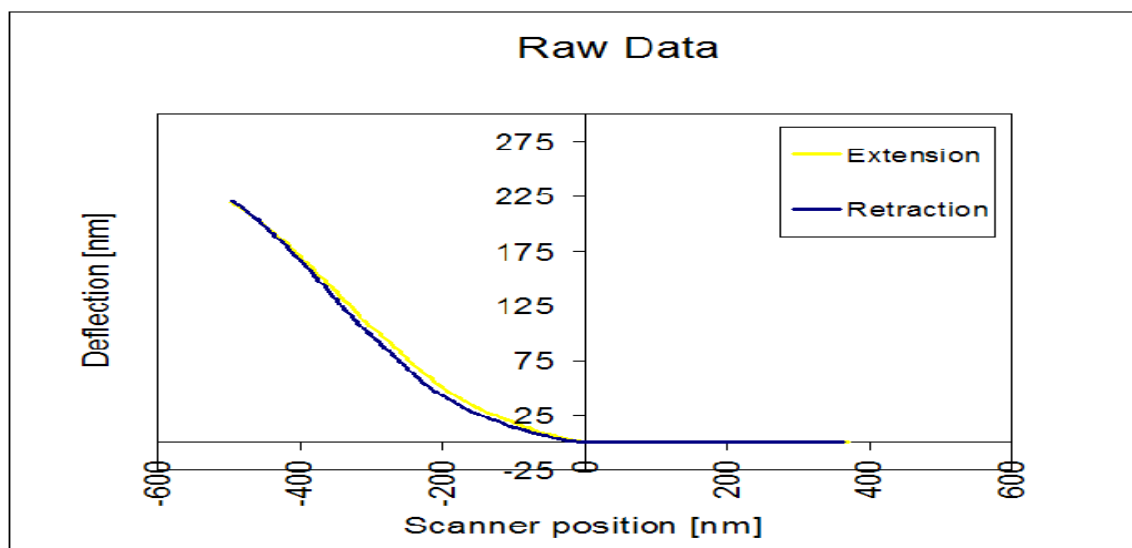### 10.5.   Uniaxial Tensile Testing

LabVIEW Program Instructions

INITIALIZE complete.vi

This program was designed to center the sample and the marker positions to be in the camera's line of sight. In the front panel, click the 'run' button on the menu. Adjust the contrast on the sliding bars in such a way that only the markers are present and they are in red. Then use the up and down buttons to move the sample up and down into the camera's viewing screen. The lamp is highly recommended to help the camera detect the contrast between the markers and the background color. Pull the sample in or out in such a way that the force read on the force transducer is as close to zero as possible. The value can be found in the front panel under the camera's viewing screen window.

 All four marker positions must be small enough to be present before and during the test. If one or more of the markers moved out of the viewing screen, the program will report and error message and none of the data points will be recorded. Once the sample is centered on the viewing screen and the force transducer is close to zero, click the stop 'button.' Record the final values on the contrast bars. These values will be used in the next program. Then close the program.

UNIAXIAL FINAL.vi

This program was designed to run the experiment. It was used for the biaxial, uniaxial, and stress relaxation test. Open the program and click on the tab options for the desired test. For the uniaxial tension test, click on the 'uniaxial' tab. Select the appropriate axis for the displacement direction. Then input the dimensions of the samples, the strain rate, the maximum strain, the number of cycles, the contrast values found from the previous program, and the arm length of the force transducer. After all of the required fields are complete, click 'run' button on the menu. The test will start. Click 'replace' in the popup window to replace old data in the spreadsheet file. The data from every test can be found in the file called 'sampledata' found on the desktop. To perform the stress relaxation test, click the stress relaxation tab. Input the required fields as in the uniaxial tension test. The program is set to 600 seconds of stretch time. This time can be adjusted in the block diagram of this program.

Below are results from each sample used to analyze the final results for Uniaxial Tension Test.

8/0.08% at 10% Strain: Sample P

Strain Rate	Stiffness	Avg.	STDEV	Uncertainty	% Error
0.01	24851	28406	1754.632	7.06%	6.2%
	28925			6.07%	
	28833			6.09%	
	29179			6.01%	
	29232			6.00%	
	29418			5.96%	
0.05	24735	22595	2324.505	9.40%	10.3%
	24855			9.35%	
	24370			9.54%	
	21522			10.80%	
	20075			11.58%	
	20011			11.62%	
0.1	30382	29189	1330.713	4.38%	4.6%
	28827			4.62%	
	30004			4.44%	
	28463			4.68%	
	30415			4.38%	
	27043			4.92%	

8/0.08% at 10% Strain: Sample Q

Strain Rate	Stiffness	Avg.	STDEV	Uncertainty	% Error
0.01	22782	24033	784.7995	3.44%	3.3%
	23758			3.30%	
	24046			3.26%	
	24027			3.27%	
	25169			3.12%	
	24418			3.21%	
0.05	23235	23976	889.3198	3.83%	3.7%
	24199			3.68%	
	25257			3.52%	
	24546			3.62%	
	22809			3.90%	
	23809			3.74%	
0.1	23625	22778	1200.786	5.08%	5.3%
	23266			5.16%	
	23244			5.17%	
	22758			5.28%	
	23380			5.14%	
	20396			5.89%	

8/0.08% at 10% Strain: Sample R

Strain Rate	Stiffness	Avg.	STDEV Total	Uncertainty	% Error

Strain Rate	Stiffness	AVG	STDEV	Uncertainty	%Error
0.01	23453 24567 25180 25033 24970 24665	24645	627.653	2.68% 2.55% 2.49% 2.51% 2.51% 2.54%	2.5%
0.05	21545 23812 23762 24210 24472 24256	23676	1079.095	5.01% 4.53% 4.54% 4.46% 4.41% 4.45%	4.6%
0.1	26183 24062 24064 22561 22162 20977	23335	1827.908	6.98% 7.60% 7.60% 8.10% 8.25% 8.71%	7.8%

8/0.08% at 10% Strain: Sample G

Strain Rate	Stiffness	AVG	STDEV	Uncertainty	%Error
0.01	21901 23453 23407 24859 25684 26700	24334	1746	8.0% 7.4% 7.5% 7.0% 6.8% 6.5%	7.2%
0.05	19290 21801 22095 21291 20063 21092	20939	1069	5.5% 4.9% 4.8% 5.0% 5.3% 5.1%	5.1%
0.1	27869 26580 25270 25174 24767 24809	25745	1233	4.4% 4.6% 4.9% 4.9% 5.0% 5.0%	4.8%

8/0.08% at 10% Strain: Sample O

Strain Rate	Stiffness	AVG	STDEV	Uncertainty	%Error
0.01	27012 22602 29782 25261 26322	26235	2340	8.7% 10.4% 7.9% 9.3% 8.9%	8.9%

				8.9%	
	17067			22.9%	
	22289			17.6%	
0.05	23831	22217	3914	16.4%	17.6%
	17987			21.8%	
	26052			15.0%	
	26073			15.0%	
	29819			9.7%	
	25951			11.1%	
0.1	23880	27806	2884	12.1%	10.4%
	30974			9.3%	
	30162			9.6%	
	26049			11.1%	

8/0.08% at 10% Strain: Sample J

Strain Rate	Stiffness	AVG	STDEV	Uncertainty	%Error
	19525			4.5%	
	20408			4.3%	
0.01	20481	20379	876	4.3%	4.3%
	19285			4.5%	
	20933			4.2%	
	21643			4.0%	
	15952			6.5%	
	18063			5.7%	
0.05	18557	17949	1032	5.6%	5.7%
	17849			5.8%	
	18636			5.5%	
	18637			5.5%	
	18778			3.6%	
	19491			3.4%	
0.1	20254	19938	670	3.3%	3.4%
	20217			3.3%	
	20504			3.3%	
	20384			3.3%	

8/0.08% at 10% Strain: Sample T

Strain Rate	Stiffness	Avg.	STDEV	Uncertainty	% Error
	2021			14.72%	
	2463			12.07%	
0.01	2466	2544	297.3467	12.06%	11.7%
	2762			10.76%	
	2773			10.72%	
	2780			10.70%	
0.05	2060	2264	441.9792	21.45%	19.5%
	2365			18.69%	
	2072			21.33%	

Strain Rate	Stiffness	Avg	STDEV	Uncertainty	% Error
	1607			27.50%	
	2786			15.86%	
	2693			16.41%	
0.1	3633	3400	525.2454	14.46%	15.4%
	3809			13.79%	
	3567			14.72%	
	3905			13.45%	
	2827			18.58%	
	2661			19.74%	

8/0.08% at 10% Strain: Sample U

Strain Rate	Stiffness	Avg	STDEV	Uncertainty	% Error
	3318			4.21%	
	2969			4.70%	
0.01	3368	3224	139.695	4.15%	4.3%
	3222			4.34%	
	3197			4.37%	
	3271			4.27%	
	2593			10.85%	
	2998			9.38%	
0.05	3134	3101	281.2861	8.98%	9.1%
	3321			8.47%	
	3201			8.79%	
	3361			8.37%	
	2638			14.64%	
	3020			12.79%	
0.1	2199	2833	386.1409	17.56%	13.6%
	3204			12.05%	
	2748			14.05%	
	3188			12.11%	

8/0.08% at 10% Strain: Sample V

Strain Rate	Stiffness	Avg	STDEV	Uncertainty	% Error
	1810			12.25%	
	2442			9.08%	
0.01	2200	2069	221.7749	10.08%	10.7%
	1958			11.33%	
	1974			11.23%	
	2032			10.91%	
	1478			20.36%	
	1767			17.03%	
0.05	1971	1909	300.9828	15.27%	15.8%
	1880			16.01%	
	1961			15.35%	
	2399			12.55%	

Strain Rate	Stiffness	Avg	STDEV	Uncertainty	% Error
	1869			23.60%	
	2838			15.54%	
0.1	3001	2712	440.9633	14.69%	16.3%
	2597			16.98%	
	2981			14.79%	
	2988			14.76%	

8/0.08% at 10% Strain: Sample W

Strain Rate	Stiffness	Avg	STDEV	Uncertainty	% Error
	1860			21.59%	
	2651			15.15%	
0.01	2899	2443	401.5897	13.85%	16.4%
	2757			14.57%	
	2107			19.06%	
	2382			16.86%	
	2556			13.19%	
	3352			10.06%	
0.05	3371	3100	337.1767	10.00%	10.9%
	3072			10.98%	
	3386			9.96%	
	2867			11.76%	
	3166			15.69%	
	2992			16.61%	
0.1	3636	3646	496.9156	13.67%	13.6%
	3797			13.09%	
	3973			12.51%	
	4314			11.52%	

8/0.08% at 10% Strain: Sample X

Strain Rate	Stiffness	Avg	STDEV	Uncertainty	% Error
	3481			8.91%	
	3473			8.93%	
0.01	2902	3182	310.0252	10.68%	9.7%
	2718			11.40%	
	3285			9.44%	
	3232			9.59%	
	2805			9.55%	
	3251			8.24%	
0.05	3501	3181	267.8121	7.65%	8.4%
	3371			7.95%	
	3244			8.26%	
	2916			9.18%	
0.1	4280	5308	545.939	12.76%	10.3%
	5129			10.64%	
	5532			9.87%	

	5635			9.69%	
	5517			9.89%	
	5756			9.49%	

8/0.08% at 10% Strain: Sample Y

Strain Rate	Stiffness	Avg	STDEV	Uncertainty	% Error
0.01	(Outlier)344	1899	174.9096	50.85%	9.2%
	2486			7.04%	
	2231			7.84%	
	2145			8.15%	
	2008			8.71%	
	2178			8.03%	
0.05	2366	3426	573.9224	24.26%	16.8%
	3352			17.12%	
	4027			14.25%	
	3647			15.74%	
	3409			16.83%	
	3755			15.28%	
0.1	3884	5318	771.7644	19.87%	14.5%
	5037			15.32%	
	5905			13.07%	
	5708			13.52%	
	5499			14.03%	
	5879			13.13%	

Summary of results

Bis/Acrylamide	Sample	Young's Modulus (kPa)	STDEV (kPa)	Average E	STDEV	%Error
8/0.08%	G	23.7	2.5	23.8	2.5	10.37%
	O	25.4	2.9			
	J	19.4	1.3			
	P	26.7	3.6			
	Q	23.6	0.7			
	R	23.9	0.7			
5/0.025%	T	2.7	0.6	3.1	0.6	19.29%
	U	3.1	0.2			
	V	2.2	0.4			
	W	3.1	0.6			
	X	3.9	1.2			
	Y	3.5	1.7			

Range of Results		
Bis/Acrylamide	Stiffness Range (kPa)	Poisson'sRatio
8/0.08%	19-25	0.45±0.5
5/0.025%	2-4	

Q-Test

A Q-test was used to determine whether if the stiffness value obtained within a group is an outlier. Due to the mathematical and statistical equations involved in a Q-Test, the test was used to determine only one suspicious outlier stiffness value out of one set of strain rate. Below is the mathematical steps used to determine outlier. When there are six samples (N=6), the $Q_{Critital}$ value is equal to 0.56. If the result from Q test is greater than or equal to the $Q_{Critical}$ value, the suspicious data point is indeed an outlier.

The equation for Q-Test is;

$$\frac{|\text{suspicious value} - \text{value cloesest to the suspicious value}|}{\text{Range}} = Q$$

The Q test was applied to a set of stiffness values only when the percent error for each strain rate exceeded 20%.

Sample Y

A Q-Test was used to determine whether if the stiffness value 344 is an outlier in the group of six stiffness values at 0.01 strain rate.

$$\frac{|344 - 2008|}{2486 - 344} = 0.77$$

Therefore, the stiffness value 344 was omitted from the calculation.

SPSS results for both concentrations.

Univariate Analysis of Variance
Between-Subjects Factors

		Value Label	N
5/0.025%	7	T	18
	8	U	18
	9	V	18
	10	W	18
	11	X	18
	12	Y	17
Strain Rate	1	0.01	35
	2	0.05	36
	3	0.1	36

Descriptive Statistics

Dependent Variable: Stiffness

5/0.025%	Strain Rate	Mean	Std. Deviation	N
T	0.01	2543.950	297.3467	6
	0.05	2263.933	441.9792	6
	0.1	3400.117	525.2454	6
	Total	2736.000	641.8220	18
U	0.01	3224.300	139.6950	6
	0.05	3101.467	281.2861	6
	0.1	2832.583	386.1409	6
	Total	3052.783	318.1161	18
V	0.01	2069.350	221.7749	6
	0.05	1909.283	300.9828	6
	0.1	2712.183	440.9633	6
	Total	2230.272	475.1548	18
W	0.01	2442.667	401.5897	6
	0.05	3100.433	337.1767	6
	0.1	3646.200	496.9156	6
	Total	3063.100	640.1957	18
X	0.01	3181.700	310.0252	6
	0.05	3181.183	267.8121	6
	0.1	5308.117	545.9390	6
	Total	3890.333	1095.9935	18
Y	0.01	2209.640	174.9096	5
	0.05	3426.033	573.9224	6
	0.1	5318.417	771.7644	6
	Total	3736.171	1414.1476	17
Total	0.01	2623.429	519.1409	35
	0.05	2830.389	658.1503	36
	0.1	3869.603	1194.3030	36
	Total	3112.334	1000.5596	107

Tests of Between-Subjects Effects

Dependent Variable: Stiffness

Source	Type III Sum of Squares	df	Mean Square	F	Sig.
Corrected Model	90724333.472(a)	17	5336725.498	30.853	.000
Intercept	1029109069.568	1	1029109069.568	5949.639	.000
@50.025	32438208.357	5	6487641.671	37.507	.000
StrainRate_A	32228800.490	2	16114400.245	93.163	.000
@50.025 * StrainRate_A	25265741.635	10	2526574.163	14.607	.000
Error	15394330.407	89	172970.005		
Total	1142587080.590	107			

Corrected Total	106118663.879	106			

a R Squared = .855 (Adjusted R Squared = .827)

Estimated Marginal Means
5/0.025%

Dependent Variable: Stiffness

5/0.025%	Mean	Std. Error	95% Confidence Interval	
			Lower Bound	Upper Bound
T	2736.000	98.028	2541.221	2930.779
U	3052.783	98.028	2858.004	3247.562
V	2230.272	98.028	2035.493	2425.051
W	3063.100	98.028	2868.321	3257.879
X	3890.333	98.028	3695.554	4085.112
Y	3651.363	101.243	3450.196	3852.530

Univariate Analysis of Variance
Between-Subjects Factors

		Value Label	N
Strain Rate	1	0.01	36
	2	0.05	36
	3	0.1	36
8/0.08%	1	P	18
	2	Q	18
	3	R	18
	4	G	18
	5	O	18
	6	J	18

Descriptive Statistics

Dependent Variable: Stiffness

Strain Rate	8/0.08%	Mean	Std. Deviation	N
0.01	P	28406.33	1754.632	6
	Q	24033.33	784.800	6
	R	24644.67	627.653	6
	G	24333.91	1746.307	6
	O	26234.91	2339.949	6
	J	20379.10	876.348	6
	Total	24672.04	2823.102	36
0.05	P	22594.67	2324.505	6
	Q	23975.83	889.320	6
	R	23676.17	1079.095	6
	G	20938.66	1068.954	6
	O	22216.62	3914.259	6
	J	17949.11	1031.871	6
	Total	21891.84	2787.305	36

0.1	P	29189.00	1330.713	6
	Q	22778.17	1200.786	6
	R	23334.83	1827.908	6
	G	25744.74	1232.521	6
	O	27805.89	2883.770	6
	J	19938.12	669.905	6
	Total	24798.46	3539.860	36
Total	P	26730.00	3489.571	18
	Q	23595.78	1091.942	18
	R	23885.22	1329.275	18
	G	23672.44	2446.966	18
	O	25419.14	3798.404	18
	J	19422.11	1361.629	18
	Total	23787.45	3326.139	108

Tests of Between-Subjects Effects

Dependent Variable: Stiffness

Source	Type III Sum of Squares	df	Mean Square	F	Sig.
Corrected Model	908227482.502(a)	17	53425146.030	17.451	.000
Intercept	61111006363.850	1	61111006363.850	19961.141	.000
StrainRate	194326925.003	2	97163462.501	31.737	.000
@80.08	547860962.004	5	109572192.401	35.790	.000
StrainRate * @80.08	166039595.495	10	16603959.550	5.423	.000
Error	275534883.851	90	3061498.709		
Total	62294768730.203	108			
Corrected Total	1183762366.353	107			

a R Squared = .767 (Adjusted R Squared = .723)

The Poisson's Ratios were found from each test and each sample. The table below shows the sample name and its corresponding Poisson's ratio from every test.

Poisson's Ratio											
G	J	O	P	Q	R	T	U	V	Y	W	X
0.5	0.37	0.36	0.49	0.47	0.48	0.5	0.49	0.46	0.45	0.43	0.38
0.48	0.33	0.35	0.49	0.49	0.47	0.49	0.48	0.48	0.44	0.43	0.39
0.48	0.38	0.35	0.49	0.49	0.47	0.49	0.49	0.5	0.44	0.41	0.41
0.5	0.43	0.38	0.48	0.5	0.48	0.5	0.49	0.53	0.48	0.44	0.42
0.53	0.4	0.37	0.49	0.52	0.47	0.51	0.49	0.51	0.46	0.43	0.4
0.51	0.4	0.39	0.49	0.49	0.47	0.52	0.49	0.49	0.51	0.42	0.39
0.5	0.38	0.34	0.41	0.45	0.48	0.51	0.49	0.5	0.46	0.44	0.4
0.5	0.31	0.32	0.41	0.49	0.48	0.5	0.49	0.5	0.43	0.46	0.4
0.48	0.32	0.31	0.4	0.46	0.47	0.48	0.49	0.51	0.51	0.44	0.4

0.47	0.32	0.31	0.38	0.48	0.48	0.47	0.49	0.48	0.53	0.45	0.41	
0.48	0.31	0.29	0.37	0.47	0.47	0.47	0.5	0.49	0.51	0.45	0.4	
0.49	0.32	0.35	0.33	0.46	0.47	0.49	0.5	0.49	0.52	0.45	0.4	
0.38	0.37	0.37	0.48	0.47	0.47	0.51	0.49	0.49	0.48	0.46	0.37	
0.37	0.35	0.36	0.46	0.47	0.45	0.49	0.5	0.5	0.47	0.46	0.4	
0.44	0.37	0.36	0.45	0.44	0.44	0.48	0.5	0.5	0.45	0.45	0.41	
0.45	0.38	0.35	0.43	0.44	0.45	0.49	0.49	0.49	0.45	0.45	0.44	
0.44	0.36	0.32	0.43	0.43	0.44	0.46	0.5	0.5	0.44	0.43	0.45	
0.45	0.35	0.38	0.41	0.43	0.43	0.47	0.5	0.5	0.41	0.43	0.44	
0.47	0.36	0.35	0.44	0.47	0.47	0.49	0.49	0.50	0.47	0.44	0.41	**Avg. sample**

0.45	**Average Total**
0.05	**stdev.**

Stress Relaxation Test Results

Stress Relaxation 5/0.025% Polyacrylamide Gel
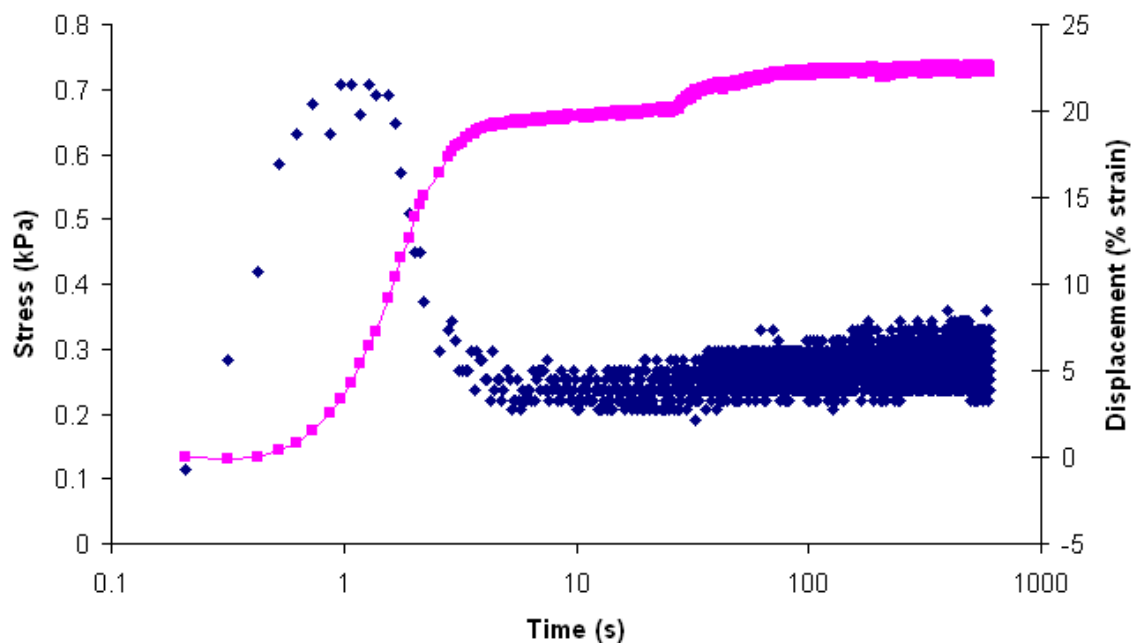
Stress Relaxation 5/0.025% Polyacrylamide Gel
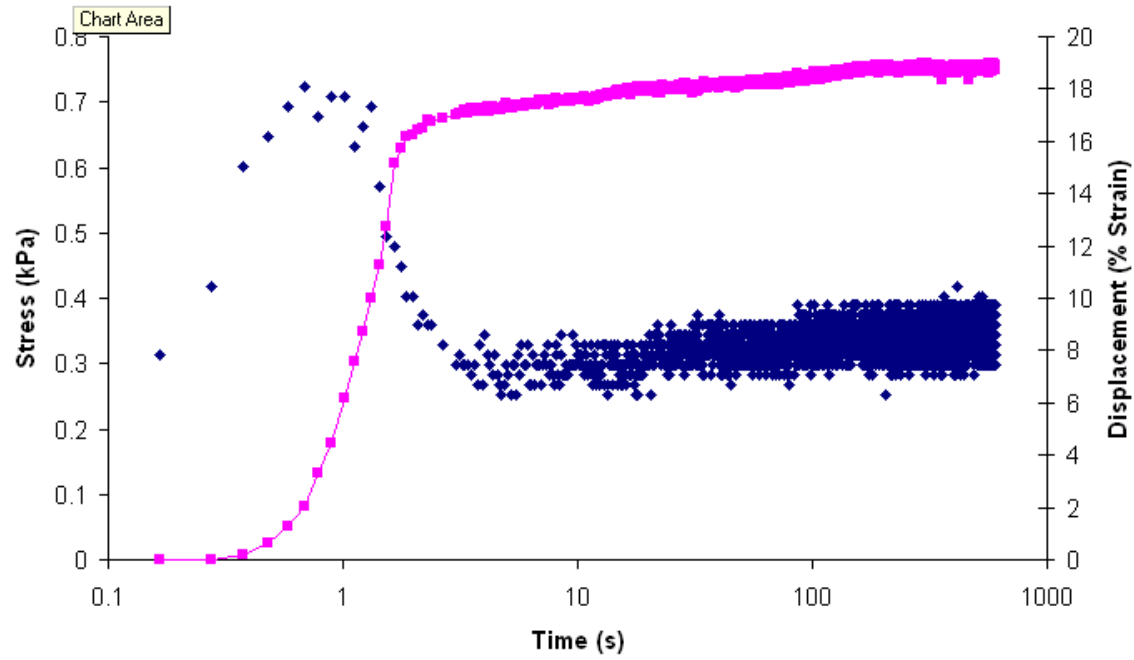
Stress Relaxation Test
5/0.025% Polyacrylamide Gel
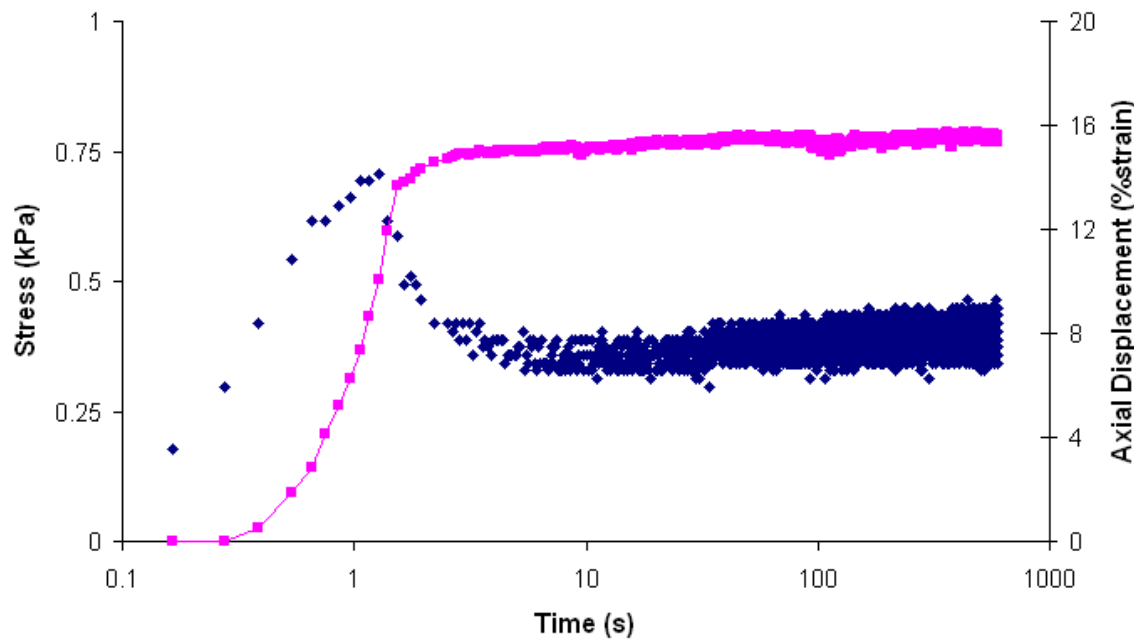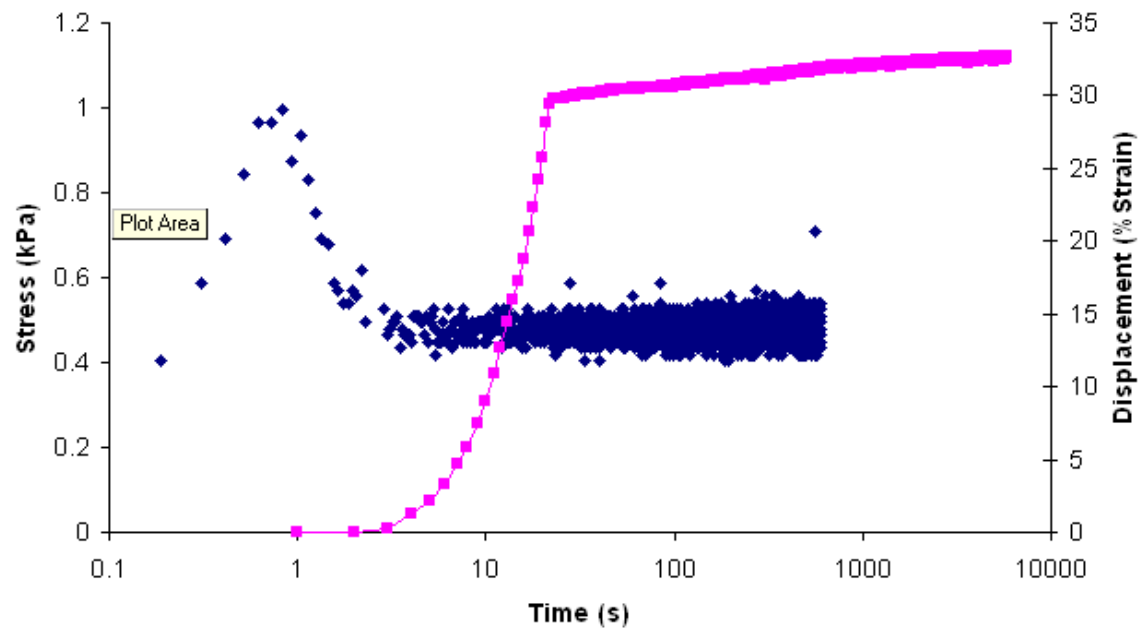
119

Stress Relaxation 5/0.025% Polyacrylamide Gel

Stress Relaxation Test 8/0.08% Polyacrylamide Gel
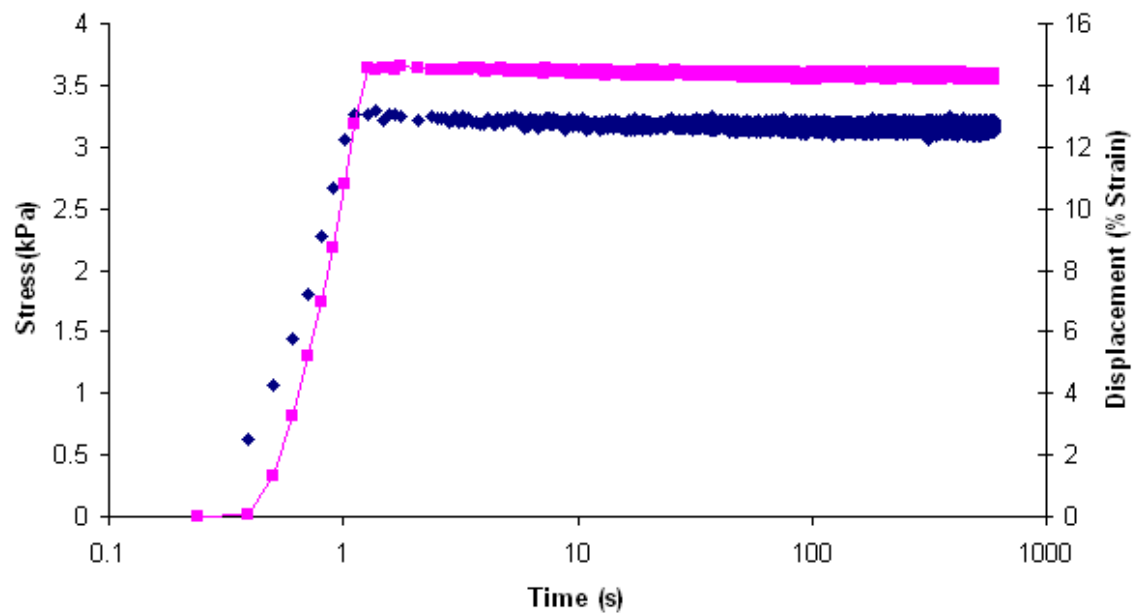
Stress Relaxation Test 8/0.08% Polyacrylamide Gel
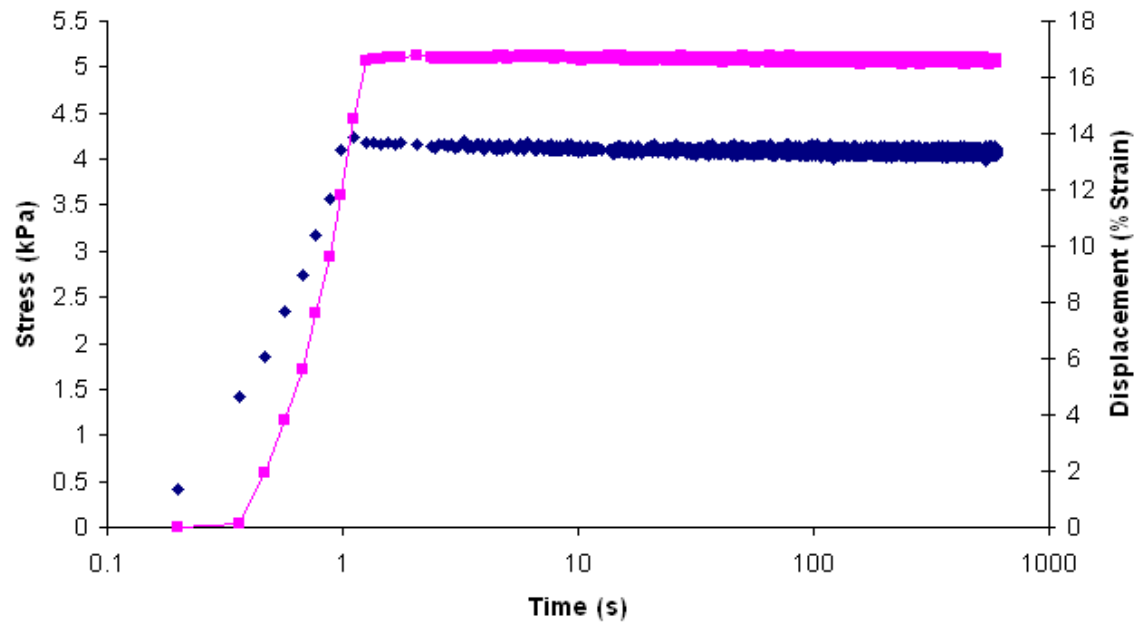
Stress Relaxation Test
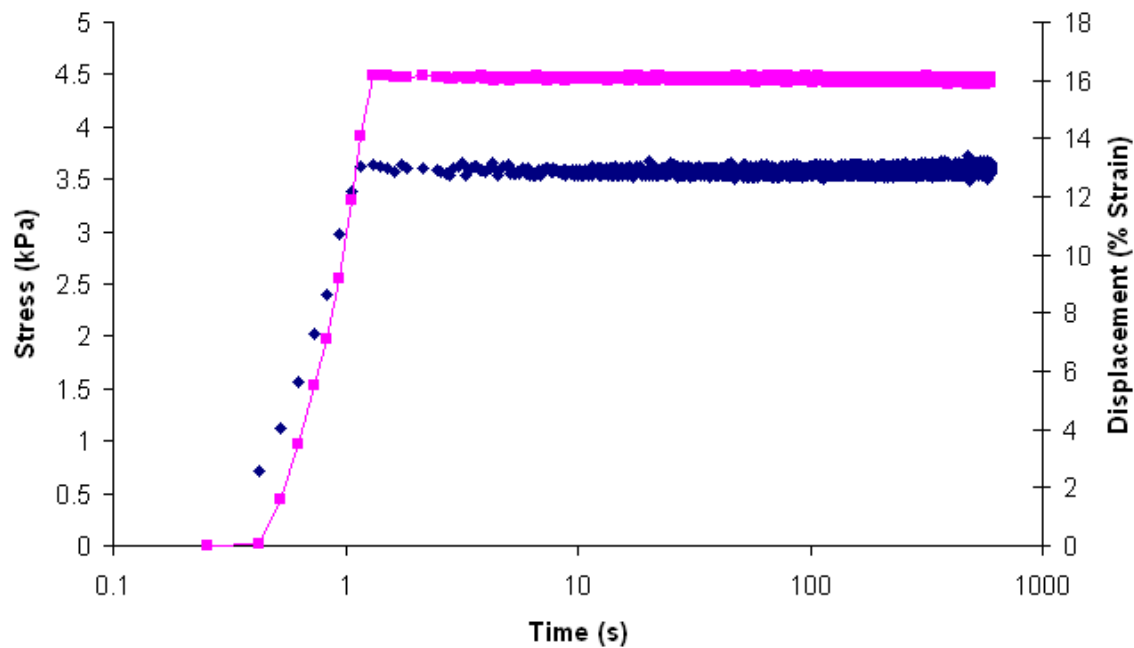
Stress Relaxation Test 8/0.08% Polyacrylamide Gel
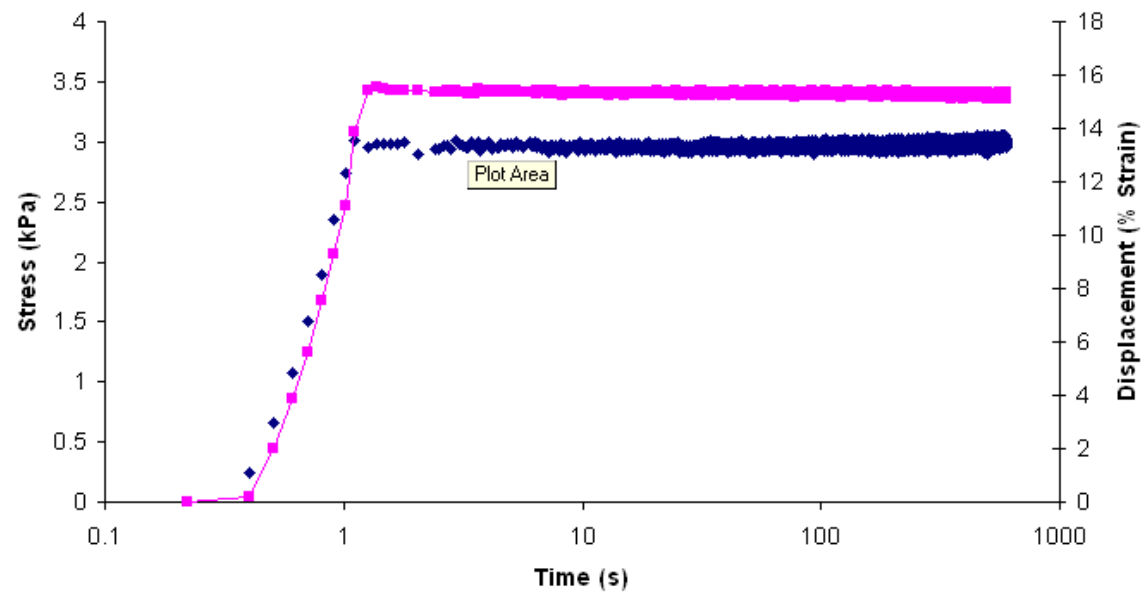
10.6.   Rheology

Initial Data for Rheometry: The following results were produced using polyacrylamide gels which were polymerized in open petri dishes. As discussed within the report, polymerizing the polyacrylamide gels within a closed glass plate environment produces more reliable results. These results still prove that the material is predominately elastic with consistent high G' values and low G" values. The phase angles are also below 10°, also indicating a high degree of elasticity.

Time sweep test 8%/0.08% (a)
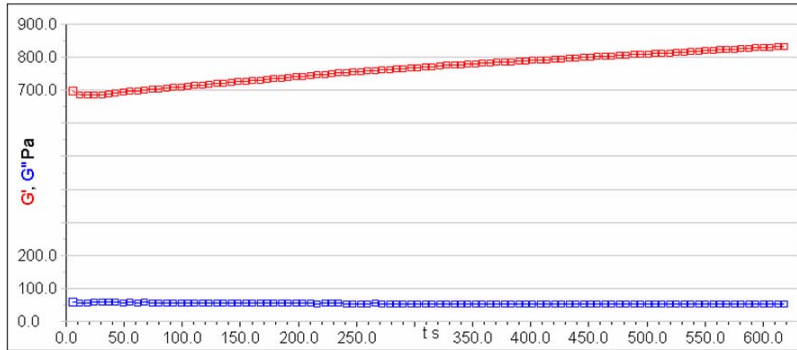
Strain sweep test 8%/0.08% (a)
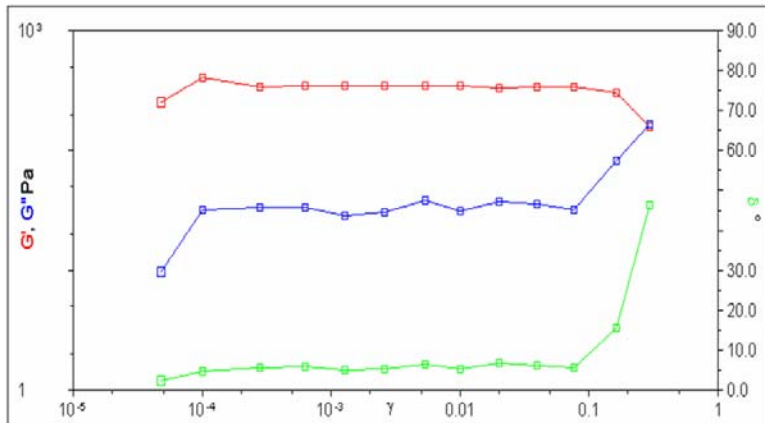
Time sweep test 5%/0.025% (a)
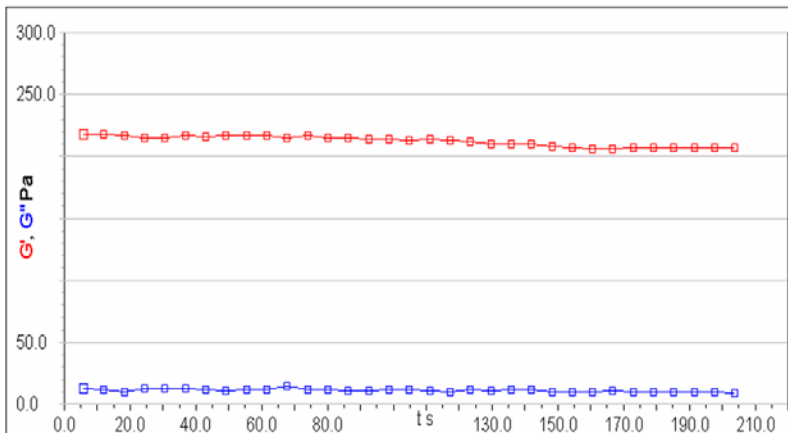
Strain sweep test 5%/0.025% (a)
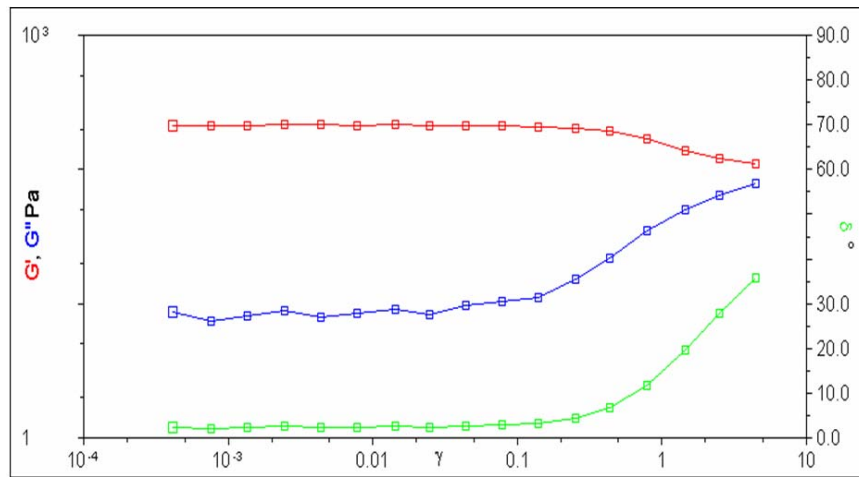
Frequency sweep test 5%/0.025% (a) (squares) and 8%/0.08% (a) (triangles)
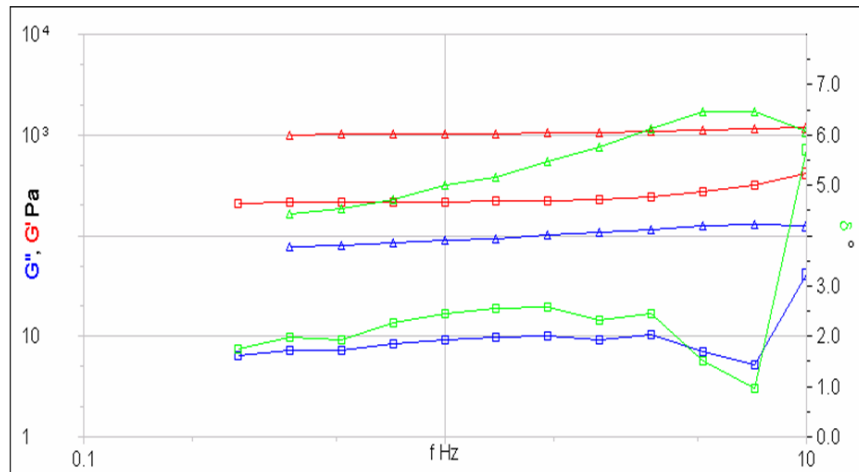
Time sweep test 5%/0.12% (a)
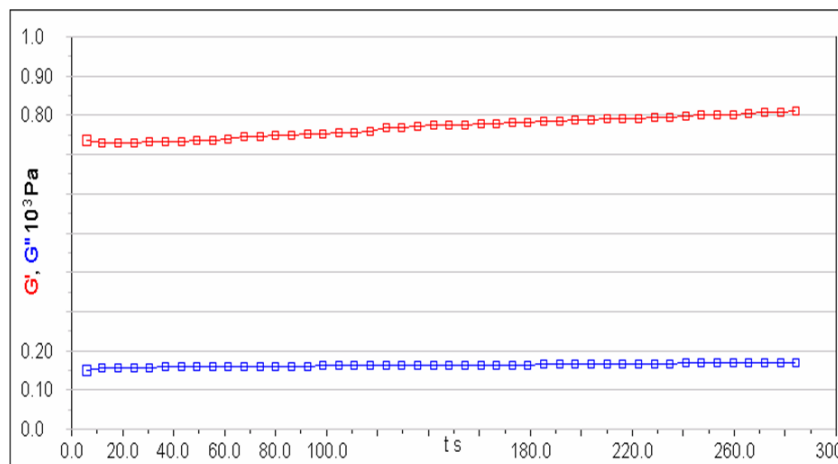
Frequency sweep test 5%/0.12% (a)
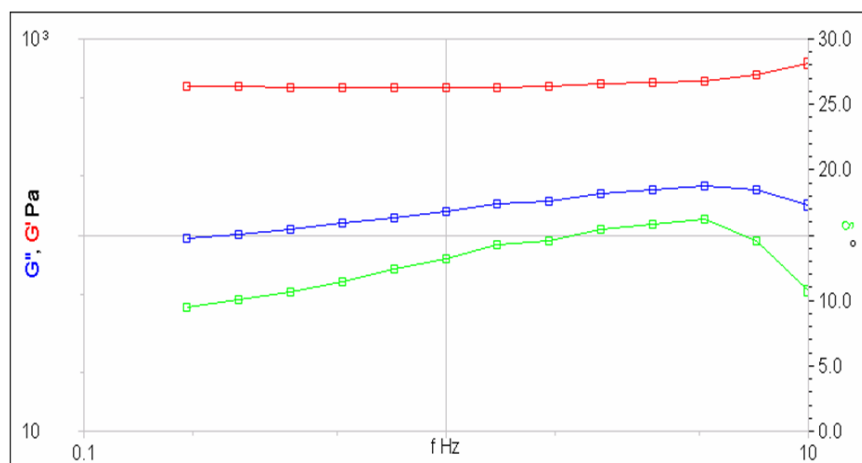
Strain sweep test 5%/0.12% (a)
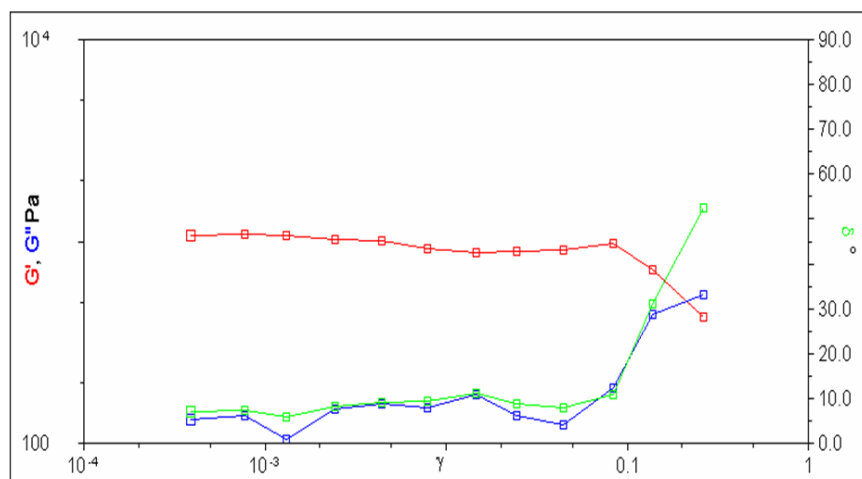
The next 21 samples represent gels tested with both the smooth and serrated parallel plate methods. The results are summarized in table format.

Time sweep test 5%/0.025% (a)
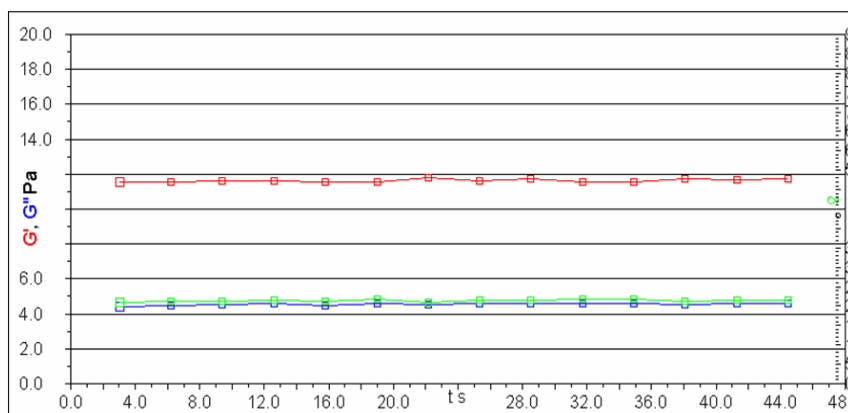
Frequency sweep test 5%/0.025% (a)
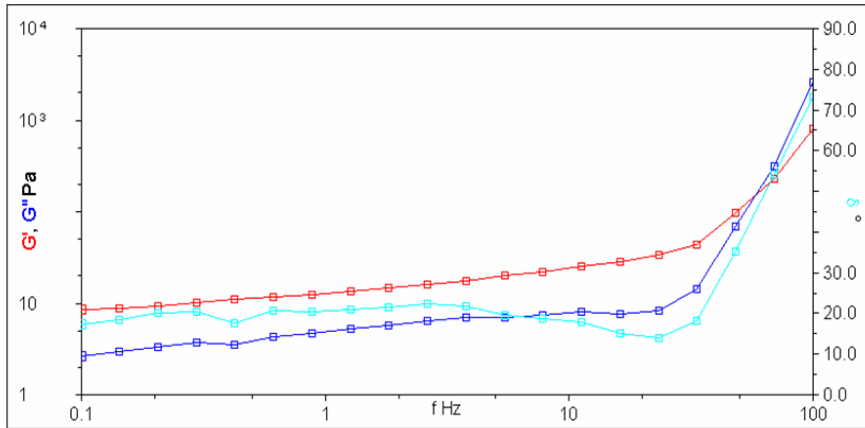
Strain sweep test 5%/0.025% (a)
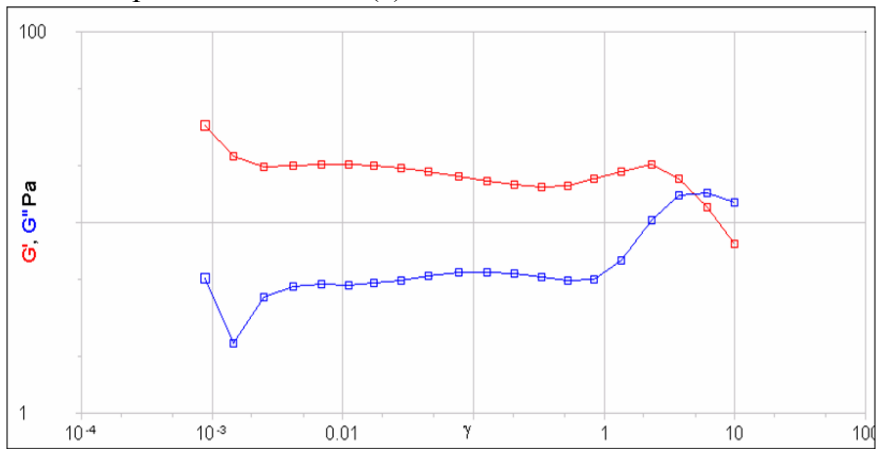
Time sweep test 5%/0.025% (b)
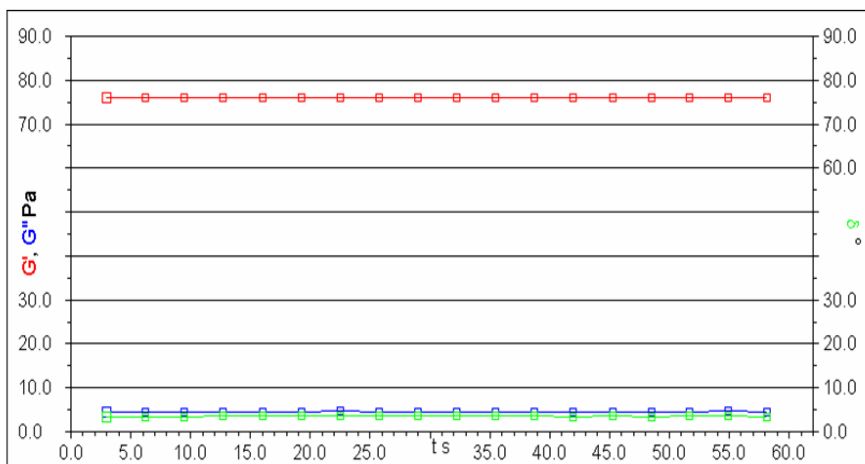
Frequency sweep test 5%/0.025% (b)
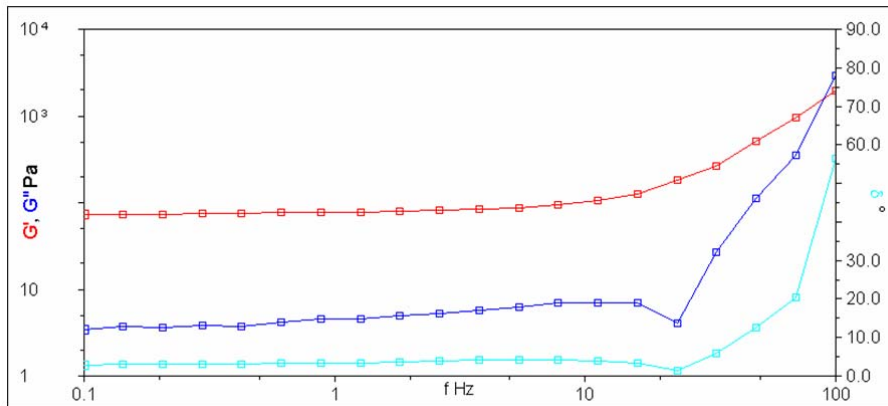
Strain sweep test 5%/0.025% (b)
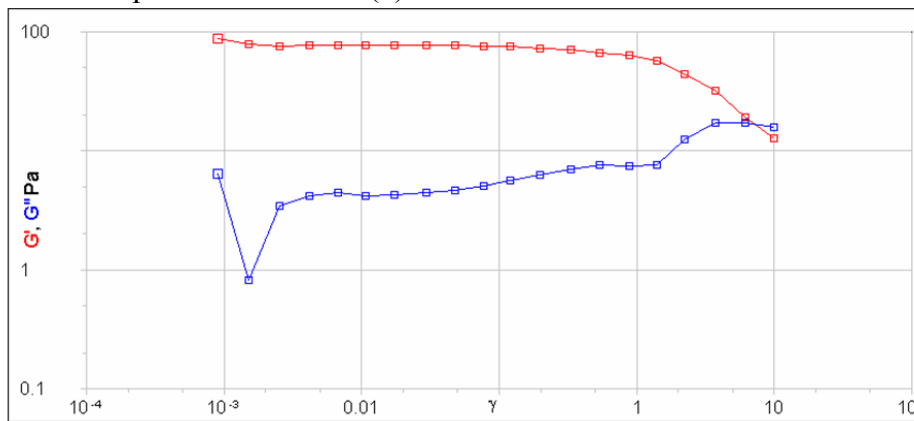
Time sweep test 5%/0.12% (a)
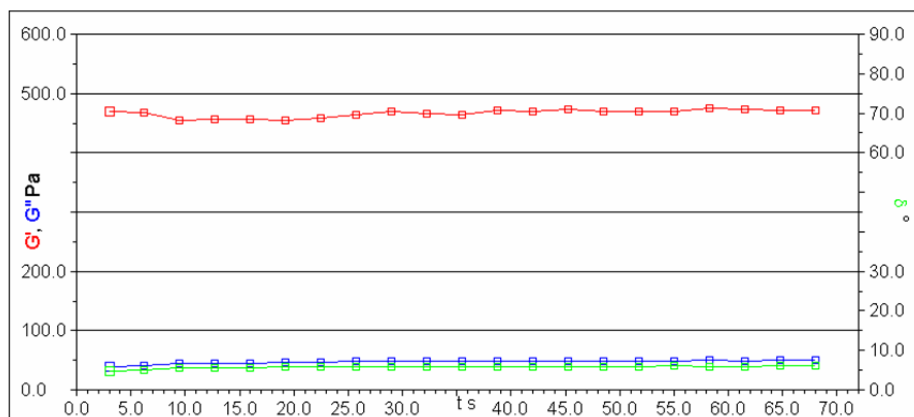
Frequency sweep test 5%/0.12% (a)
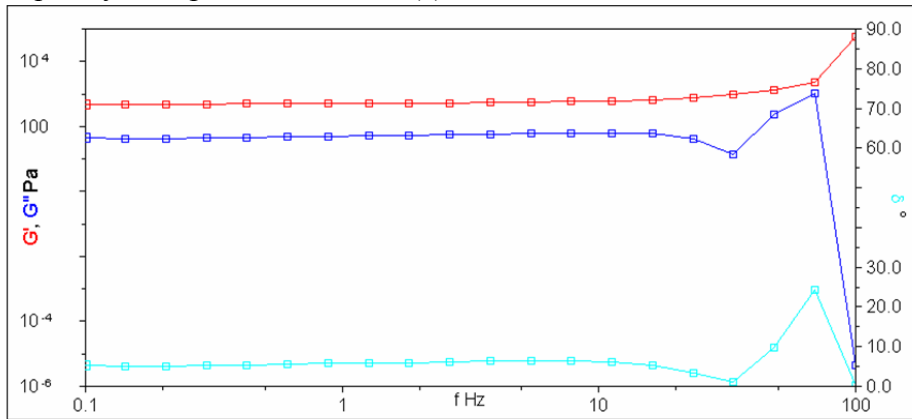
Time sweep test 8%/0.08% (a)
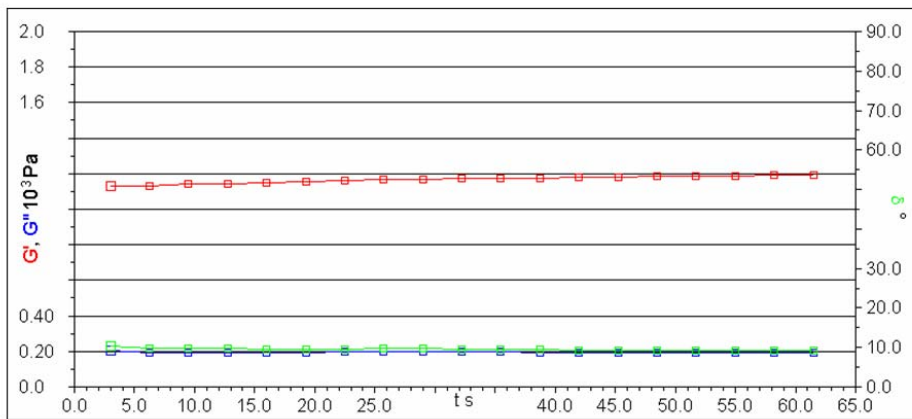
Frequency sweep test 8%/0.08% (a)
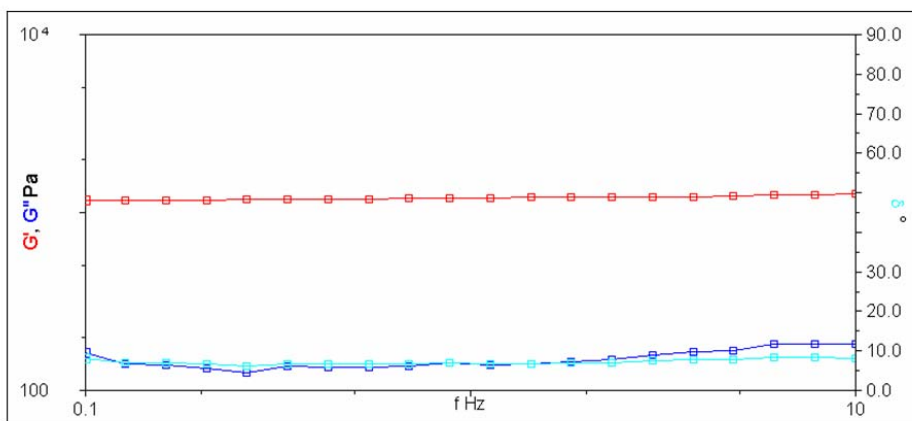
Strain sweep test 8%/0.08% (a)
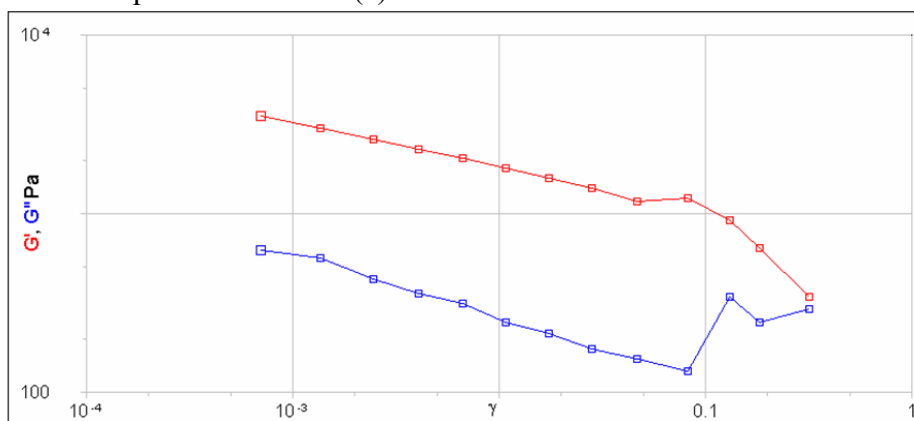
Time sweep test 8%/0.08% (b)
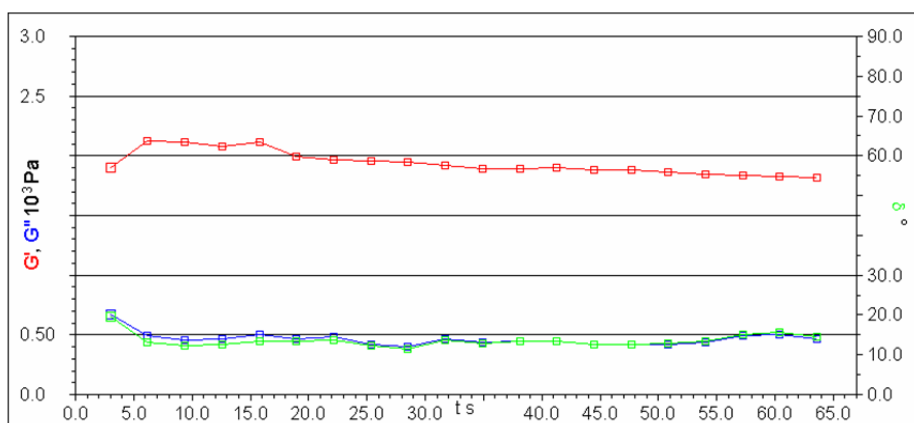
Frequency sweep test 8%/0.08% (b)
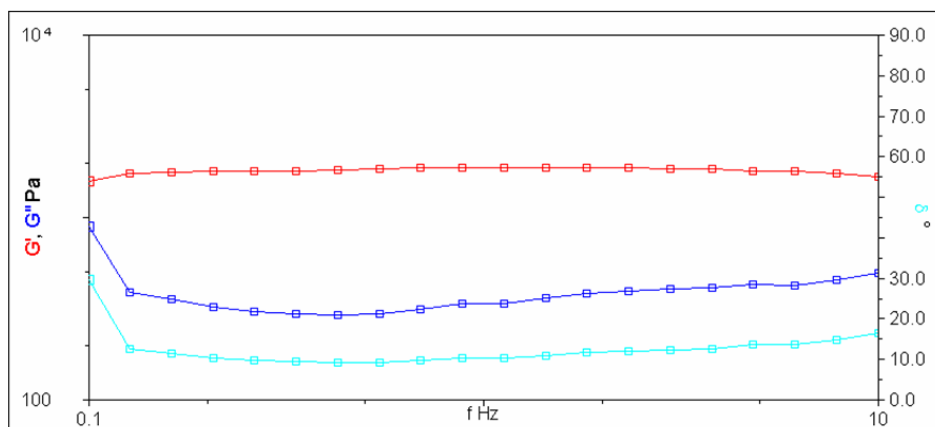
Strain sweep test 8%/0.08% (b)
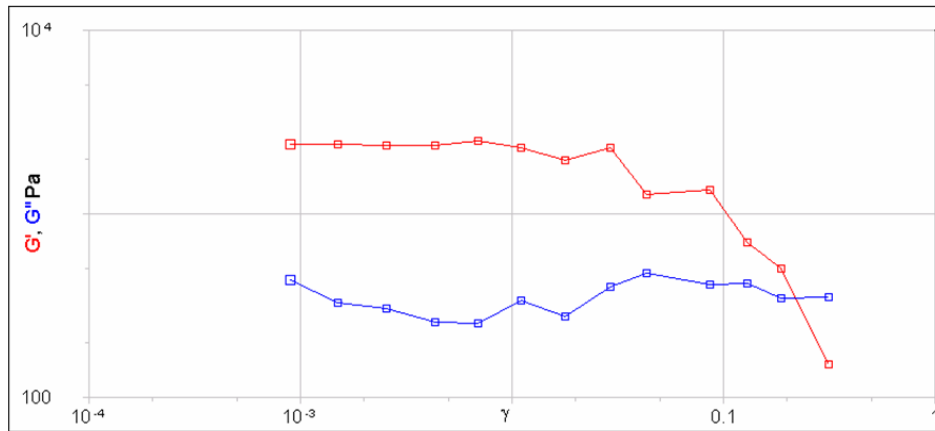
Time sweep test 8%/0.12% (a)
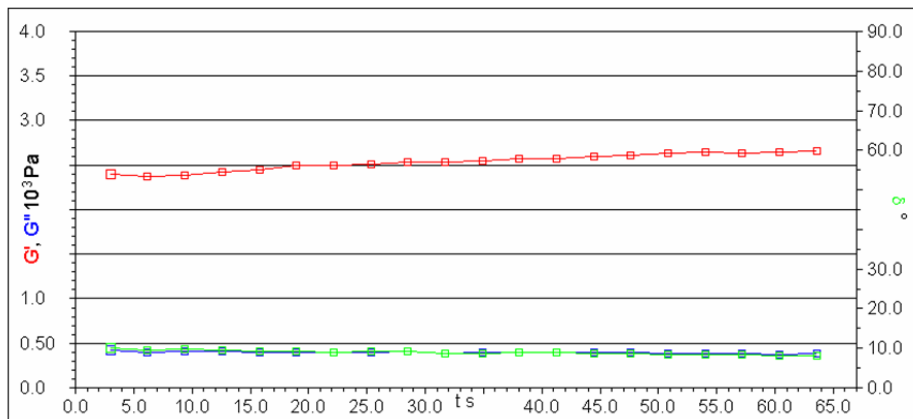
Frequency sweep test 8%/0.12% (a)
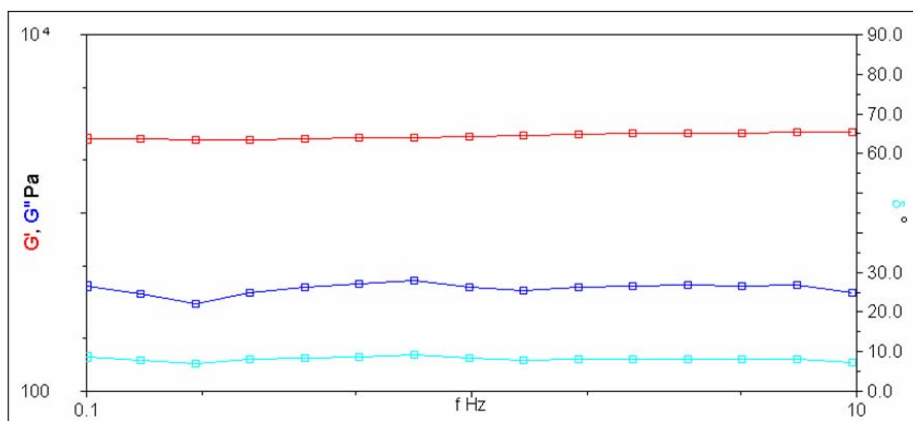
Strain sweep test 8%/0.12% (a)
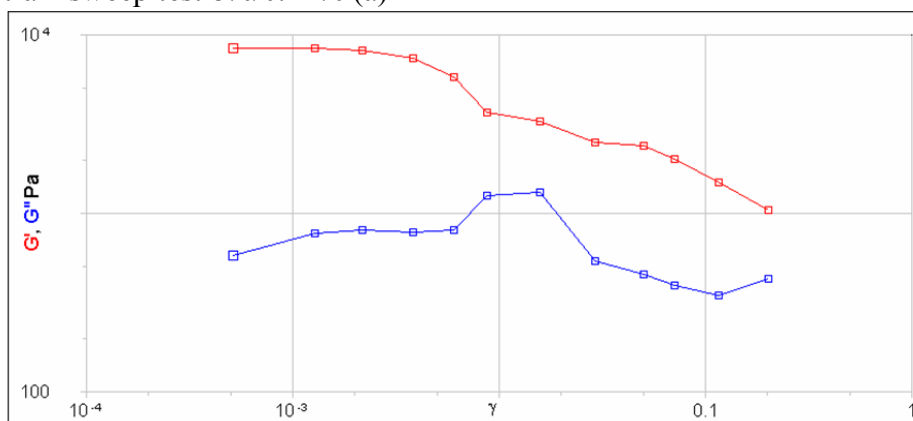
Time sweep test 8%/0.12% (b)
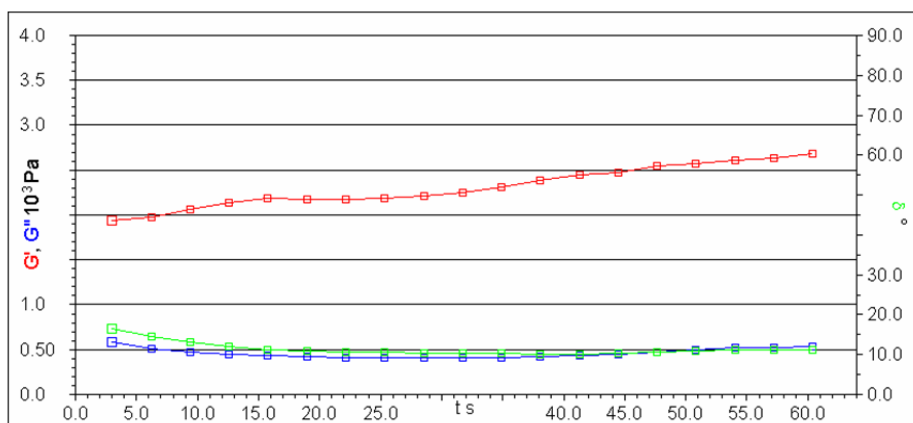
Frequency sweep test 8%/0.12% (b)
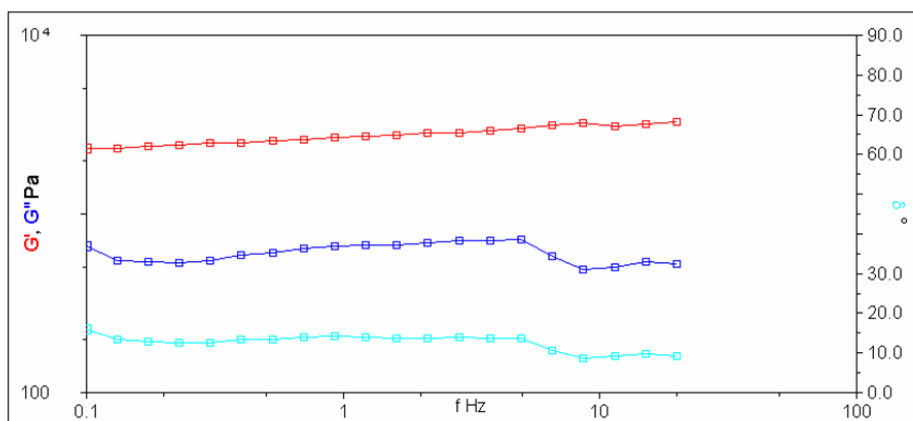
Strain sweep test 8%/0.12% (b)
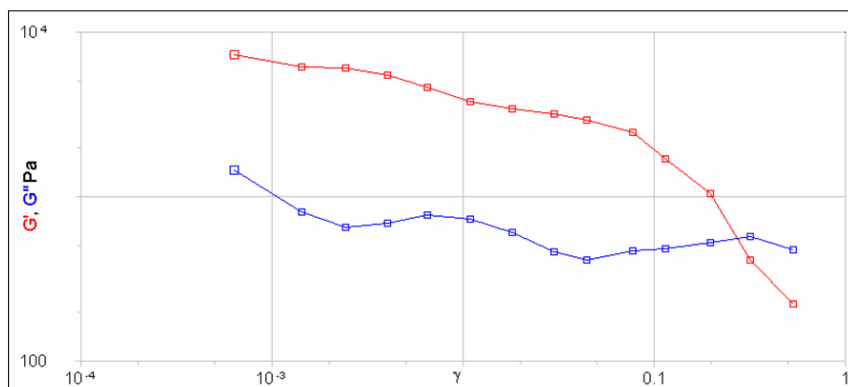
Using the smooth parallel plate method, the results in Table I were obtained using the time sweep method on the Bohlin Gemini rheometer. The elastic modulus values are calculated from the shear modulus using a Poisson's ratio of 0.4.

Test #1	Shear Modulus (Pa)		Elastic Modulus (Pa)
8%/0.08%	764±44		1834
5%/0.12%	768±26		1843
5%/0.025%	212±4		509

Table I: Preliminary Polyacrylamide Shear and Elastic Moduli

Using the serrated parallel plate method, the results in Table II were found also with the time sweep method.

Test #2	Shear Modulus (G') (Pa)			Elastic Modulus (E) (Pa)	
	A	B		A	B
8%/0.12%	2308±226	2529±91		5539	6070
8%/0.08%	1164±20	1933±100		2794	4639
5%/0.12%	466±7	X		1118	X
5%/0.025%	76±0.07	12±0.08		182	29

Table II: Polyacrylamide Shear and Elastic Moduli

There is very little reproducibility in these results. It is interesting to note that the serrated parallel plate method gave significantly higher results than the parallel plate method. This may be caused by slipping in the parallel plate system.

Testing #3:
The next data set also compares the smooth and serrated parallel plate methods. The polyacrylamide gels were again polymerized in an open environment in a plastic petri dish. The average results are represented in table form.

Time sweep test 8%/0.08% (a) – Smooth PP
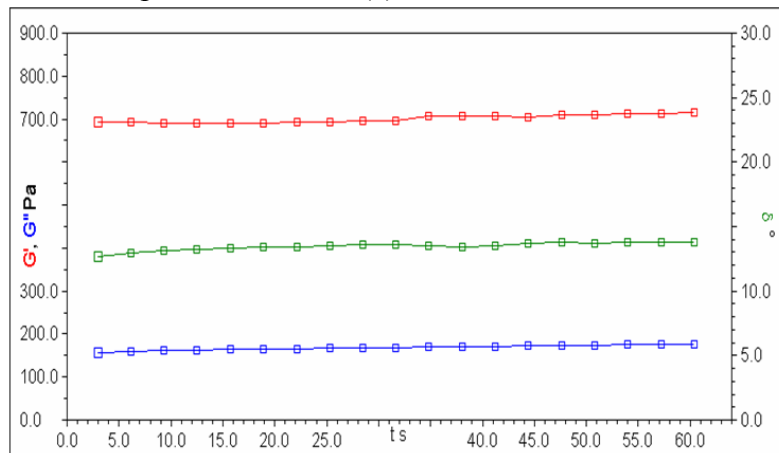
Frequency sweep test 8%/0.08% (a) – Smooth PP
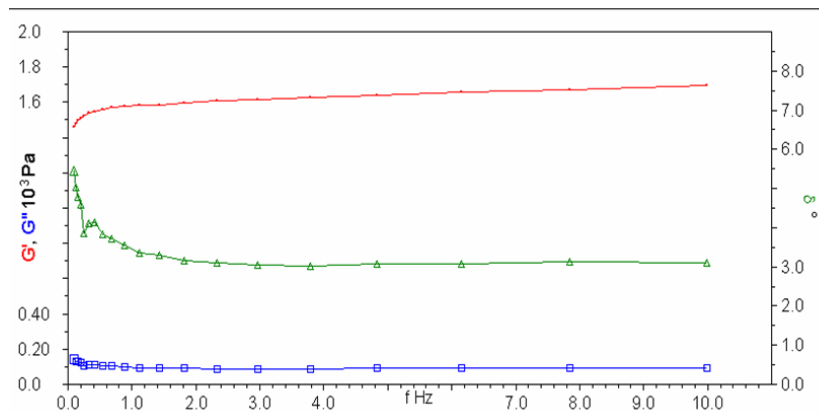

Smooth Parallel Plates 8%/0.08%:

Sample	Shear Modulus (Pa)	Elastic Modulus (Pa)
8%/0.08% (a)	720	2020
8%/0.08% (b)	700	1960
8%/0.08% (c)	330	920

Serrated Parallel Plates 8%/0.08%:

Sample	Shear Modulus (Pa)	Elastic Modulus (Pa)
8%/0.08% (d)	10	30
8%/0.08% (e)	1480	4140
8%/0.08% (f)	2360	7000

The following graphs represent polyacrylamide gels which were tested using a titanium vane tool, rather than the parallel plate method.

Time sweep test 8%/0.08% (a) – Ti Vane Tool
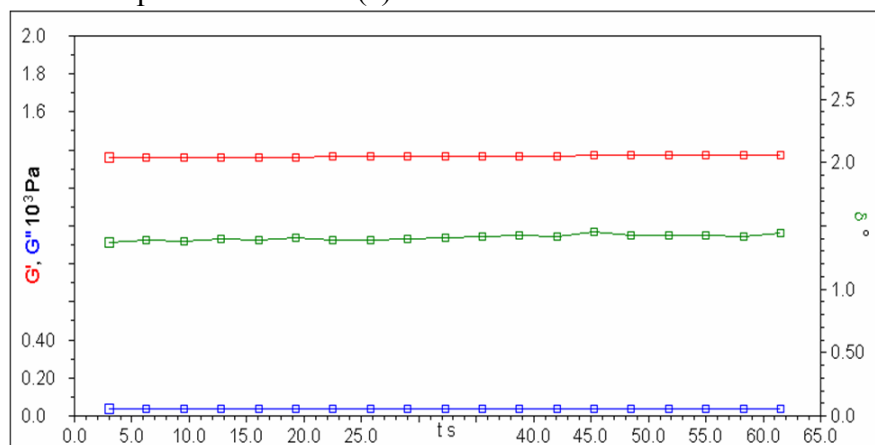
Frequency sweep test 8%/0.08% (a) – Ti Vane Tool (0.1 – 10 Hz)
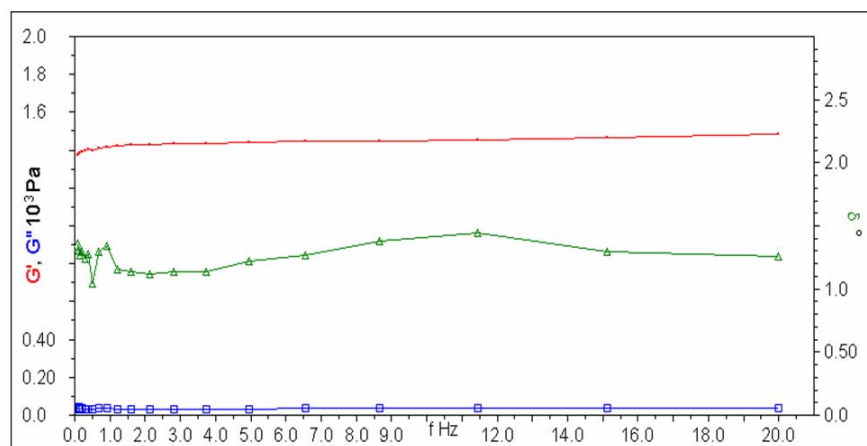
Frequency sweep test 8%/0.08% (a) – Ti Vane Tool (10 – 50 Hz)
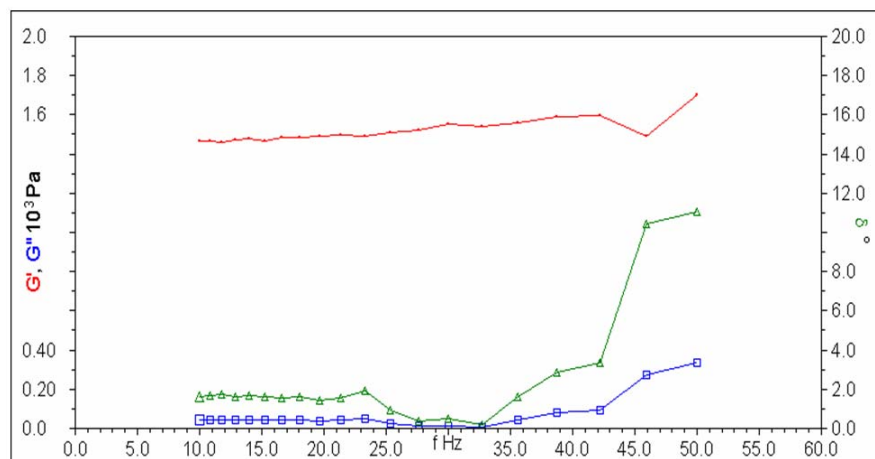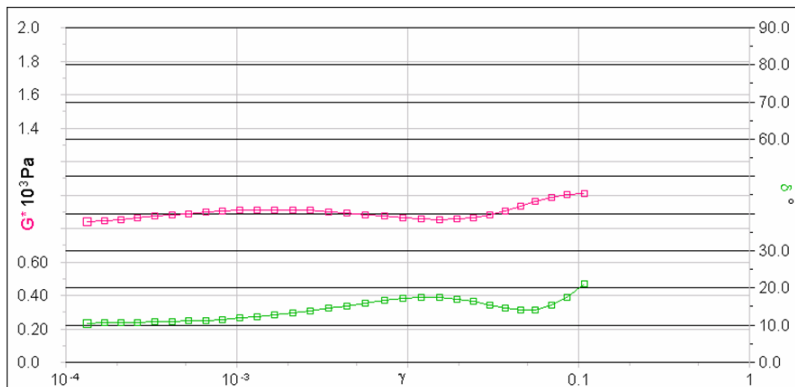
Titanium Vane Tool 8%/0.08%:

Sample	Shear Modulus (Pa)	Elastic Modulus (Pa)
8%/0.08% (d)	1360	3800

The next data set represents strain sweeps run on numerous samples of the same concentrations of acrylamide and bisacrylamide.
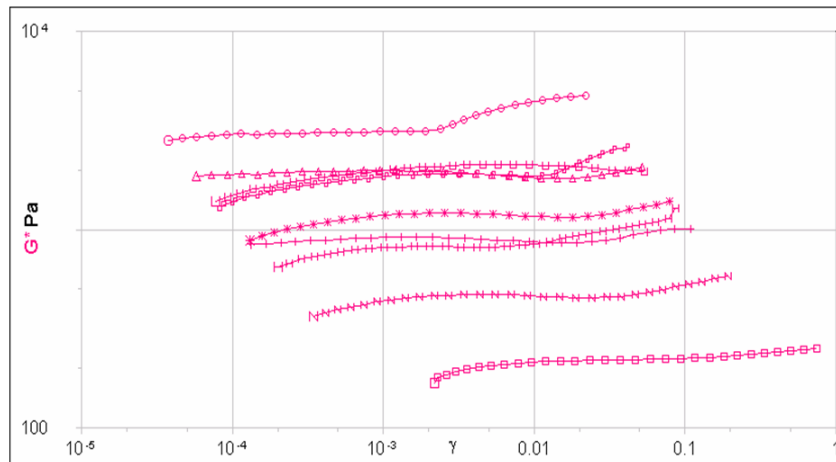
Strain sweep test 8%/0.08% (a)
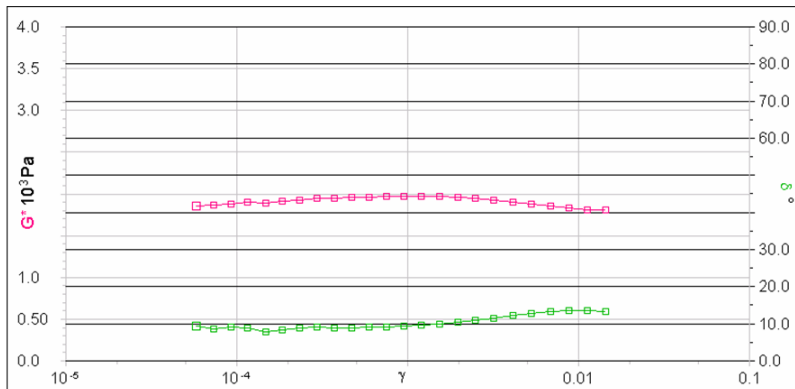
Strain sweep test 8%/0.08% (b)
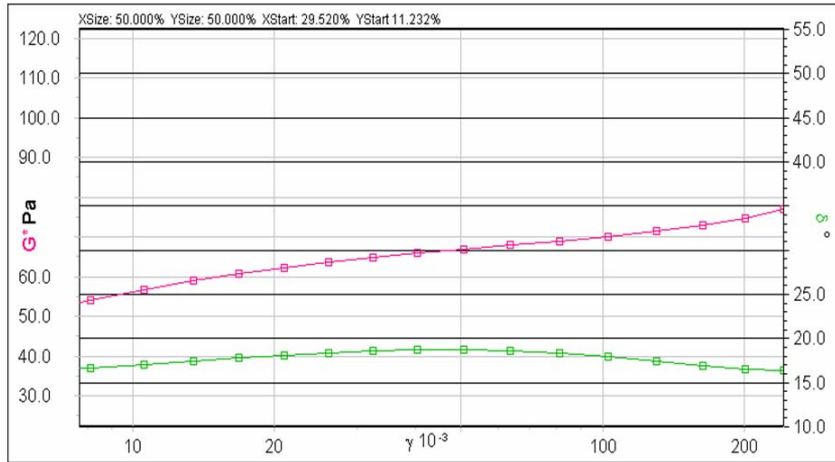
Strain sweep test 8%/0.08% (c)
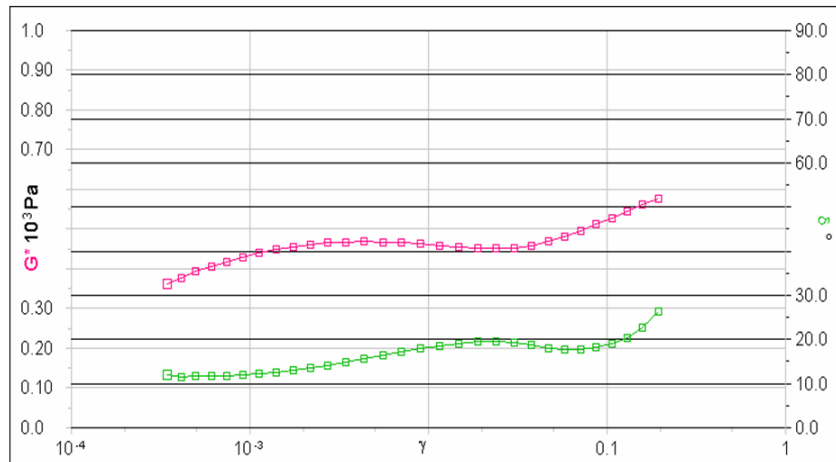
Strain sweep test 8%/0.08% (8 samples)

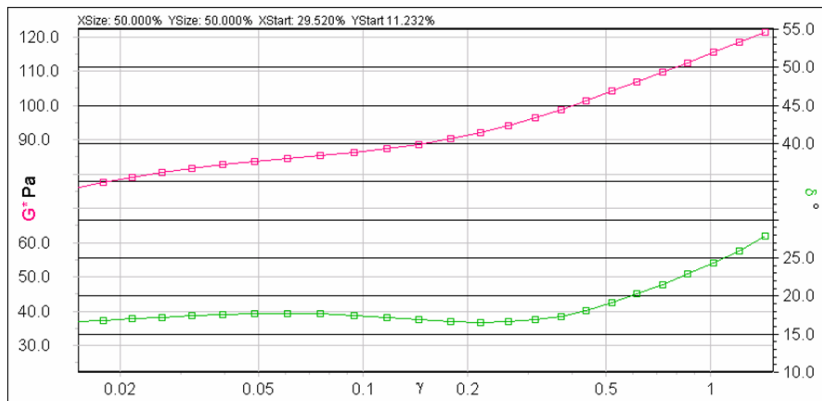Strain sweep test 8%/0.08% (8 samples)

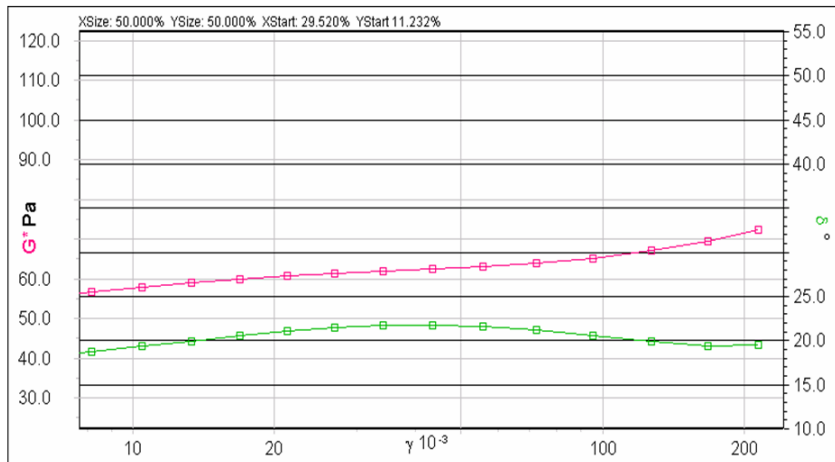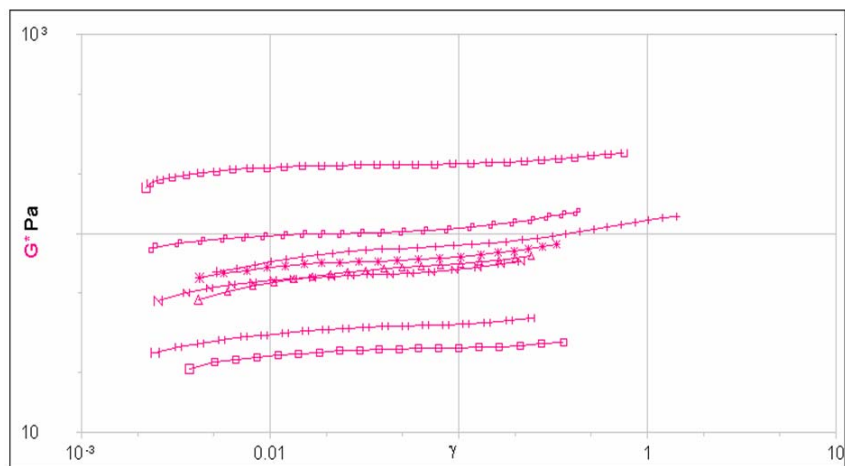| 8%/0.08% Sample	Complex Modulus (Pa)	Elastic Modulus (Pa)
a	1904	5331
b	894	2503
c	461	1291
d	1902	5326
e	1148	3214
f	866	2425
g	1851	5183
h	3435	9618

Strain sweep test 5%/0.025% (a)

Strain sweep test 5%/0.025% (b)

Strain sweep test 5%/0.025% (c)
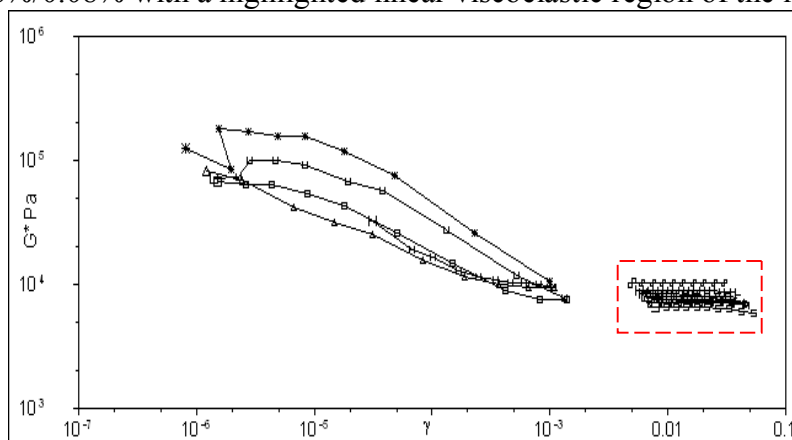
Strain sweep test 5%/0.025% (8 samples)

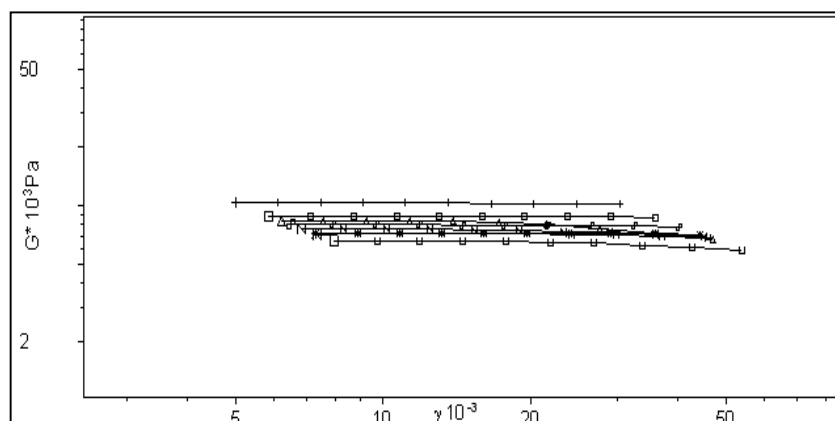Strain sweep test 5%/0.025% (8 samples)

5%/0.025% Sample	Complex Modulus (Pa)	Elastic Modulus (Pa)
a	64	179
b	90	252
c	60	168
d	216	605
e	103	288
f	73	204
g	32	90
h	25	70

Again, one can notice that there is very little reproducibility in the numbers. The gels were not produced in the same batch, nor were they polymerized in the glass plate set up. The next two sets of data represent gels that were from the same polyacrylamide solution and polymerized in between the two sheets of glass.
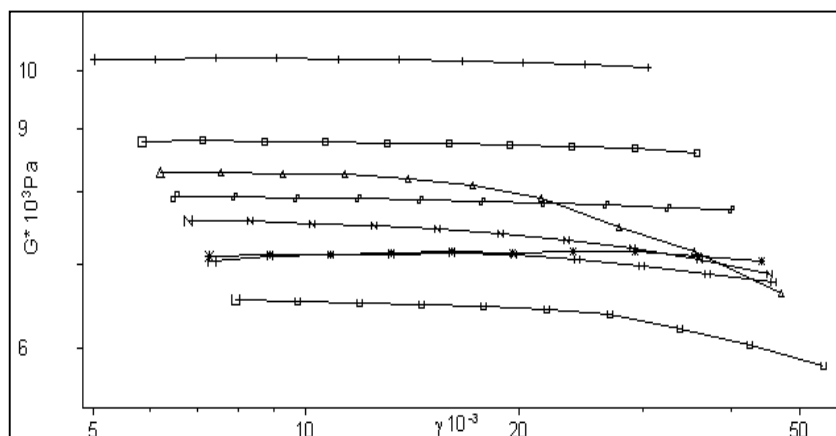
Strain Sweep of 8%/0.08% with a highlighted linear viscoelastic region of the material
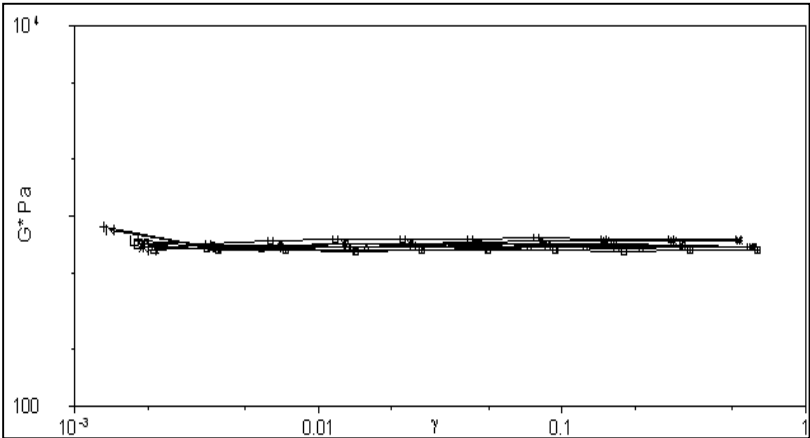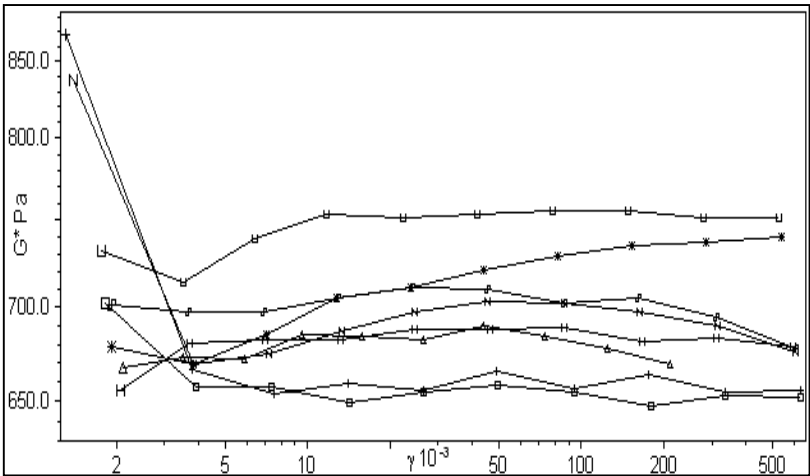

Strain Sweep 8% / 0.08% (8 samples) Linear Region

Strain Sweep 8% / 0.08% (8 samples)Linear Region (Zoom)

Strain Sweep 5% / 0.025% (8 samples) Linear Region

Strain Sweep 5% / 0.025% (8 samples) Linear Region (Zoom)

Sample (8%/0.08%)	Initial Gap (μm)	Initial Thrust (g)	Complex Modulus (Pa)	Elastic Modulus (Pa)

1	6051	70.0	7900	22120
2	6241	70.4	8254	23111
3	6195	72.9	8764	24539
4	6111	73.0	10200	28560
5	6247	70.4	7510	21028
6	6224	70.8	6508	18222
7	5984	70.9	7129	19961
8	5921	75.2	7113	19916
		AVE	7922	22182
		STDEV	1163	3255

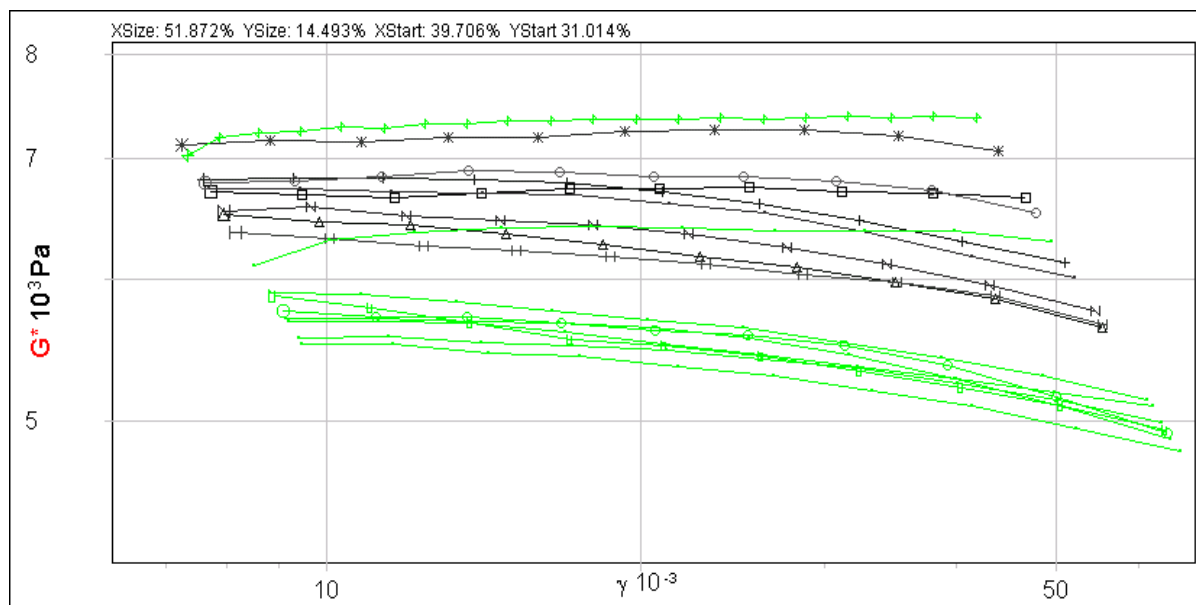| Sample (5%/0.025%)	Initial Gap (μm)	Initial Thrust (g)	Complex Modulus (Pa)	Elastic Modulus (Pa)
1	4964	27.4	697	1953
2	4471	26.0	672	1881
3	4526	30.5	657	1840
4	4383	29.0	654	1830
5	4376	33.7	674	1887
6	4250	28.2	738	2067
7	4376	31.0	685	1917
8	4398	31.4	682	1910
		AVE	682	1911
		STDEV	27	75

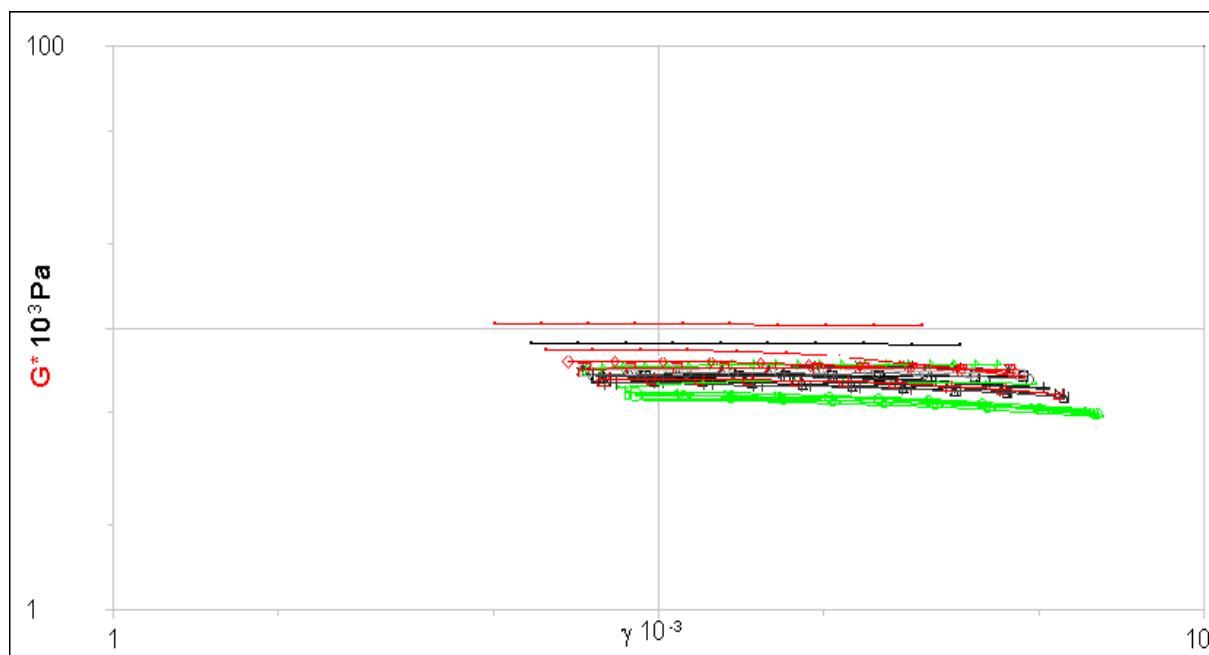Figure 1: Strain Sweep 8%/0.08% Linear Region Zoom

Figure 2: Strain Sweep 8%/0.08% Linear Region
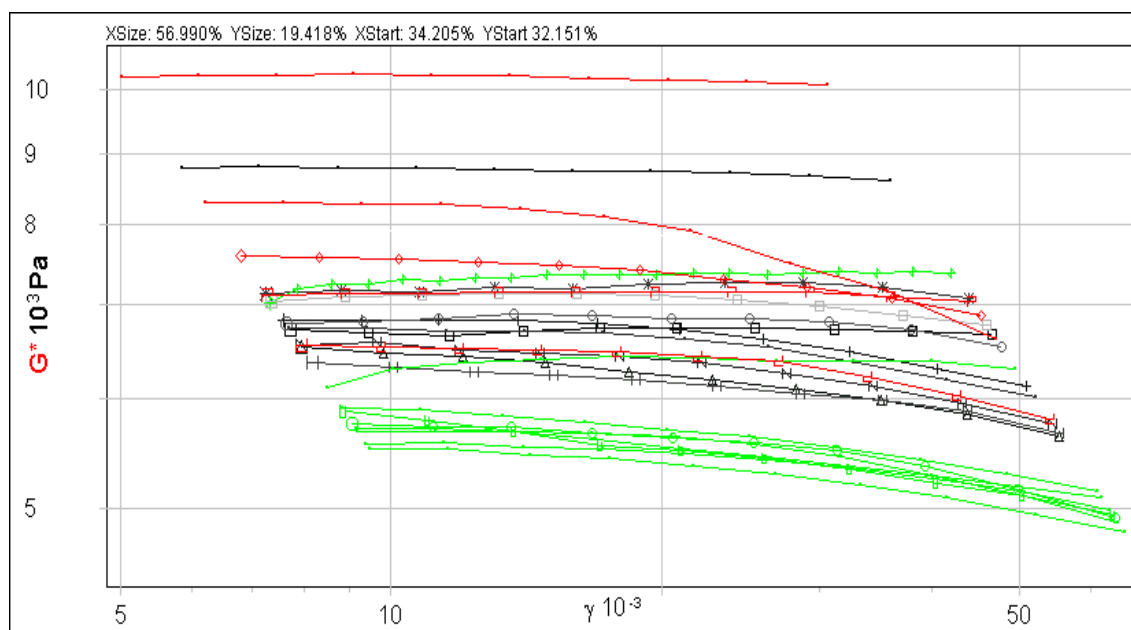
Figure 3: Strain Sweep 8%/0.08% Linear Region Zoom

(8%/0.08%) Sample	Drying Time (min)	Complex Modulus (Pa)
1	0	6267
2	30	8114
3	60	6127
4	90	7875
5	120	7795
6	150	9214
7	180	6932

Strain Sweep 8%/0.08% Linear Region Dehydration: inconsistent alteration of the complex modulus values over drying time.

(8%/0.08%) Sample	Thrust (g)	Complex Modulus (Pa)
1	10	3592
2	20	3377
3	30	2295
4	50	4204
5	70	6605
6	90	5613
7	110	6052
8	130	6153
9	150	6379
10	200	6423
11	250	6130
12	300	5686

Strain Sweep 8%/0.08% Linear Region Thrust Range: low thrusts (< 70 g) result in inconsistent data. High thrusts do not appear to significantly alter the properties of the gel.

(8%/0.08%)	Initial Gap (µm)	Initial Thrust (g)	Complex Modulus (Pa)	Elastic Modulus (Pa)
1	6051	70.0	6729	19514
2	6241	70.4	6267	18174
3	6195	72.9	6605	19155
4	6111	73.0	6352	18421
5	6247	70.4	6605	19155
6	6224	70.8	7267	21074
7	5984	70.9	6174	17905
8	5921	75.2	6835	19822
		AVE	6604	19152
		STDEV	353	1023

Table 8: Strain Sweep data from Set 1 (black) Figure 1 directly above.

(8%/0.08%)	Initial Gap (µm)	Thrust (g)	Complex Modulus (Pa)	Elastic Modulus (Pa)
1	5297	70.1	5579	16179
2	5994	70.9	7354	21327
3	5496	70.8	6404	18572
4	5583	70.3	5545	16081
5	5845	70.8	5437	15767
6	5539	70.5	5632	16333
7	5798	70.6	5511	15982
8	5642	70.5	5692	16507
		AVE	5894	17093
		STDEV	663	1923

Table 9: Strain Sweep data from Set 2 (green) Figure 1 directly above.

(5%/0.025%)	Initial Gap (µm)	Initial Thrust (g)	Complex Modulus (Pa)	Elastic Modulus (Pa)
1	4964	27.4	697	2021
2	4471	26.0	672	1949
3	4526	30.5	657	1905
4	4383	29.0	654	1897
5	4376	33.7	674	1955
6	4250	28.2	738	2140
7	4376	31.0	685	1987
8	4398	31.4	682	1978
		AVE	682	1979
		STDEV	27	77

Table 10: Strain Sweep data from the top (red) group in Figure 2 and Figure 3 directly above.

(5%/0.025%)	Initial Gap (μm)	Thrust (g)	Complex Modulus (Pa)	Elastic Modulus (Pa)
1	4146	29.2	676	1960
2	4140	30.4	574	1665
3	4290	29	600	1740
4	4336	29.6	625	1813
5	4270	30	701	2033
6	4248	30.1	627	1818
7	4229	29.2	707	2050
8	4132	29.7	671	1946
		AVE	648	1878
		STDEV	48	140

Table 11: Strain Sweep data from the bottom (black) group in Figure 2 and Figure 3 directly above.